UNIVERSITY OF CAPE COAST

MEASUREMENT OF ABSORBED DOSE TO ORGANS AT RISK IN HIGH DOSE RATE BRACHYTHERAPY OF THE CERVIX

JUSTICE AVEVOR

2020

UNIVERSITY OF CAPE COAST

MEASUREMENT OF ABSORBED DOSE TO ORGANS AT RISK IN HIGH DOSE RATE BRACHYTHERAPY OF THE CERVIX

BY

JUSTICE AVEVOR

Thesis submitted to the Department of Physics, School of Physical Sciences, College of Agriculture and Natural Sciences, University of Cape Coast, in partial fulfillment of the requirements for the award of Doctor of Philosophy Degree in Physics

MARCH 2020

DECLARATION

Candidate's Declaration

I hereby declare that this thesis is the result of my own original research and that no part of it has been presented for another degree in this university or elsewhere.

Candidate's Signature: ..... Date: .....

Name: Justice Avevor

Supervisors' Declaration

We hereby declare that the preparation and presentation of the thesis were supervised in accordance with the guidelines on supervision of thesis laid down by the University of Cape Coast.

Principal Supervisor's Signature: ..... Date: .....

Name: Dr. Joseph Amoako

Co-Supervisor's Signature: ..... Date: .....

Name: Prof. George Amoako

ABSTRACT

Radiation dose to bladder and rectum in the treatment of cervical cancer using high dose rate brachytherapy is a limiting factor to the delivery of the prescribed dose to the target. The objective of this study is to determine absorbed dose to the bladder and rectum (organs at risk) in the treatment of cervical cancer using multisource high dose rate brachytherapy treatment system in order to establish an in-vivo dosimetric and quality assurance protocol for patient treatment. A phantom was constructed using perspex for the measurement of dose distribution to the bladder and rectum. Gafchromic EBT3 films were used as dosimeters for measuring doses received by the bladder and rectum. The variation between doses calculated by the treatment planning system (TPS) and the doses measured by the Gafchromic EBT3 film at the bladder point was 15.38% (mean) ranging from -29.03% to 43.75%. The variation between doses calculated by the TPS and the doses measured by the film at rectum point was 14.73% ranging from -47.22% to 51.06%. Two mathematical algorithms were developed from the study to enable dose estimation to the bladder and rectum for error detection, variation analysis and verification of the treatment system. The variation between doses calculated by the TPS and the doses calculated by the model at the bladder point was 9.53% ±8.04. The variation between doses calculated by the TPS and the doses calculated by the model at the rectal point was 13.57% ±8.46. The results of the proposed models are within the ± 15% uncertainty proposed for dose delivery in radiation therapy (Hanson et al., 1994). The model is therefore recommended for clinical applications.

KEY WORDS

Brachytherapy

Dose

Gafchromic EBT3 Films

Organs at risk

Phantoms

Treatment Planning System

ACKNOWLEDGEMENTS

Much effort from individuals and organizations has gone into the completion of this research work. I would like to express my sincere gratitude to my supervisors Dr. Joseph Amoako and Prof. George Amoako for their immense contribution to make this study a better one. I would like to thank the National Centre for Radiotherapy and Nuclear Medicine for allowing me access into the facility to be used for this study.

I am also grateful to Dr. Samuel Nii Tagoe, Mr. Evans Sasu and Amos Asiedu for their contribution towards this work. My appreciation also goes to the University of Cape Coast, the Graduate School and the department of Physics for all the efforts and contributions towards this study.

Finally, I wish to thank my family especially my parents Wallace Yao Anthony Avevor and Catherine Atsupui Tamekloe, my brother Mawuli Avevor, my wife Solace Avevor and my wonderful sons Enam and Elolo Avevor.

DEDICATION

To my sons: Enam and Elolo Avevor.

.

TABLE OF CONTENTS

LIST OF TABLES

LIST OF FIGURES

LIST OF ACRONYMS

2D	Two-dimensional
3D	Three-dimensional
AAPM	American Association of Physicists in Medicine
ACCIRAD	Accidents and near misses in Delivery Radiotherapy
ANOVA	Analysis of Variance
AP	Anterior-Posterior
BT	Brachytherapy
CT	Computed Tomography
CTV	Clinical Target Volume
EBRT	External Beam Radiotherapy
EBT	Electronic Benefit Transfer
GTV	Gross Tumor Volume
GYN	Gynaecology
H& D	Hurter and Driffield
HDR	High Dose Rate
HPV	Human Papillomavirus
IAEA	International Atomic Energy Agency
ICRP	International Commission on Radiological Protection
ICRU	International Commission on Radiation Units and Measurements
IMRT	Intensity Modulated Radiotherapy

ISA	Inter-Source Attenuation
ISP	International Specialty Products
IVD	In-Vivo dosimetry
LAT	Lateral
LDR	Low-Dose Rate
MDR	Medium-Dose Rate
MRI	Magnetic Resonance Imaging
NCRNM	National Centre for Radiotherapy and Nuclear Medicine
NCRP	National Council on Radiation Protection and Measurements.
NPP	Normal Probability Plot
OAR	Organs at Risk
OD	Optical Density
PDR	Pulse Dose rate
PMMA	Polymethylmethacrylate
PTW	Physikalisch-Technische Werkstätten
QA	Quality Assurance
RGB	Red Green Blue
ROSIS	Radiation Oncology Safety Information System
RPOP	Radiation Protection Patients
SAD	Source-Axis Distance
SAFRON	Safety in Radiation Oncology
SPSS	Statistical Package for the Social Sciences

SSD	Source-Surface Distance
TG	Task Group
TLD	Thermoluminescent Dosimeter
TPS	Treatment Planning System
TRS	Technical Report Series
WHO	World Health Organization

LIST OF SYMBOLS AND CONSTANTS

Symbol	Meaning	Unit
ψ	Energy Fluence	J/m^2
Φ	Particle Fluence Rate	$m^{-2}s^{-1}$
(Λ)	Dose Rate Constant	$cGyh^{-1}U^{-1}$
$\dot{D}$	Dose Rate	Gy/min
$D_{w,cal}$	Absorbed Dose to Water Phantom	Gy/min
H_T	Equivalent Dose	S_v
I_O	Initial Intensity	W/m^2
K_{TP}	Pressure-Temperature Correction	nC
S_k	Air Kerma Strength	$U(1U = 1\ cGy\ cGycm^2h^{-1})$
D	Depth	Cm
D	Distance	M
$\dot{X}$	Exposure Rate	$C\ Kg^{-1}S^{-1}$
C	Cerma	Gy
D	Dose	Gy
E	Effective Dose	S_v
$G(r,\theta)$	Geometry Function	cm^{-2}
I	Intensity	W/m^2
K	Kerma	Gy
L	Source Active Length	M
M	Dosimeter Reading	nC/min

X	Exposure	$(\mathrm{C/kg})$.
Φ	Particle Fluence	m^{-2}
Ψ	Energy Fluence Rate	$\mathrm{Jm}^{-2}\mathrm{s}^{-1}$
β	Angle Covering Active Source	Radian

CHAPTER ONE

INTRODUCTION

This chapter presents an overview of the background of cervical cancer and the challenges associated with its treatment using high dose rate brachytherapy. The statement of problem, the objectives of the study and the relevance and justification have been outlined in this chapter. Furthermore, the scope and delimitation and the organization have also been presented.

Background to the Study

Cervical cancer occurs when normal cells on the cervix grow out of control. This type of cancer can be effectively treated if detected early. The World Health Organization (WHO, 2017), has approximated close to a million patients who are living with this disease. Cancer of the cervix is associated with infection by human papillomavirus (HPV)(WHO). It is caused by a long-term infection with HPV. Majority of cervical cancer cases (>80%) occur in low- and middle-income countries. According to 2017 census in Ghana, there were about 8.57 million women of ages 15 years and above who are at risk of developing cervical cancer (WHO, 2017). It is the leading cancer among women in Ghana and the most frequent cancer among women between 15 and 44 years of age (WHO, 2012).

There are various treatment options available for cervical cancer. One common treatment option is radiation therapy or radiotherapy. During radiotherapy, the cancerous cells are exposed to ionizing radiation to cause a rapid breakdown of the cell's deoxyribonucleic acid (DNA) which results in cell death. This treatment option is divided into external beam radiation therapy and brachytherapy (BT) or internal radiation (WHO, 2017).

BT is a terminology that describes the short distance cancer treatment with radiation from small, encapsulated radionuclide sources. This treatment type is achieved by putting the radioactive sources directly into or near the volume to be treated. The dose is then delivered continuously, either over a short period of time (temporary implants) or over the lifetime of the source to a complete decay (permanent implants). Most common BT sources emit gamma photons; however, in a few specialized situations β or neutron emitting sources are used (Mayles, Nahum, and Rosenwald, 2007).

BT can use sources that are loaded within body cavities (intracavitary), sources that are implanted into tissues (interstitial), trains of sources within the lumen of organs, such as the bronchus or oesophagus (intraluminal), or sources supported in a mould over a tumor (superficial BT). The prime example of intracavitary BT is the use of radioactive sources within applicators in the uterus and vagina, whilst the best example of interstitial BT would be the use of radioactive needles in the treatment of carcinoma of the tongue. Intraluminal BT is a relatively new technique made possible by high dose rate micro-sources, which need only remain within the lumen for a few minutes, thus avoiding the problems of obstruction. Superficial BT has largely been replaced by the use of high energy electrons for tumors of the skin, but may still have a place in the treatment of tumors in the upper airways and oropharynx. It is also occasionally used in the treatment of vaginal and vulvar cancers (Mayles, Nahum, and Rosenwald, 2007).

Historically, BT developed because of the inadequacy of external radiotherapy in treating deep-seated tumours. The gynaecological organs were particularly suitable for treatment by BT because of their accessibility through

the vagina. Similarly, the treatment of head and neck cancer relied heavily on interstitial brachytherapy because of the ease of access through the mouth and nose. As a consequence, systems were developed for both intracavitary and interstitial therapy in several major radiotherapy centres, particularly Paris, Stockholm and Manchester (Mayles, Nahum, & Rosenwald, 2007).

In the first half of the 20th century, all of these centres used radium, which had the advantage of a long half-life, making recalibration and replacement of sources unnecessary. Radium produces a high energy emission that is not preferentially absorbed in bone by the photoelectric effect. Therefore, it can be used to deliver large doses to tumours adjacent to bone that would be at risk of osteonecrosis if treated with low-energy orthovoltage X-rays. This latter advantage became less important as high energy external-beam therapy improved in the 1950s and 1960s and, as the daughter product of radium was radon gas, radium was phased out of use and replaced with caesium, which has solid decay products (Mayles et al, 2007).

Various applicator designs were created to allow live-source implantation techniques to be replaced by either manual or remote after-loading, whereby the radioactive source was only introduced into the applicators after the applicators were correctly positioned, be they intracavitary or interstitial applicators. Today, newly developed systems allow radioactive sources to be remotely after-loaded by either cable-driven or pneumatic techniques, enabling the activity of the radioactive sources to be increased to allow low-medium and high-dose-rate brachytherapy with complete staff protection (Palmer, Nisbet, & Bradley, 2013).

There are ongoing remarkable innovations and progressive transitions in BT treatments. There is also a drift away from using the conventional technique where dose distributions are pre-determined and a shift from 2D to 3D approach of the overall treatment process. Quality assurance procedures must match the same rate of progress with the new trends in the treatment planning of BT and dose delivery to ensure a high level of accuracy in dosimetry and quality. Conventional techniques of quality control are based entirely on isolated source-strength measurements with very little or no independent determination of the actual dose delivered. This type of technique is not enough for modern 3D-based BT which demands a multi-dimension verification measurement of the dose delivered when using applicators in clinical treatment and the potential of significant patient-specific dose distribution optimization (Palmer, Nisbet, & Bradley, 2013).

One challenge with BT treatment is that there are no laid down protocols for quality control measurements of the 3D dose distribution delivered using the high dose rate (HDR) treatment equipment (Palmer, Bradley, & Nisbet, 2012). Dose distribution measurements in BT are herculean due to high, steep dose gradients (6% per mm at the target volume in HDR gynecology treatments) and levels of discrepancies in dose deposition around the region of interest. The systems used in the measurements must be adequate and flexible to allow the use of the various designs of applicators of HDR and make available sufficient data within the maximum extent of the applicator dimensions (Palmer, Nisbet, & Bradley, 2013).

Over the years, a lot of investigators have used radiochromic films in BT dosimetry to determine peculiar measurements and to also verify the Monte

Carlo generated TG- 43 based source model data (Sureka, 2007; Lliso, 2011; Aldelaijan, 2011). Nonetheless, publications that involve the use of the new Gafchromic EBT3 film BT dosimetry are few. Publications on quality control procedures for dosimetry in BT are also limited. The few available ones are entirely based on point dose measurements, making use of ion chamber or alanine (CarlssonTedgren and Grindborg, 2008). There is therefore, the need to develop analytical techniques and practical measurement which is required both for routine in-clinic quality checks of BT equipment performance and for independent verification of the 3D BT dosimetry system.

Accuracy, careful planning and delivery are major requirements in treating cervix cancer using high dose rate brachytherapy. This is crucial because a major part of the treatment site is in close proximity to critical organs and healthy tissues. It is important that the HDR system used in the treatment performs very effectively and accurately to affect a series of planned source dwells treatment. Dose delivery accuracy depends on source positioning, because of the short distances between target and source, steep dose gradients and large inverse square law corrections for any geographic errors. In BT treatment, even small geometric uncertainties or errors may result in large dose discrepancies from the original treatment plan. These discrepancies may result in inadequate dose delivery to the target and/or increased dose to organs at risk and healthy tissues (Elfrink et al., 2001).

In-Vivo Dosimetry

In-vivo dosimetry (IVD) is an important quality assurance technique for HDR BT for the cancer of the cervix. IVD is the only practical way to check the delivered dose during radiotherapy and BT. Through IVD, discrepancies in the dose delivered and the dose calculated using TPS may be determined. IVD supplies the needed information which aids in assuring precise, targeted and conformal dose delivery. Reports have proven that IVD is feasible and can be performed to predict dose delivery to the rectum and bladder during HDR brachytherapy using Co-60 source (Zaman et al., 2014).

The error types during BT treatments and their rates of occurrence are not well known. This knowledge gap is partially due to the absence of independent verification systems of the sequence in treatment in the clinical workflow routine. It is accepted that real-time IVD can make available efficient error detection and treatment verification within the field of IVD. However, the non-existence of high accuracy IVD systems that are straightforward for clinicians has hindered the widespread implementations of the systems (Kertzscher, Rosenfeld, Beddar, Tanderup, & Cygler, 2014).

Modern BT is growingly implementing the three-dimensional (3D) imaging treatment planning systems (TPS) based and remote afterloading [for HDT BT]. Due to these evolutions, the use of manual procedures, which are a common source of errors in radiotherapy has reduced. (Ashton, Cosset, Levin, Martinez, and Nag, 2004; Lopez, Andreo, Cosset, Dutreix, and Landberg 2000; IAEA, 2000; WHO, 2008). However, BT still typically involves more manual procedures during catheter/applicator insertion, treatment planning and treatment delivery than external beam RT (EBRT). Again, the verification of

treatment delivery is not advanced in BT as it is in EBRT. This makes BT more susceptible to errors than EBRT.

Application of 3D imaging in BT has enhanced the frequent implementation of individualized adaptive approaches via dose optimization and geometry of implants. The accuracy of dose delivery, conformality of dose to target and the reliability of the treatment flow are becoming very important. There is an improvement in understanding the correlation between dose and its effects on the patients and staff by the availability of the 3D dose distributions. This has paved way for an improved prospect to plan and direct treatments according to certain dose constraints in the balancing and prioritization between the target and organ-at-risk (OAR) doses. The effects of dose variations are more pronounced, particularly for patients with target and/or OAR doses close to constraint values, hence the need to control the precision of dose delivery (Tanderup, Nesvacil, Potter, Kirisits, 2013).

There is a need to establish procedures for error detections and variations in future treatment verification so as to improve the overall accuracy of treatment delivery. This must be included in the context of high dose gradients in BT which makes treatment delivery and precise dose measurements very challenging, because a small error or geometric discrepancy can result in large dose variation from the intended treatment plan. These discrepancies can result in inadequate dose delivered to the target and/or increased OAR doses.

Errors in BT treatment are classified into human errors (e.g. incorrectly specified source strength, erroneously connected source transfer guide tubes and gross applicator reconstruction errors) or equipment malfunctions (e.g. defective afterloader stepping-motor and flaws in the control software). There

is limited information on these kinds of errors during treatment in BT and their rates of occurrence. Avalaible sources of information addressing errors during RT include dedicated databases as reported by Chambrette, Hardy, & Nenot (2001); Cunningham, Coffey, Knoos & Holmberg (2010); Holmberg, Malone, Rehani, McLean, Czarwinski (2010) and published reports (IAEA, 2010). There is a possibility, however, that a significant portion of these errors are not known to the RT community since treatment centers are not subject to guidelines that demand public reporting when treatment errors are detected. Also, there are no control methods to monitor the flow of treatment in BT that are independent of the treatment delivery system; hence it is likely that these errors remain unknown in the entire treatment.

Uncertainties in BT Treatments and the need for IVD Dosimetry

Uncertainty analyses occupy a significant part of the literature and cover different aspects of BT treatment workflow. Uncertainties related to treatment planning arise partly from source calibration uncertainties (DeWerd et al., 2011) and imperfections of the dose calculation protocols. Currently, the TPSs in use incorporate the American Association of Physicists in Medicine Task Group (TG)-43 dose calculation protocol (Rivard et al., 2004), which works with the assumption that a patient is made of water and as such does not take into account tissue heterogeneities and inter-source dose attenuation. Additionally, there are challenges with these TPs when it comes to the implementation of the dose calculation protocols and the source parameters. (DeWerd et al., 2011 and Rivard et al., 2004).

The uncertainties with the TPS are further improved by the interobserver variability in the volumetric delineation of clinical targets and OARs (Rivard et

al, 2004; Kirisits et al, 2007; & Hellebust et al 2013) and by systematic effects of source positioning and applicator reconstructions. (Petriet al., 2013; Hellebust et al., 2007; Tanderup et al., 2008; De Leeuw et al., 2009; Haack, Nielsen, Lindegaard, Gelineck, Tanderup, (2009); Wills et al, 2010; Haie-Meder et al, 2005). The imperfections confronting the TG-43 dose calculation protocol (DeWerd et al., 2011) is being resolved by developing model-based dose calculation methods, which are in contrast to the TG-43 account for individualized patient anatomy and tissue heterogeneities (Hellebust et al., 2010, Beaulieu et al., 2012).

Several factors like, organ movements, treatment planning and contouring can affect treatment outcomes. The effects of these factors on clinical outcomes have not been well reviewed even though discrepancies in dosimetry of BT have been well described. Nonetheless, series of reports have been published by investigators to enhance the likelihood of describing BT discrepancy budgets that encompass the whole treatment workflow beginning from source calibration to the delivery of treatment (Tanderup, Nesvacil, Potter, Kirisits (2013), Rivard, Venselaar, & Beaulieu, 2009). The findings from these investigations detail the significance of geometric variations induced by organ and applicator movements, (Kirisits et al, 2014) which complicate and potentially compromise accumulated dose calculations in the organs. Inter- and intrafraction deformations of the rectum, bladder and prostrate have been studied, (Nesvacil et al, 2013; Buchali, 1999; Hellebust, Dale, Skjønsberg, & Rune, 2001; Holloway et al, 2009; Jamema et al, 2013)and the dosimetric impact owing to more general anatomical variations has been evaluated in a multicentre comparison of cervix BT (Kirisits et al, 2014). Organ–applicator

movements during imaging of patients to the delivery of treatment stages have been identified as a major source of error (Tanderup et al, 2008; Cherpak, Cygler, & Perry, 2013; Hoskin, Cook, Bouscale, & Cansdale, 1996; Kim et al, 1996; Bahena et al, 1998; Datta et al, 2001; Hoskin et al 2003; Wulf et al 2004) and their effects have been further analyzed. In BT of cervical cancer, inter- and intrafraction uncertainties that are due to the movements of organs and deformations account for 20-25% of the D2 cm^3 parameter (minimum dose to the most irradiated 2 cm^3) per fraction and is the most important component in the uncertainty budget for OARs (Tanderup et al., 2013).

The knowledge about BT treatment errors comes from published reports (Lopez, Andreo, Cosset, Dutreix, & Landberg, 2000; IAEA, 2000; IAEA, 2017) and databases, such as (Radiation Oncology Safety Information System) ROSIS, (Cunningham, Coffey, Knoos, & Holmberg, 2010), (Safety in Radiation Oncology) SAFRON [Holmberg, Malone, Rehani, McLean, & Czarwinski, 2010, IAEA,2017) and (Accidents and near misses in delivery radiotherapy) ACCIRAD (Chambrette, Hardy, Nenot, 2001) which is limited to the information that clinics are willing and able to share. Several of the reported BT error types could have been detected with real-time IVD, for instance, there have been a case of an HDR unit malfunction, where the BT source had broken loose from the guide wire and remained inside the patient (IAEA, 2017). If real-time IVD was more frequently implemented in the clinical workflow routine, in addition to consensus recommendations for image-guided BT (Potter, 2006; Dimopoulos et al, 2012), our knowledge about BT errors and their occurrence rates could improve, provided the reporting is open and honest.

Statement of Problem

The goal in HDR brachytherapy treatment is to deliver high dose to the cervix whilst sparing or minimizing dose to the bladder and the rectum (organs at risk) which are in close proximity to the cervix. However, most frequent clinical complications such as rectal ulceration, fistulas and urinary bladder obstruction, are being reported as a result of high dose delivered to parts of the bladder and rectum. There is a need to establish an in-vivo dosimetric protocol for error detections, variation analysis and verification in the HDR BT treatment flow in order to improve the overall accuracy of treatment delivery.

Objectives

The main objective of this study is to determine the absorbed dose to the bladder and rectum (organs at risk) in HDR BT of cervical cancer in order to establish an in-vivo dosimetric and quality assurance (QA) protocol for patient treatment.

The specific objectives are:

i. To construct an inhouse anatomical water phantom for dose distribution measurements during BT treatment.
ii. To determine the dose distribution (measured dose) during treatment and compare it with the optimized dose (planned dose) calculated by the TPS for empirical validation and system verification.
iii. To develop mathematical algorithms for dose determination to the bladder and rectum for error detection and dose variation analysis.

Relevance and Justification

This study has become necessary because the BT system of cervical cancer treatment at the National Center for Radiotherapy and Nuclear Medicine (NCRNM), Accra has been changed from low dose rate (LDR) to high dose rate BT. Avevor, Tagoe, Amuasi & Fletcher, assessed dose to the bladder and rectum in LDR intracavitary BT of the cervix using Gafchromic films. They reported deviation between TPS and film dose for the bladder at the distance of 0.5 cm to be 16.3 % (range -35.33 to +39.37) At a distance of 1.5 cm, the deviation was 19.4% ranging from -49.48 to +30.39. For the rectum, they reported 23.1% deviation between TPS and film dose at a distance of 0.5 cm. (range -42.42 to +40.41) At a distance of 1.5 cm, the deviation was 22.5% ranging from -49.45 to +46.48 (Avevor, Tagoe, Amuasi & Fletcher, 2017). With the switch from LDR to HDR, there is a need to establish a dosimetric protocol for error detections, variation analysis, and verification of the HDR BT treatment system so as to improve the overall accuracy of treatment delivery. This work is therefore a further study based on the recommendations of Avevor, Tagoe, Amuasi & Fletcher 2017.

Scope and Delimitation

The data used in this research was collected at the NCRNM, Korle-Bu Teaching Hospital, Accra and all the dose measurements were done with the in-house phantom constructed as described in chapter three. Microsoft SPSS was used for modelling. Visual Studio codes were used to design the dose conversion model.

Organization of the Study

This thesis is arranged in a chronological order of five chapters. Chapter one begins with a short introduction that presents the problem under study describing the importance of the work. It also provides the context within which the problem is occurring pointing out knowledge gaps, and controversies to be resolved. Furthermore, chapter one gives relevant knowledge to the study and the objectives of the research. Chapter two reviews relevant literature on works significant to the research problem and also gives the theoretical framework of the study. Chapter three addresses the research design, materials used, data collection procedures, data processing analysis and various methods employed in arriving at the goal of the research. Chapter four is a compilation of the results obtained from the research and the discussion of these results. Summary, conclusions, recommendations and suggestions for further research are presented in chapter five giving an overview of the entire dissertation.

Chapter Summary

Cancer of the cervix is a leading cancer among women in Ghana (WHO, 2017). There are various treatment modalities available for the treatment of this type of cancer. BT treatment is a major treatment modality used for cervical cancer. It is a short distant treatment where small encapsulated radioactive

sources are placed within or near the volume to be treated. In BT treatment of the cervix, applicators are used to allow live-source implantation, which allows the radioactive sources to travel to the region of interest. HDR BT is a faster way of treating patients. However, one major challenge with HDR BT is the lack of laid down procedures for quality control measurements of the 3D dose distribution delivery.

Gafchromic films are the latest dosimeters for measuring dose distribution in intracavitary BT; however, there are few publications on HDR BT that make use these films as dosimeters. In treatment delivery for cancer of the cervix using HDR BT, careful planning and accuracy are major requirements. This is very important because of the critical organs (bladder and rectum) and healthy tissues that are in close proximity to the cervix. IVD is a QA technique and a practical way of checking dose delivery during BT. BT makes use of TPS which plans and calculates the doses that must be delivered to the treatment site. However, these TPS have shortcomings with the algorithm being used and thus leads to uncertainties in the BT treatment. IVD is therefore needed to check these uncertainties for effective treatment outcome. Other factors like organ movements and contouring do affect treatment outcome. Based on these uncertainties, the study seeks to verify the treatment delivery system, establish a dosimetric protocol and QA for patient and staff safety. The chapter contains detailed objectives of the study, relevance and justification, scope and delimitation and how the study has been organised.

CHAPTER TWO

LITERATURE REVIEW

Introduction

The degree of clinical accuracy required in BT for dose delivery to a patient has received great attention over the years. These considerations are generally based on differences in radiation response between tumors and normal tissues. This chapter addresses the need for precision in treatment delivery. The chapter also details the concepts and theoretical frameworks of high dose rate BT as it relates to the research being undertaken. The complications of the TPS being used for the BT treatment have also been outlined.

HDR BT

One major advantage of BT is that it delivers high dose to the target at the same time spares surrounding healthy tissues. With proper case selection and delivery technique, HDR BT has great promise when cases are properly selected with the right technique for delivery. This is because the short treatment times, avoidance of radiation exposure and patients need not to be on admission. Also, optimization of the dose distribution is achieved by varying the dwell time of the source at each dwell position using the single stepping source. Mistakes in HDR BT can be extremely harmful to patients due to short treatment times which do not permit time for correction; hence treatment delivery needs careful execution. The training of personnel engaged in the treatment is very crucial (Nag et al., 2000).

BT procedures were previously carried out by placing the radioactive source near or into the tumor directly (“hot”loading). This led to exposure of

radiations to the physicians performing the treatment. In order to reduce these hazards and increase the accuracy of treatment delivery, manually afterloaded techniques were introduced. In this technique, catheters, hollow needles or applicators were first inserted into the tumor, then loaded with the radioactive source.

Medical personnel and visitors are now being protected from radiation exposure by the introduction remote-controlled insertion. The treatment room that houses the patient is shielded with lead and with cameras mounted within, the medical physicist is able to control and monitor the treatment procedure from outside. Needles, catheters, or hollow applicators are then inserted into the cancerous region (tumor) and transfer tubes are used to connect the shielded radioactive source inside the HDR aferloader. A remote control is then used to draw the source which passes through the tube into the tumor. BT procedures that are remote-controlled can be carried out using low-dose-rate (LDR), medium-dose rate (MDR), or HDR techniques (Nag et al., 1993).

The usual dose rate employed in current HDR BT units is about 100-300 Gy/h. The use of remote-controlled BT (whether it is LDR, MDR, or HDR BT) eliminates the dangers of radiation exposure. Patient discomfort and applicator movements are minimized by the use of HDR, because treatment times are short which are done on outpatient basis. Also, modern HDR afterloaders employ the use of single stepping source which permits dose distribution optimization by varying the dwell time of the radioactive source at each dwell position. As much as optimization can aid in the distribution of the radiation dose, it must not be utilized as a substitute for an implant that is poorly placed.

Inappropriate examples of optimization strategies have been provided by Nag and Samsami (2000) which can result in suboptimal dosimetry plans and clinical challenges (Nag and Samsami, 2000).

General Considerations and Uncertainties Associated with BT

In BT treatment, the tolerance of the normal tissue is often the limiting factor for the dose that can be delivered to the patient. The relation between dose and biological effect is described by dose effect curves. For normal tissue complication, dose effect curve is generally steeper than for a local tumor control, and the same level of biological response is usually found at a higher dose level for normal tissue than for tumors (Larry, DeWerd, Mark, Rivard, & Hans, 2012).

The term accuracy is taken usually separately for clinical aspects and physics aspects. This is often associated with geometrical miss and dosimetrical deviations, respectively. From clinical studies, it was concluded by the International Commission on Radiation Units and Measurements (ICRU Report 24, 1976) that the available evidence for certain types of tumor points to the need for accuracy of ±5% in delivery of absorbed dose to a target volume if the eradication of the primary tumor is sought. Closer limits were considered virtually unachievable at the time of writing that report. In the ICRU report, no indication is given about the confidence level of this 5% value, that is, whether it concerns one or two standard deviations or an action level.

One decade later, Mijnheer, Battermann, and Wambersie, (1987) discussed the clinical observations of normal tissue reactions. These authors concluded that an increase in the absorbed dose of ±7% can result in observable

and unacceptable normal tissue complication probabilities. If information from one radiotherapy center is transferred to another, unacceptable risks are involved if the overall treatment in the absorbed dose is larger than ±7%. The authors have intimated that this value should be interpreted as twice the standard deviation of the absorbed dose. Therefore, they concluded that a total uncertainty of ±3. 5% (1 source distance) in the absorbed dose at the dose specification points is desirable and should be strived for in routine clinical practice (Mijnheer et al., 1987).

Similarly, Brahme, Chavauradra, and Landberg, (1988) in their study concluded that a relative standard deviation in tumor control probability for less than ±10%, and preferably less than ±5% is needed to have a reasonable probability of distinguishing the outcome from comparable studies with patient groups of a few hundred persons. To maintain a high quality of treatment, the loss in tumor control probability due to dose variations should not be more than 5% and preferably 3% to the target. When transformed into a recommended tolerance level for accuracy in dose delivery, a value of 3% relative standard deviation in the absorbed dose was proposed. The action level, above which it is recommended to work to improve the accuracy in dose delivery, is at a relative standard deviation of 5% (Brahme et al. 1988).

To achieve a 3.5% (1SD) in the physical dose delivery requires accurate and reproducible calibration of the treatment delivery machine and high precision in dose calculation procedures. These considerations form the basis of the many national and international recommendations for quality assurance of

equipment and audit procedures for radiotherapy treatments (Mijnheer et al., 1987).

There are significant patient-specific clinical uncertainties related to interfraction and intrafraction movement of both target and adjacent OARs. Individual patients will also exhibit variable radiation response characteristics related to both tumor and normal tissues. A final consideration and perhaps the greatest variable in clinical practices relates to the target and OAR delineation by the clinician with considerable interobserver and intraobserver variations seen. When the tumor or parts of it are not irradiated or not treated with the intended dose, the success of the therapy will be reduced drastically. In particular, in BT, it should be considered that treatments are often given in one or a very low number of fractions in comparison to the EBRT. For the dose delivery to a brachytherapy target volume, uncertainties will be encountered in contouring (interobserver and intraobserver variabilities), afterloader performance (both with spatial and temporary uncertainties), imaging (reconstruction, volume interpolation, fusion), and dose calculation in inhomogeneous media. At the patient level, there will be intrafraction and interfraction movements, organ motion, and swelling. (Brahme et al. 1988)

Dose Calculations in BT using TG-43 Formalism

Dosimetry in BT employs two main calculation methods for dose distribution calculation around the radioactive source. These are the Sievert integral and modular dose calculation models (TG-43). The commonly used method is the TG-43. This is because it makes use of the quantities measured in the medium to determine the dose rates. As of the year 2012, the international

standard for dose calculation in BT is the TG-43 formalism. This formalism was developed by AAPM Task Group No.43 and published in 1995. Most treatment planning software vendors have implemented the TG-43 formalism. (Nath et al., 1995)

TG-43 Formalism

In 1995, the AAPM TG-43 published a report on the dosimetry of sources used in interstitial BT. In this report, there was an introduction of dose calculation formalism that made use of new quantities like air kerma strength (S_K), dose rate constant (Λ), geometry function (G (r,θ)), radial dose function (g (r)), and anisotropy function (F (r,θ)). These new quantities introduced, take into account the spatial distribution of radioactivity within the source, geometry, scattering in water surrounding the source and self-filtration of the source (Nath et al., 1995). The absorbed dose rate distribution around a sealed BT source according to this formalism at point P with polar coordinates (r, θ) can be determined using the following formalism:

According to the protocol as shown in equation 1, the dose rate $(\dot{D})$ at a point $P(r,\theta)$ in water can be expressed as

$$\dot{D}(r,\theta) = \Lambda\, S_k \frac{G(r,\theta)}{G(r,\theta)}\, g(r) F(r,\theta) \qquad (1)$$

where r is the distance from the origin to the point of interest P and θ is the angle with respect to the long axis of the source. θ_0 defines the source transverse plane and is equal to $\theta/2$ radians as shown in Figure 1, S_k is the air kerma strength of the source, Λ is the dose rate constant in water, $G(r,\theta)$ is the

geometry function, $g(r)$ is the radial dose function, and $F(r,\theta)$ is the anisotropy function.

Air Kerma Strength

Air kerma strength, S_k, as shown in equation 2 accounts for BT source strength and is defined as the product of air kerma rate at a calibration distance (d) in free space, this is often assumed to be 1 m, along the transverse axis of the source and the square of the distance (d^2),

$$S_k = k(d)d^2 \quad (2)$$

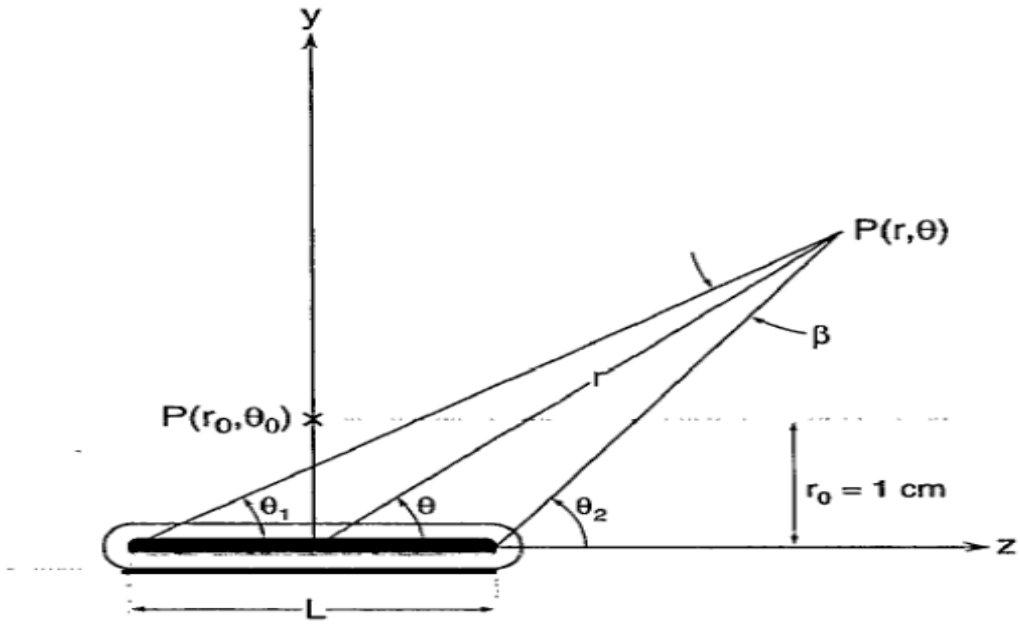

Figure 1: BT Sources Geometry used in TG-43 formalism

The unit of S_k is $U(1U = 1\ cGy\ cGycm^2h^{-1})$

Source : Nath et al., 1995

Dose Rate Constant

Dose rate constant, (Λ), is defined as dose rate at 1 cm along transverse axis ($\theta_o = \pi/2$) of the source per unit air kerma strength (U) in a water phantom. Dose rate constant of a BT source is derived as:

$$\Lambda = \dot{D}(r_{o,}\theta_o)/S_k \quad (3)$$

Λ has units of $cGyh^{-1}U^{-1}$. As indicated in the AAPM TG-43 report, the effects of the spatial distribution of radioactivity within the source, geometry, scattering in water surrounding the source and self-filtration of the source are considered by this parameter.

Geometry Function

Spatial distribution of radioactivity within the source and the slump of the photon fluence with distance from the source are considered by Geometry function, G (r, θ), with the unit ofcm^{-2}. For point sources, the geometry function indicates the inverse square law.

$$G(r,\theta) = \begin{cases} r^{-2}, point\ source \\ \dfrac{\beta}{Lr\sin\theta}, Line\ source \end{cases} \quad (4)$$

As it is shown in Figure 1, L is the source's active length and $\beta = \theta_2 - \theta_1$ is the angle covering active source from the point(r, θ).

Radial Dose Function

Radial dose function, $g(r)$, takes into account slump of dose rate arising from absorption and scattering in the medium on the transverse axis of the source and can be affected by self-filtration, and encapsulation.

According to AAPM Task Group 43, radial dose function is defined as:

$$g(r) = \frac{\dot{D}(r,\theta_o)G(r,\theta_o)}{\dot{D}(r,\theta_o)G(r,\theta_o)} \quad (5)$$

Equation 5 is defined just on transverse axis, which means $\theta_o = \frac{\pi}{2}$.

Anisotropy Function

Angular variation of photon absorption and scattering in the encapsulation and the medium at different distances and angles from the source is taken into account by anisotropy function, $F(r,\theta)$

$$F(r,\theta) = \frac{\dot{D}(r,\theta)G(r,\theta_o)}{\dot{D}(r,\theta_o)G(r,\theta)} \quad (6)$$

where $\theta o = \frac{\pi}{2}$

Like $g(r)$, applying geometry function in equation 6 is suppressing the effect of inverse square law on the dose distribution around the source.

Several studies were carried out after the TG-43 formalism was published by the AAPM to determine the dosimetry parameters of BT sources. The limitations of the formalism and its advantages were verified (Liu et al., 2004; Meigooni et al., 2003, 2005; Melhus & Rivard, 2006; Parsai et al., 2009; Rivard et al., 2004, 2007; Sina et al., 2007, 2009, 2011; Song & Wu, 2008; Zehtabian et al., 2010).

TG-43 Updater Version 1

In 2004, Rivard et al., published an updated version of TG-43 (named TG-43U1), in which they added several corrections to the original protocol as depicted in equation 7:

$$\dot{D}(r,\theta) = \Lambda S_k \frac{G_L(r,\theta)}{G_L(r_O,\theta_o)} g_L(r) F(r,\theta) \quad (7)$$

Equations 9 and 10 includes additional notation compared with the corresponding equation 1 in the original TG-43 formalism, namely the subscript ‘‘L’’ has been added to be used for geometry function and it denotes the line source approximation. The S_k definition in TG-43U1 differs in two key ways from the original AAPM definition of S_k.

The quantity Air-kerma strength, S_k as shown in equation 8, is the air-kerma rate, $K_\delta(\mathrm{d})$, in vacuo and due to photons of energy greater than δ, at distance d from the source, multiplied by the square of the distance which should be located on the transverse plane of the source. This distance (d) can be any distance large relative to the maximum linear dimension of the radioactivity distribution, typically of the order of 1 meter.

$$S_k = K_\delta(d)d^2 \qquad (8)$$

When S_k is obtained experimentally, the measurements should be corrected for photon attenuation and scattering in air and any other medium interposed between the source and detector, as well as photon scattering from any nearby objects including walls, floors, and ceilings (Rivard et al., 2004).

The low-energy or contaminant photons (e.g., characteristic X-rays originating in the outer layers of steel or titanium source cladding) would increase $K_\delta(d)$ without contributing significantly to dose at distances greater than 0.1 cm in tissue. Therefore, a cutoff energy δ (i.e. 5 keV for low-energy photon emitting brachytherapy sources) should be considered in calculating $K_\delta(d)$.

In TG-43U1 dose-calculation formalism, a subscript X has been added to the notation $g(r)$ as shown in equation 9 and geometry function of the original protocol. This protocol presents tables of both $gp(r)$ (point source

approximation) and $gl(r)$ (Line source approximation) values; $gx(r)$ is equal to unity at $r_o = 1\ cm$.

$$g_X(\mathrm{r}) = \frac{\dot{D}(\mathrm{r},\theta_O)G_X(r_O,\theta_o)}{\dot{D}(r_O,\theta_o)G_X(r,\theta_o)} \tag{9}$$

The 2D anisotropy function, $F(r,\theta)$, is defined as:

$$g_X(\mathrm{r}) = \frac{\dot{D}(\mathrm{r},\theta_O)G_X(r_O,\theta_o)}{\dot{D}(r_O,\theta_o)G_X(r,\theta_o)} \tag{10}$$

The definition of 2D anisotropy function is identical to the original TG-43 definition, other than inclusion of a subscript L, which is added to geometry function.

Generally, the TG-43U1 includes:

I. A revised air-kerma strength $S_k$definition.

II. b. Not using apparent activity for specification of source strength

III. c. Distance-dependent one-dimensional anisotropy function

IV. d. Guidance on extrapolating tabulated TG-43 parameters to long and short distances

V. e. Minor correction of the original protocol and its implementation (Rivard et al., 2004).

Limitations of TG-43 and TG-43U1 Dose Calculation Formalisms

The dosimetry parameters employed by the TG-43 and TG-43U1 dosimetry formalisms are obtained for BT source which is single. Its location is at the center of a fixed volume, homogeneous liquid water phantom (Nath et al., 1995; Rivard et al., 2004, 2007). It must be noted that these algorithms do not

take into account several factors that affect the high-quality clinical outcomes (Rivard et al., 2009).

Inhomogeneities

The TG-43 dose algorithm assumes that dosimetry is carried out in a uniform medium (water) phantom. Therefore, inhomogeneities like bony and soft tissues have not been accounted for in the formalism. Inhomogeneities are very crucial especially in certain implant regions like the head, neck and lung. The dosimetry parameters of the BT source can be altered as a result of these existing inhomogeneities.

Inter-Source Attenuation (ISA) and Applicator Influence

ISA is very significant in clinical situations where many BT sources are used in patient treatment. The effect of applicators and other BT sources (ISA) on dosimetry is not considered when using the TG-43 formalism inside a homogenous water phantom. (Markman, Williamson, Dempsey, and Low, 2001). The structures of BT sources and the applicators are composed of materials with densities and atomic numbers which are not comparable to that of water. Materials whose atomic numbers are very high have photoelectric effect more pronounced in them so the parameters of the TG-43 are different when the effects of the shields in the applicator and other sources are considered when compared to that of water without consideration of these factors (Rivard et al., 2009). For easy identification, radio-opaque markers (i.e. silver markers $Z = 47$) are used during post implant CT localization in LDR BT. This can result in some discrepancies when using the TG-43 dose calculation protocol. When the applicator in use is composed of materials whose atomic

numbers are not comparable to that of water (i.e. stainless $steel = 26$), this would lead to certain degree of error.

The difference between the TG-43 parameters of BT sources in applicator materials is highly dependent on the energy of BT sources. Consequently, not considering the ISA and the applicator effects are more pronounced for BT sources emitting low energy gamma rays.

Several researchers have investigated the effects of shields of some other materials (like radio opaque markers, components of the applicator and other sources). They have reported that the radiation attenuation in such materials can affect the dose distribution around the BT sources and therefore needs to be taken in consideration (Fragoso, 2004; Fragoso et al., 2004; Parsai et al., 2009; Perez-Calatayud et al.,2004, 2005; Sina et al., 2007, 2011; Siwek et al., 1991).

Units of Measurement in Dosimetry

Radiation effects and its measurements need several specifications of the radiation field at the region or point of interest. Dosimetry involves methods for a quantitative determination of the amount of energy deposited by directly or indirectly ionizing radiations in a given medium. Some units of measurement and quantities have been defined in this chapter for describing radiation beam, commonly used dosimetric quantities and their units.

Photo Fluence and Energy Fluence

The following quantities are used to describe a mono-energetic ionizing radiation beam: particle fluence, energy fluence, particle fluence rate and energy fluence rate. These quantities are usually used to describe photon beams and may also be used in describing charged particle beams.

Particle Fluence

Particle fluence as defined in equation 11 is a very important basic quantity, involving the number of particles per unit area. Suppose N particles pass through an area A. The particle fluence for the area A is defined as

$$\Phi = \frac{N}{A} \tag{11}$$

which is usually expressed in units of m^{-2} *or* cm^{-2} (ICRU 2011).

Energy Fluence

The energy fluence, ψ, as defined in equation 12 is the rate of change of dR by dA, where dR is the radiant energy incident on a sphere of cross sectional area, dA

$$\Psi = \frac{dR}{dA} \tag{12}$$

The unit of energy fluence is J/m^2 (ICRU, 2011).

Particle Fluence Rate

The particle fluence rate $\dot{\Phi}$, as defined in equation 13 is the the rate of change of dΦ by dt, where dΦ is the increment of the fluence in time interval dt

$$\dot{\Phi} = \frac{d\Phi}{dt} \tag{13}$$

It has units of $m^{-2}s^{-1}$ (ICRU, 2011).

Energy Fluence Rate

The energy fluence rate $\dot{\Psi}$ (also referred to as intensity) as defined in equation 14 is the rate of dψ by dt, where dψ is the increment of the energy fluence in the time interval dt,

$$\dot{\psi} = \frac{d\Psi}{dt} \tag{14}$$

The unit of energy fluence rate is W/m^2 or $Jm^{-2}s^{-1}$(ICRU, 2011).

Exposure

Exposure measures the amount of ionization in air produced by X- or gamma-ray radiation. Its SI unit is the coulomb per kilogram(C/kg). Exposure is measured under conditions of electronic equilibrium. For photon energies above 3 MeV, the ranges of secondary electrons become a significant fraction of the photon attenuation lengths and the departure from equilibrium may be significant. Thus, exposure is not defined above photon energies of 3 MeV (Attix, 1998).

Exposure Rate

The exposure rate as shown in equation 15, $\dot{X}$, is the rate of change of $d\dot{x}$ by dt, where $d\dot{x}$ is the increment of exposure in the time interval dt, thus:

$$\dot{\mathrm{X}} = \frac{d\dot{\mathrm{X}}}{dt} \tag{15}$$

The unit is $C\ Kg^{-1}S^{-1}$ (ICRU, 2011).

Kerma

Kerma as defined in equation 16, is an acronym for Kinetic Energy Released per unit Mass. It is a non-stochastic quantity applicable to indirectly ionizing radiations such as photons and neutrons. It quantifies the average

amount of energy transferred in a small volume from the indirectly ionizing radiation to directly ionizing radiation without concerns to what happens after this transfer. It is the mean energy transferred from the indirectly ionizing radiation to the charged particles (electrons) in the medium dt $d\bar{E}_{tr}$ per unit mass dm:

$$K = \frac{d\bar{E}tr}{dm} \tag{16}$$

The unit of kerma is joule per kilogram (J/kg). The name for the unit of kerma is the gray (Gy), where 1 Gy = 1 *J/kg* (ICRU, 2011).

CERMA

CERMA is the Converted Energy per unit Mass. It is a non-stochastic quantity applicable to directly ionizing radiations such as electrons and protons. It quantifies the average amount of energy converted in a small volume from directly ionizing radiation, such as electrons and protons in collisions with atomic electrons without concerns about what happens after this transfer.

$$C = \frac{dE_c}{dm} \tag{17}$$

where dE_c is the converted energy and dm is the mass.

CERMA as shown in equation 17 is measured joule per kilogram (J/kg). KERMA is measured in Gy. Cerma differs from kerma in that: Cerma involves the energy lost in electronic collisions by the incoming charged particles. Kerma involves the energy imparted to outgoing charged particles (ICRU, 2011).

Absorbed Dose

Absorbed dose as defined in equation 18 is a non-stochastic quantity. It is applicable to both directly and indirectly ionizing radiations. For indirectly

ionizing radiation, the energy is imparted to matter in a two-step process. In the first step (resulting in kerma), the indirectly ionizing radiation transfers energy as kinetic energy to secondary charged particles. In the second step, these charged particles transfer a major part of their kinetic energy to the medium (finally resulting in absorbed dose) and loose some of their energy in form of radiative losses (bremsstrahlung, annihilation in flight).

The absorbed dose is related to the stochastic quantity energy imparted. The absorbed dose (D) is defined as the mean energy **ε** imparted by ionizing radiation to matter of mass m in a finite volume V by

$$D = \frac{d\varepsilon}{dm} \tag{18}$$

The energy imparted ε is the sum of all the energy entering the volume of interest minus all the energy leaving the volume, taking into account any mass-energy conversion within the volume. Pair production for instance decreases the energy by 1.022 MeV, while electron-positron annihilation increases the energy by the same amount. It must be noted that because electrons travel in the medium and deposit energy along their tracks, this absorption of energy does not take place at the same location as the transfer of energy described by kerma. The unit of absorbed dose is joule per kilogram (J/kg). Its unit of measurement is referred to as Gray (Gy), (ICRU, 2011).

Equivalent Dose

The equivalent dose in tissue T is given by the expression in equation 19:

$$H_T = \sum W\, D_{T,R} \tag{19}$$

where $D_{T,R}$ is the absorbed dose averaged over the tissue or organ T, due to radiation R.

In radiological protection, it is the absorbed dose averaged over a tissue or organ. It is weighted for the radiation quality of interest. The weighting factor is called the radiation weighting factor, W_R and is selected for the type and energy of the radiation incident on the body. This weighted absorbed dose, called the equivalent dose, is strictly a dose. The unit of equivalent dose is the joule per kilogram with the special name of sievert (Sv)(ICRU, 2011).

Effective Dose

The effective dose is the sum of the weighted equivalent doses in all the tissues and organs of the body. It is given by the expression in equation 20:

$$E = \sum W_T \, . H_T \qquad (20)$$

where H_T is the equivalent dose in tissue or organ T and W_T is the weighting factor for tissue T. The relationship between the probability of stochastic effects (primarily cancer and genetic effects) and equivalent dose is found to depend on the organ or tissue irradiated. The effective dose combines the equivalent doses to the various body organs and tissues in a way which correlates well with the total stochastic effects (ICRU, 2011).

Gafchromic Films

Introduction

Gafchromic EBT film has special characteristics that are meant for utilization for medical physicist and dosimetrist working in the radiotherapy centers. In common with previous Gafchromic films, EBT film is self-developing, but it also incorporates numerous improvements in ISP's radiochromic film technology (ISP, 2009). Some of these improved features include:

I. Dose range 1 cGy – 800 cGy; EBT film is ten times more sensitive than its previous generation Gafchromic HS film and MD-55
II. Energy independent from the keV range into the MeV range
III. Uniformity better than 1.5%
IV. Larger with two different formats; 8"x10" and 14"x17"
V. Faster and lower post-exposure density growth
VI. Will withstand temperatures up to 70 ºC

Configuration and Structure of Gafchromic EBT

Gafchromic EBT is made by laminating two coatings. The coatings are manufactured to a single specification. The EBT laminate is identified by its batch number. At all steps of the manufacturing process the intermediates and components are identified by their batch numbers. The configuration of Gafchromic EBT film is shown in Figure 2.

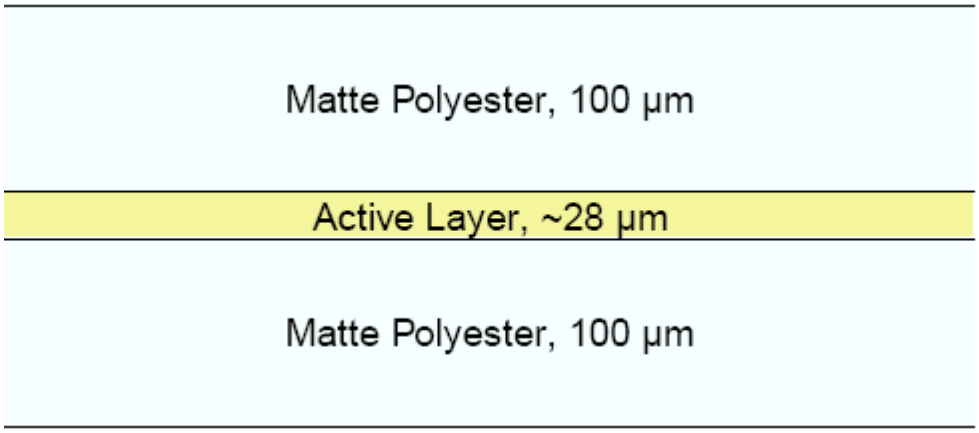

Figure 2: Gafchromic EBT3

Source: ISP, 2011

Gafchromic EBT Dosimetry Film Characteristics

The Gafchromic film has been designed with high sensitivity to measure the absorbed dose of high-energy photons used in IMRT in the 1 cGy to 800 cGy dose range. The response to photons has been found to be energy-independent in the MeV range and measurements at energies down to about 30 keV reveal that the sensitivity changes by less than 10% (ISP, 2009).

Optical Density to Dose Relationship

Coloration occurs when the film is exposed to ionizing radiation. The coloration is as a result of attenuation of some of the visible light coming through the developed film, making its appearance 'grey'. The reduction in light passing through the film is a measure of its 'blackness' or 'optical density' (OD).

In film dosimetry, an important assumption is that the dose to the film is reflected in the resulting optical density of that film. This relationship can be expressed as follows:

$$OD = log_{10}\left(\frac{I_o}{I}\right) \quad (21)$$

where I_O is the light intensity with no film present and I is the light intensity after passing through the film. Since I_O/I has an exponential relationship to the dose, the optical density is appropriately linear with dose. The wide use of the film as a dosimeter is due to acceptance of this relationship. The Gafchromic film has an advantage over other dosimeters such as its mapping ability; dose can be analyzed on area on the film unlike other dose detectors where dose is measured at a point. With the Gafchromic film, a 2D OD fluence map can be achieved. Film dosimetry results can be verified by a second detector (e.g. point dose measurements using an ionization chamber) to provide useful dosimetric information.

Potential Variables of Film Dosimetry

The major concern in using the Gafchromic film as a detector is the fragility of the optical density and how it relates to the dose. The sensitivity of the film to the dose can be used to express this relationship. There are discussions that suggest that the sensitivity of the film is affected by variables such as; film plane orientation, the beam energy of the photon, experimental design, post-irradiation conditions, emulsion differences between film batches, and densitometer types used or more broadly the analysis tool (software).

Phantoms

Dosimetry investigations in radiotherapy involve mostly the use of phantoms. This is because the Perspex materials used in the construction of these phantoms mimic the anatomical properties of the human tissues. Phantoms therefore, represent the human body and have been in use for investigations as far as treatments with radiations are concerned. In 1896, after Wilhelm Conrad Rontgen discovered x rays, her wife's hand was first used for the world's first ever x ray images. The effects were harmful due to high doses of radiation received and that resulted in erythema and cell squamation. As a result, nobody was willing to volunteer for radiation exposures meant for experimental purposes. This led to the development of phantoms by physicists to simulate patients for dose measurements and to also verify the effectiveness of the system.

In designing a phantom, the materials are selected based on the intended use of the phantom. The thickness of the material, the size, shape of the phantom fabricated will depend on what it is fabricated for. Phantoms that are meant to use dosimeters like film or TLDs also have different designs and fabrications. Every material used in the phantom design must simulate human tissues, but the properties of these materials vary with the amount of radiation energies incident upon them. The materials will be tissue equivalent based on a range of energies they receive; they cannot be tissue equivalent over all range of energies.

Several characteristics can be used in the measure of tissue equivalence of the phantom such as the physical density (ρ) and effective atomic number (Z_{eff}). These parameters provide information on the physical properties of the

material but do not provide much insight about its radiological properties. The electron density of the material is a parameter that provides insight into how the material will behave in a radiation environment. The commonly accepted and mostly widely used parameter that is used to measure the tissue equivalence of a material is the mass energy-absorption co-efficient (μ_{en}/ρ). This is because it gives indication as to how much energy is deposited in the tissue of interest. There are materials available that simulate tissue very accurately but one must keep in mind that the radiological properties are of much concern and these properties also depend highly on the amount of radiation energy incident upon it (Dewerd and Kissick, 2014).

Phantoms for dosimetry are used when there is a need to simulate the conditions of a procedure to measure dose at certain points of interest. It is dangerous to place a human being in a beam for dose measurements. It is even more impractical to place radiation dosimeters in the human to measure dose distribution. This was what led to the construction of Dosimetry phantoms which holds water and slabs of tissue equivalent materials were designed to hold the dosimeters in place for dose distribution measurements in tissues without unnecessary exposure of radiations to persons involve in the process.

Dosimetry in Water Phantoms

The characteristics of radiochromic films such as physical toughness, energy dependence and automatic development has given it an advantage for use in dosimetry over other solid-state detectors and the radiographic film. For medical and industrial applications, dosimetric evaluations must be carried out in water (liquid water environments) for accurate determination of doses. There

are different types of constructions of the radiochromic film. Depending on the type of film used for water dosimetry, the properties may vary (AAPM, 1998).

There are a few challenges which may be encountered in water dosimetry such as: (a) the effects of water on the film dosimeter during exposure (neither TLDs nor radiographic films are suitable for water dosimetry without some sort of protective coating placed over them); and (b) the film response due to the orientation with respect to the beam direction in the water. A lot of detectors depict directional dependence when exposed to radiation beams. This is because there are variations which are microscopic on the path of the radiation beam before interaction measurement point within the detector (AAPM, 1998).

Densitometry Systems: Evaluation of Radiochromic Film Dose

Ideally, information from the analogue film must be converted into a digital form for accurate dose quantification. A 2D data set can be obtained from a digitized film; providing information on the film coloration due to the dose deposited in that region. Although theoretically the ultimate limit of resolution is the dimension of each ‘‘activated’’ molecule on the film, practically the spatial resolution of the data set is limited by the sampling rate set in the scanner/densitometer software. Sometimes it is more useful to sample at a rate which is consistent with the data required for a specific patient treatment and the spatial resolution of the planning software used to calculate the patient absorbed dose during therapy. In this way, the planning data set and the dosimetry data set can be superimposed and a comparison made between the expected and actual dose. To maximize the confidence in the measured dose, it is necessary to establish an accurate relationship between the dose and the pixel

value i.e. a correct change in the pixel value for the given required doses. The pixel value is equivalent to the light intensity transmitted through the irradiated film. This can be expressed as follows

$$OD = -log_{10}\left(\frac{Mean\ Pixel\ Value_{exposed}}{Mean\ Pixel\ Value\ _{unexposed}}\right) \quad (22)$$

Films with favorable characteristic curve must be selected (i.e. dose response) or the films can be exposed to radiation appropriately (to the most effective dose) to achieve this, so that the pixel values being measured falls within the linear portion of the dose response curve (AAPM, 1998).

The accuracy needed requires a correct bit level of data acquisition. An 8-bit software analysis tool (256 resolutions) would be inadequate if it does not allow the accuracy level required to be seen. By using 256-bits of information, a 1-pixel change is approximately 0.5%. This may not be adequate. As such, normally scientists use 12- or 16-bit scanning resolution for film analyses or use the direct analogue signal for data processing (AAPM, 1998).

Film Sensitivity and Calibration

In calibrating a radiochromic film, a large well-characterized uniform radiation field must be used. The film must be positioned in such a way that it falls on the central portion of a large photon beam (such as a 40 cm × 40 cm) at depth of interest (preferably ≥5 cm). Another dosimeter should be used to determine the beam calibration characteristics (e.g. ionization chamber), to permit direct calibration of the film in terms of absolute dose within the dose range of interest (AAPM, 1998). Relationship between film response and absorbed dose must be established and plotted as a curve often called calibration

curve (or sensitometric curve). The slope of the calibration curve decreases as dose increases. The calibration curve can provide information for conversion of film response to dose and vice versa. The relationship between dose and film response can also be tabulated. The change in film response per unit absorbed dose can be represented by a single number for a net optical density up to 1.0. This number, defined here as film average sensitivity, is the average change in response (i.e., readout) per unit absorbed dose calculated over the lower, most linear portion of the calibration curve. This number depends on one or more of the following: (1) the wavelength used for readout, (2) the particular densitometer used for readout, (3) film batch, (4) the delay between irradiation and readout, (5) beam quality of the calibration source, and (6) other factors such as temperature and humidity. Figure 3 shows the dose-response curves of MD-55-1 film measured by a laser densitometer (632.8nm) for three radionuclides. The square, circle, and plus symbols are for ^{125}I, ^{137}Cs, and ^{60}Co, respectively.

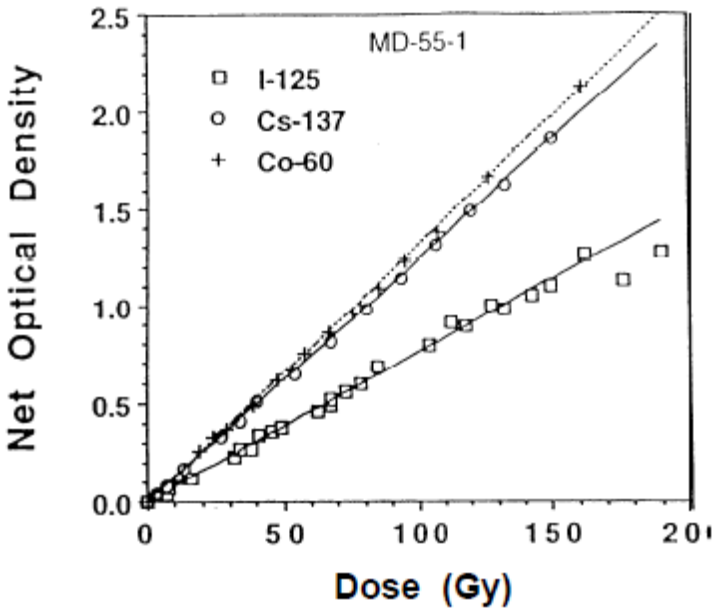

Figure 3: The Dose-Response Curves Of MD-55-1 Film Measured by a Laser Densitometer (632.8 Nm) for three Radionuclides, the Square, Circle, and plus Symbols are for 125I, 137Cs, and 60Co, respectively; the dotted and solid lines near the symbols indicate

Source: (AAPM Report 63, 1998).

Film Scanning

When using the film in dose measurement, an indirect method is employed. A calibration curve is required to convert the film response or optical density (OD) values to doses.

Scanning orientation and scanner uniformity are two main factors that do affect the accuracy and precision in obtaining accurate optical density values. These factors can give higher percentage difference when measuring point doses. The effects of film orientation have been discussed by some researchers and their reports well documented. The scanning of these films was done in

portrait orientation consistently to reduce the effect of orientation (Rink, Vitkin, & Jaffray, 2005, Saur and Frengen, 2008, Zeidan, et al, 2006, Martisikova, Ackermann and Jakel, 2008).

Richley et al have also reported that the manufacturer recommends scanning be done in portrait, so that the short side of the film which agree almost exactly to the coating direction of the film is parallel to the direction of the scanning. (Richley, John, Coomber, and Fletcher, 2012). The uniformity of the scanner depends on the orientation of the film because of the different light scatter conditions that are established as a result of the film active component structure. In order to get rid of the effect of light scattering, to achieve the best uniform response, films should be kept in the same location and the regions of interest on the film must be close to the centre area of the scan bed (Richley, John, Coomber, and Fletcher).

Advantages of Gafchromic Films

I. Gives permanent absolute values of absorbed dose with an acceptable accuracy and precision.
II. Film has a high spatial resolution
III. Ease of handling and data analysis.
IV. Large area dosimetry: especially for electron beam.
V. Do not require chemical processing.

Beam Calibration

Absorbed Dose to Water Phantom

In this research, the absorbed dose $D_{w,cal}$ was determined using the proposed method by the IAEA Technical Report Series TRS398 (IAEA, 2000). The dosimeter reading M, with $N_{d,w}$ calibration factor for cylindrical chamber calibration in cobalt-60 beam gave the absorbed dose to water

-temperature correction factor where P_o and T_O are respectively the pressure and temperature of the phantom at the reference depth in water as

$$D_{w,cal} = M \times N_{d,w}\ (Gy/min) \tag{23}$$

$$M = M_l \times K_{TP} \times K_{pol} \times K_{ele} \times K_{sat} \tag{24}$$

where, $M_{l=}\left(\frac{M_+}{min}\right)$ is the uncorrected dosimeter reading in nC/min.

$K_{TP} = \left(\frac{273.2+T}{273.2+T_O}\right) \times \frac{P_O}{P}$, is pressure-temperature correction factor where P_o and T_o are respectively the pressure of the room and temperature of the air in the chamber cavity at the reference calibration conditions. P and T are the pressure and temperature measured during the experiment respectively.

$K_{pol} = \left(\frac{|M_+|+|M_-|}{2M}\right)$ is the polarity correction factor where M_+ and M_- are the electrometer readings at the voltage $+V_1$ and $-V_1$ respectively; M is the absolute value of M_+ for which voltage in the chamber was calibrated. These readings are measured in nanocoulomb (nC).

K_{ele} is the dimensionless Electrometer calibration factor.

$K_{sat} = \left(\frac{\left({}^{V_1}/_{V_2}\right)^2 - 1}{\left({}^{V_1}/_{V_2}\right)^2 - \left({}^{M_1}/_{M_2}\right)} \right)$, is a dimensionless recombination correction factor where

V_1 is the normal polarizing voltage, and V_2 is the reduced polarizing voltage.

$V_1 > V_2$, M_1 and M_2 are the readings at V_1 and V_2 respectively in (nC).

The Manchester System of Dose Prescription

The NCRM uses the Manchester system of intracavitary BT practices. This system was developed to deliver a consistent dose to a tumor volume. In this system, doses are prescribed to Point A. Point A is defined to be 2 cm superior to the external cervical (or cervical end of the tandem), and 2 cm lateral to the cervical canal. Ideally, a point A represents the location where the uterine vessels cross the ureter. It is believed that the tolerance of these structures is the main limiting factor in the irradiation of the uterine cervix. Dose to Point A is prescribed only when tandems are used together with the ovoids. In procedures where only ovoids are used, doses are prescribed to the surface of the ovoids and 0.5 cm from the surface of the ovoids.

Chapter Summary

HDR BT, a major treatment modality for carcinoma of the cervix has been extensively discussed in this chapter. The tolerance of normal tissue during treatment is a major limiting factor in the treatment of the disease using HDR BT. The TPS makes use of TG-43 formalism; an algorithm developed by the AAPM. This algorithm has several challenges which make accuracy in dose delivery quite challenging.

The algorithm has been extensively discussed in this chapter and its challenges also outlined. Reports from several investigators relating to this study have been discussed in this chapter. The unit of measurement in dosimetry presented by the ICRU (2011) has also been discussed in the chapter.

Gafchromic film is the latest type of radiochromic film being used in radiotherapy dosimetry. It has several advantages that make it user-friendly and easy in handling. This type of film is colorless with a nearly tissue equivalent composition which makes it suitable for dose measurements in BT.

The TRS 398 which is the IAEA (2000) proposed protocol for beam calibration has been discussed in this chapter. The TRS 398 was used in calibrating the films for measurements. There is a relationship between the ionizing radiation that passes through the film with respect to dose. In order to measure the dose received by the film, the optical density, which is the attenuation of some visible lights passing the film is calculated and converted to dose using the calibration equation generated from the calibration. In the treatment of the cancer of the cervix, Fletcher suites of applicators are used for treatment procedure. These applicators have some effects on the dose delivered. The chapter contains the discussions of these applicators and reports from other investigators. The NCRNM uses the Manchester system of dose prescription and this has also been well documented.

CHAPTER THREE

RESEARCH METHODS

Introduction

This chapter provides the relevant information on the experimental and construction processes of the study. The calibration, measurement procedures and dosimeter (Gafchromic films) that were used are described in this chapter. Absorbed dose to critical organs (bladder and rectum) in BT treatment can be determined using varying techniques. In this study a water phantom was designed constructed for dose distribution measurements. Gafchromic films were used in measuring the doses to various points. The construction process of the phantom has been outlined. For quality assurance purposes, the Gafchromic films used in measuring the doses to the rectal and bladder points were calibrated; the outlines have been indicated in this chapter. The dose measurements were carried out using the constructed phantom.

Materials

The following materials and equipment were used in the study. Polymethyl Methacrylate (PMMA) sheets, locally constructed water phantom, tape measure, Cobalt 60 teletherapy machine, PTW water phantom (type 267), MP1 Manual Water Phantom, ionization chamber, electrometer, Gafchromic EBT3 films, EPSON Stylus C× 5900 Scanner, ImageJ Software, Multi sourced High Dose Rate (HDR) afterloader BT system, Fletcher suite applicators, Reconstruction box, HDR-plus treatment planning system, Mobile C-arm fluoroscopic X-ray unit, SPSS Statistical tool, Visual Basic Studios software.

Therathron Equinox 100 Cobalt - 60 Teletherapy Unit

Teletherapy treatment machines are Gamma ray emitting treatment units. In this study the Therathron Equinox 100 Cobalt – 60 of serial number 2771 manufactured by Best Theratronics (Canada) was used. At the time of its installation it had an initial source activity of 399.0 TBq. This was determined by the Nordion Inc Canada; manufacturer of the source on 1st August 2013. The reference beam output in water at the depth of maximum dose (0.5 cm with the water) is 189.49 cGy/min. This was measured on 12th Dec 2013. The cobalt 60 sources are encapsulated with high activity within the treatment head of the teletherapy machine with a diameter of 2 cm and length 4 cm. (Canadian Nuclear Safety Commission, 2012).

A pneumatically driven linear source drawer mechanism has been designed to move the source between the fully shielded and fully exposed positions. In order for the source to cycle from the fully shielded to the fully exposed positions and back for minimum of three times in 30 seconds, a large air reservoir is provided to aid this movement. If the air pressure drops below a preset limit, the source is automatically returned to or retained in the fully shielded position. In the event of a power failure, the source automatically returns to its fully shielded position. The Theratron Equinox, as shown in Figure 4, is designed to minimize leakage in accordance with IEC 60601-2-11 standards. The Cobalt-60 source emits two gamma rays having energies of 1.17 MeV and 1.33 MeV with a mean energy of the radiation emitted by the source is 1.25 MeV

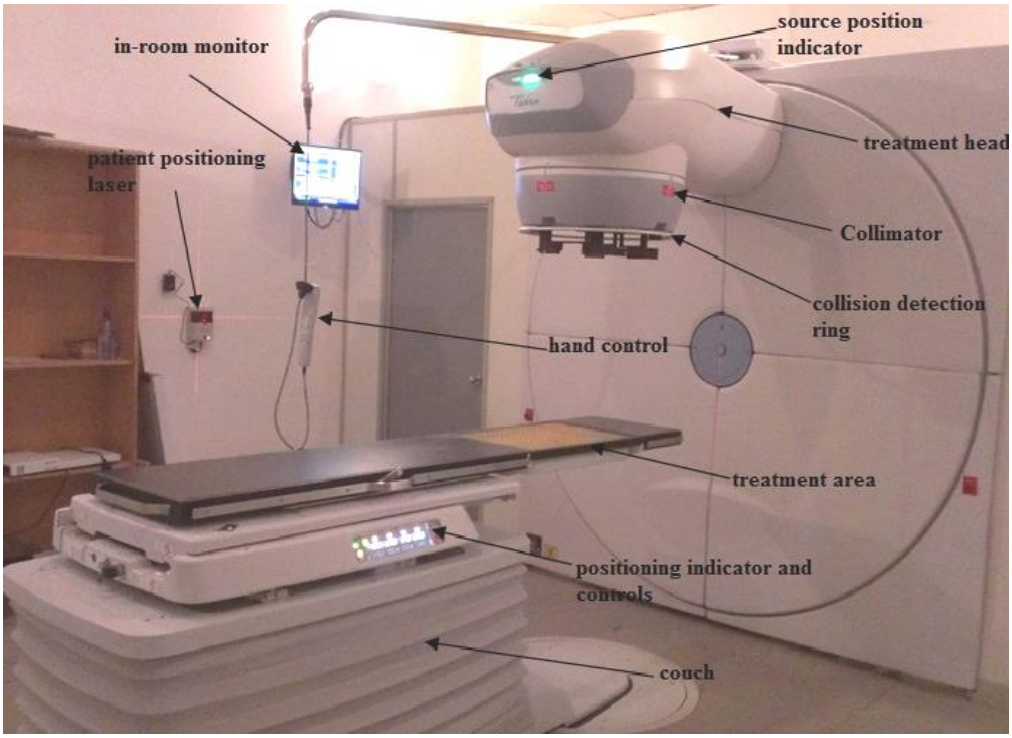

Figure 4: Therathron Equinox 100 Cobalt - 60 Teletherapy Unit

One Dimensional Manual Water Phantom

In this study a one-dimensional manual water phantom as shown in figure 5 was used to calibrate the Gafchromic EBT3 films. The MP1 was also used to access the quality of the doses and to also determine the absolute doses in line with standard dosimetric protocols. The MP1 was also used to access absorbed dose at reference points to meet the TRS 398 protocols. The vertical moving range of the MP1 is 254 mm and external horizontal dimension of 320 mm × 370 mm. In order to drain the water in the phantom after use, a tap is made at the bottom of the phantom to aid drainage.

Figure 5: One Dimensional Manual Water Phantom

Ionization Chamber

Ionization chambers incorporate three electrodes, which define the chamber sensitive air volume. The sensitive air volume is typically of the order of 0.1 to 1 cm^3 in ionization chambers used for the calibration of clinical photon and electron beams. The three electrodes are the: polarizing electrode, which is connected directly to the power supply; measuring electrode, which is connected to ground through the low impedance electrometer to measure the charge or current produced in the chamber sensitive volume; guard electrode, which is directly grounded and serves two purposes. The guard electrode defines the chamber sensitive volume and prevents the measurement of chamber leakage currents.

A cylindrical farmer type ionization chamber, model PTW31002-1505 manufactured by PTW Freiburg, Germany with Serial number of 1510 as shown in Figure 6 was used with the water phantom for the beam output measurement. It is cylindrical in shape with sensitive air volume of 0.6 cm^3. The sensitive air volume of the ionization chamber is opened to the environment; hence its readings needed to be corrected for influencing factors that will affect air density. The factors are: temperature, pressure and humidity. The chamber has calibration traceability to the International Atomic Energy Agency secondary standard laboratory. The chamber has a calibration factor, $N_{D,W}$ of 5.17 determined with chamber bias voltage + 400 V at temperature of 20 ℃ and pressure of 101.325 Kpa for humidity not exceeding 70 %. The ionization chamber was used to establish dosimetric protocol for the Gafchromic EBT3 films.

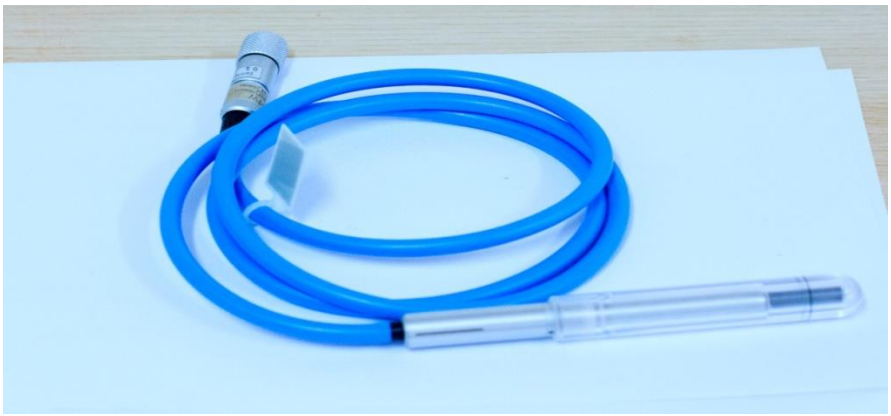

Figure 6: Farmer type Ionization Chamber

Electrometer

Electrometer is a charge measuring device which is connected to an ionization chamber to quantify the amount of ionization taking place within the sensitive volume of the chamber when exposed to ionizing radiation. The electrometer used was PTW UNIDOS model, as depicted in Figure 7. It has a serial number T10005-50316 (PTW, Freiburg, Germany). The electrometer was calibrated together with the PTW 30001 farmer type ionization chamber. During measurements the electrometer was set in the integral mode to measure charges within 60 seconds intervals. The electrometer has a polarity switch at the back, which allows the user to change the bias voltage polarity of the connected chamber. In the front of the electrometer are; a display panel which shows charge or current reading, measurement mode, duration of measurement and option menus. There are bottoms to enable the user to enter into library of chambers, select reading range and change bias voltage of chambers as well as measuring intervals.

Figure 7: PTW UNIDOS Electrometer

Gafchromic Films

Gafchromic EBT3 film with Lot# 04201601 manufactured by International Specialty Product was used. This is shown in Figure 8. Each sheet has a size of 8× 10 cm (ISP, 2011). The films used for the calibrations were cut to a size of 2 cm × 3.5 cm. The Film can measure dose from 1 cGy to 10 Gy. The film was handled in interior room light and kept in the dark case when not in use. Exposure to sunlight was avoided since the film may darken. It was exposed, measured and stored at room ambient temperature of 24 ºC. The films were interleaved with a tissue paper which provided a homogeneous environment around individual pieces of film. Figure 14 show samples of the exposed Gafchromic EBT3 films.

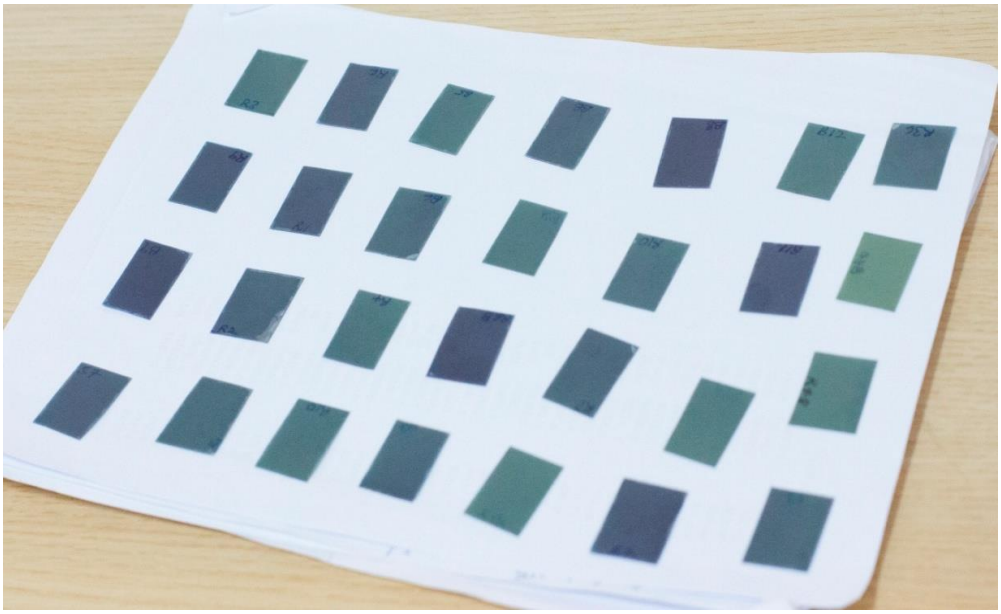

Figure 8: Gafchromic EBT3 Films

Multisource HDR Afterloader BT System

Product Description

The system consists of the following components: afterloader, operating and display elements, external signal and safety equipment accessories (applicators, treatment planning software, transport container, emergency container, and room monitoring system). Figure 9 shows an image of the Multisource High Dose Rate (HDR) Afterloader system.

Figure 9: Multisource High Dose Rate (HDR) Afterloader

Brief Description of the afterloader

Drive Systems

The dummy and radiation source are each driven by a stepper motor independent of one another. The drive systems can be calibrated using a defined calibration track. Prior to each treatment, the dummy drives into the individual channels. This checks whether the channel is unobstructed and whether the correct applicator has been connected.

Channel Multiplier

The channel multiplier enables treatment with up to 20 applicators. It positions the guide tubes in front of the exit channels from the dummy or source. The channel multiplier is ready for operation only when the channel position is correct and the inserted guide tubes are seated properly.

Source

Depending on the treatment nuclide used, either a cobalt source or an iridium source is used in the system.

Co-60: Co0.A86

Ir-192: Ir2.A85-2

Both types are certified as "special form radioactive material".

Safe

The radioactive source is held within shielding. Depending on the nuclide used, the shielding consists of a heavy steel construction with cast lead (for Ir-192 source) or consists of tungsten for Co-60 source.

Height Adjustment

The working height of the afterloader can be set (motor-driven) between 800 and 1100 mm at the afterloader control panel.

Dosimeter (optional)

The afterloader can be optionally equipped with a dosimeter manufactured by PTW for in-vivo dosimetry. A 1-channel bladder probe and 5-channel rectal probe can be connected. The measured values are evaluated in the dosimeter and transferred to the computer.

Operating and Display Elements

The afterloader is controlled and monitored using the operating and display elements located in the control room. General operation takes place at the computer. Treatments are started and interrupted at the start - stop control panel.

Other operating and display elements are located directly at the afterloader. Indicator lights signal the afterloader status. The control panel as shown in figure 10.

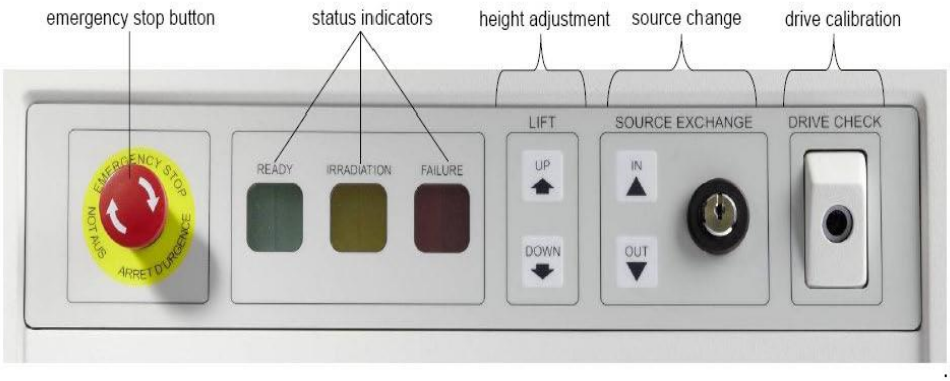

Figure 10: The Control Panel of the HDR Afterloader

Fletcher Suite of Applicators

In intracavitary BT, sources need to be placed in cavities, and to avoid migration of sources to unintended places during treatment, sources are usually placed in special devices called applicators placed in the host. The choice of an applicator is largely influenced by the BT system one is following and the anatomical site of the patient where the brachytherapy insertion needs to be done. The Oncology Centre where this study was carried out uses the Manchester system for its cervical brachytherapy implants and therefore uses Fletcher-Delcos suite of applicators for the implants. The Fletcher suite of applicators consist of two ovoid tubes (ovoids) and a number of uterine tubes called tandems. The ovoids have a diameter of 2 cm, but there are mini-ovoids with diameters of 1.5 cm. The diameter of an ovoid can be increased by putting a special cap on the ovoid to enable it fit perfectly into the cervical canal. When the uterus of the patient is removed as a result of surgery, it is only ovoids (cylinders) that are used for the treatment.

The tandems have a diameter of 0.6 cm, and come in variety of curvatures. The choice of a tandem depends on the curvature and length of the uterus of the patient undergoing brachytherapy. For any particular implant or brachytherapy insertion, pair of ovoids is used, which are on certain occasions combined with a tandem when there is an indication of tumor infiltrating into the uterus. The applicators also provide some level of radiation shielding to the bladder and rectum in close proximity to the cervix. Figure 11 shows the image of Fletcher suite of applicators.

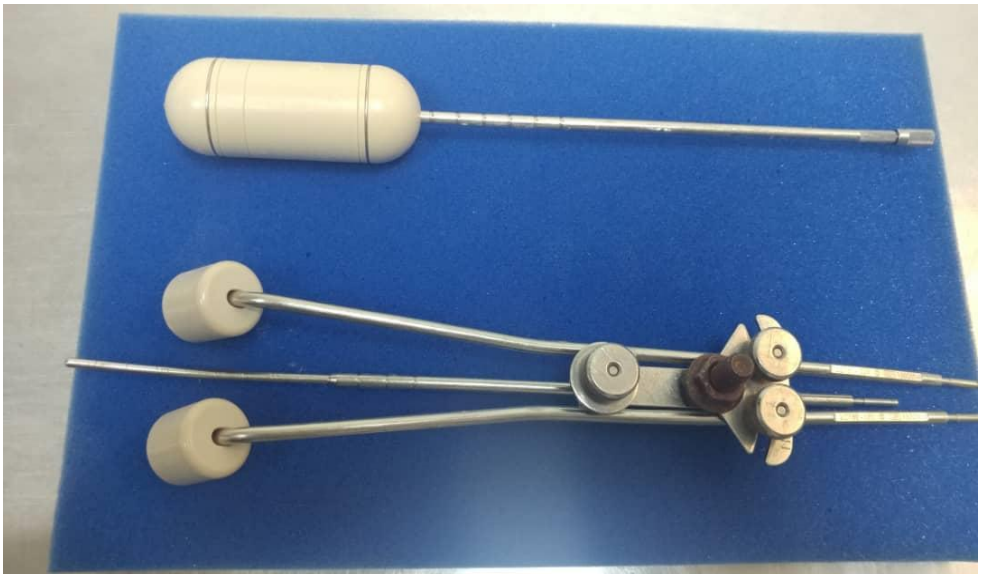

Figure 11: Fletcher Suite of Applicators

Mobile C-arm fluoroscopic X-ray Unit

A mobile C-arm is a medical imaging device that is based on x-ray technology. The name is derived from the C-shaped arm used to connect the x-ray source and X-ray detector to one another. These devices provide high-resolution X-ray images in real-time, thus allowing the physicist to monitor progress at any point during imaging procedures and immediately make any corrections that may be required. A C-arm comprises a generator (X-ray source) and an image intensifier or flat-panel detector. The C-shaped connecting element allows movement horizontally, vertically and around the swivel axes, so that X-ray images of the patient can be produced from almost any angle.

In brachytherapy procedures, the mobile C-arm unit is typically used to help guide the placement of the applicators to their correct positions and to define position of sources in relation to applicators for the treatment planning process.

This research was carried out at the National Center for Radiotherapy and Nuclear Medicine (NCRNM), the Siemens C-arm x-ray machine as shown in figure 12 was used to obtain orthogonal radiographs of insertions for treatment planning to determine duration of treatment of the procedure and to deliver the desired radiation dose. The C-arm x-ray machine is also used to check the orientation of the applicators within the host. Once the applicators are confirmed as being in the correct positions, further imaging can be performed to guide detailed treatment planning. The components are arranged on an arm shaped like the letter 'C'. The high voltage generator of the x-ray tube is fused into the frame work that support the 'C' shaped arm such that the whole assembly run on wheels making the unit mobile. The X-ray unit is connected to a cabinet-like console with a monitor having easily detachable cables. Fluoroscopy images can be visualized on the monitor. The unit has two devices for taking radiographs and performing fluoroscopy; one is hand controlled and the other is foot controlled.

Figure 12: Mobile C-arm fluoroscopic X-ray Unit

Reconstruction Box

Implant reconstruction and precise treatment planning can be done using the reconstruction box. The reconstruction box as shown in Figure 13 is made up of an acrylic frame used for imaging in BT to support non isocentric C-arm units. It gives accurate implant reconstruction with semi-orthogonal films or digital images from C-Arm. The box has a radio-opaque cross-hairs imbedded in it which can be seen on radiographic images. Using the BT TPS (HDRplus), implants can be easily reconstructed in a 3D space.

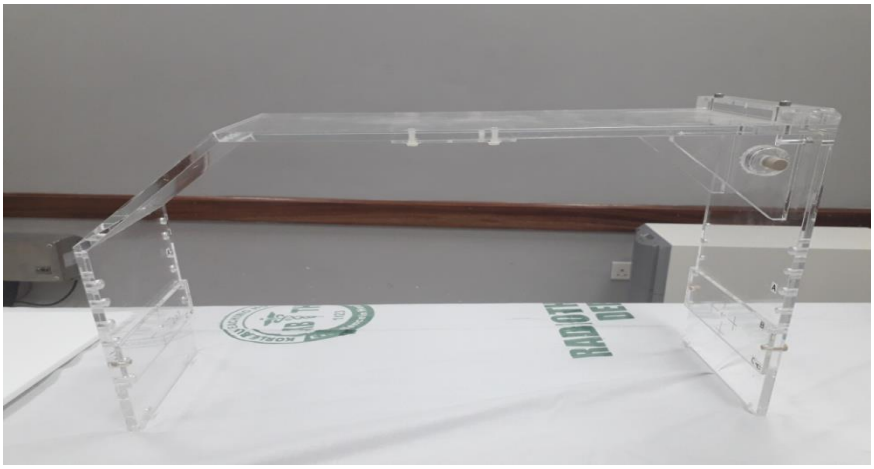

Figure 13: Reconstruction Box

Epson Stylus Scanner

The EPSON Stylus C× 5900 Scanner (USA) as depicted in Figure 14 was used in scanning the irradiated films. The films were cut to a size of 2 cm × 3.5 cm. The scanner provides sensitive response for EBT3 film at doses up to 8 Gy in the red color channel. The EBT3 film has a unique marker dye in its active layer. This improves the automatic uniformity of the film in the blue channel range. Doses from 8 Gy to 40 Gy are measured by the green channel.

Figure 14: Epson Stylus Scanner with Strips of Irradiated Gafchromic EBT3 Films arranged on it for Scanning

ImageJ Software

The ImageJ software was used in analyzing the Gafchromic films. ImageJ is a java-based processing program developed by the Institute of Health (USA). The ImageJ was used in measuring the pixel values of the film at a point (central point) on the Gafchromic EBT3 film. These pixels were then used to determine the optical densities of the film for dose measurement. The interface of the ImageJ software is depicted in Figure 15.

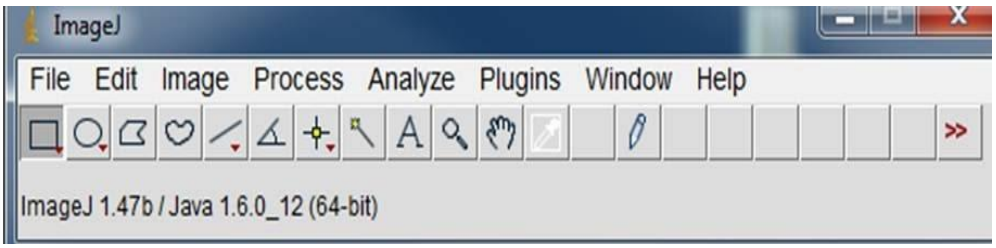

Figure 15: ImageJ User Interface

Experimental Methods

Phantom Design and Fabrication

The phantom was designed to meet certain design criteria so that it can test realistic anatomic clinical situations. Water was used as substitute for tissue and slabs were designed to hold the Gafchromic films in place to be imaged using C-arm X-ray unit. Two organs at risk (OAR) namely bladder and rectum which are in close proximity to the cervix were selected. Perspex (PMMA) sheets of thickness 6 mm and 10 mm were used in the entire design as shown in Figure 16. Computer tomography (CT) images of a real patient's cervical region were obtained from the CT scanner and these were used as a guide in constructing the bladder and rectal region of the cervix phantom.

The phantom designed is cuboid in shape with predominantly 6 mm thickness of the perspex material. It has a height of 41 cm and breadth 31 cm. The pieces of perspex material were glued to each other using Trichloromethane (chloroform) at room temperature. The chloroform was used to join the perspex sheets together. It is an organic compound with the formula $CHCI_3$. Chloroform is a colorless, volatile liquid derivative of Trichloromethane with an ether-like odour. It can be used as a solvent to bond pieces of acrylic glasses together. A perspex sheet of 10 mm was used to make one end of the phantom thicker than the other. This was done to support the reconstruction box. The reconstruction box helps in getting the magnification of the images taken during the brachytherapy procedure.

Two thin film holder slabs of dimensions $31.5 \times 2.8\ cm^2$ were fabricated by joining two sheets of 6 mm perspex together with the chloroform. A small cavity of $2.8 \times 2.5\ cm^2$ was created in the slab to represent the bladder and the rectum. These same cavities are meant to hold the Gafchromic films in place for the measurement of dose to the bladder and the rectum which are the organs at risk (OAR) in the treatment of cervical cancer. The film holders with the cavities were then positioned vertically, but anterior and posterior to each other in the cuboid shaped water phantom designed. Another holder, rectangular in shape was fabricated to hold the film holders. This holder was made from perspex sheets of thickness 6 mm and 10 mm with dimensions of $6.8 \times 6.8\ cm^2$. This is to allow for the distances between the bladder and the rectum to be varied during the dose measurements. It must be noted that the anatomical distance between

the bladder and the rectum which are posterior and anterior to the cervix vary from patients to patients.

Special clamping devices were fabricated to hold the applicators in a firm position during the intracavitary brachytherapy insertions. These special clamps were made by joining perspex of 10 mm thickness in a cuboid shape; a hole was drilled in them to enable a plastic screw to lock the applicators.

The relative electron density of the perspex sheet used in the entire design was determined to be 1.069 which is comparable to water. This makes the phantom suitable for dose measurements. A 3D view of the phantom is shown in Figure 16 and 17.

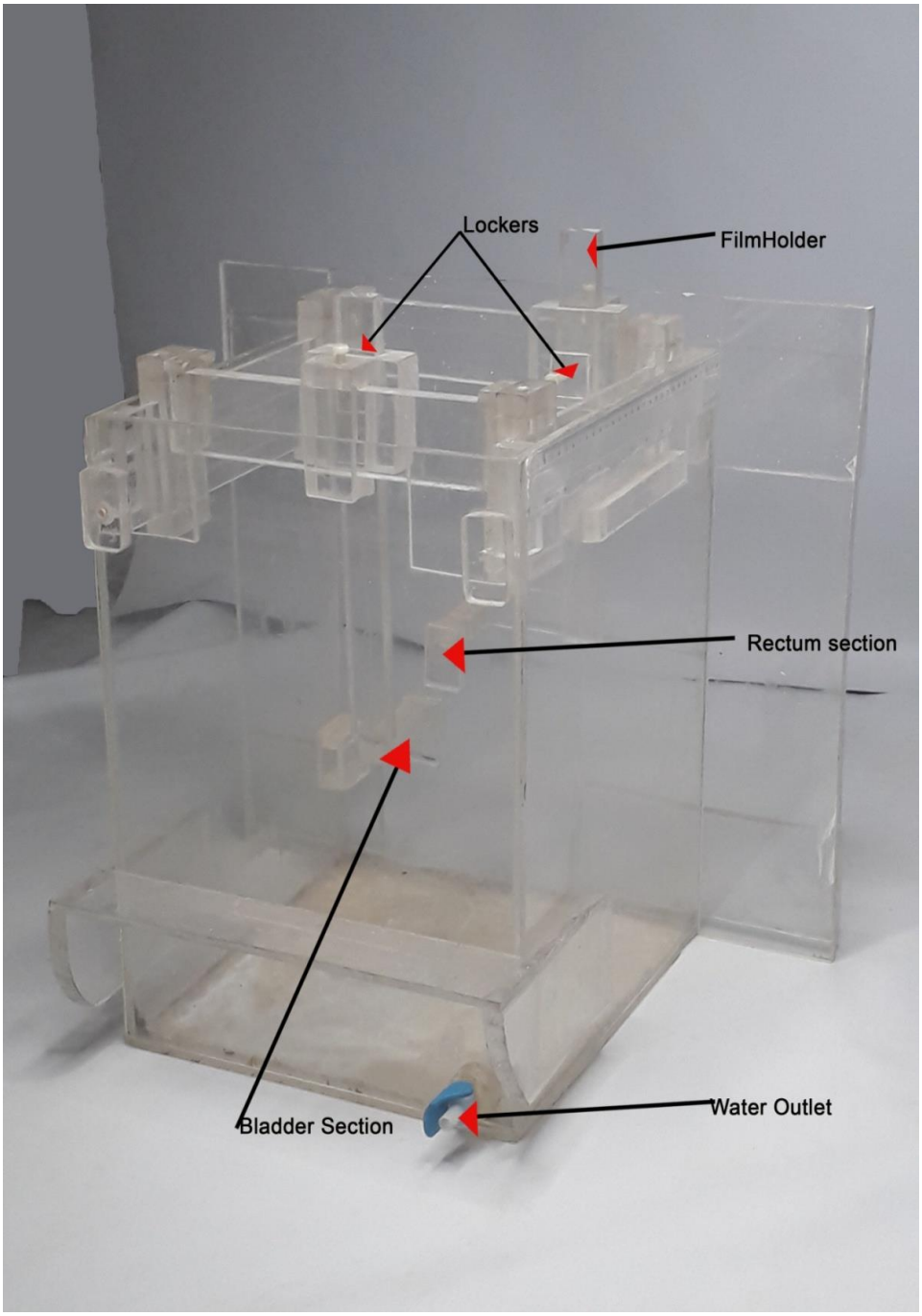

Figure 16: Locally Constructed Water Phantom

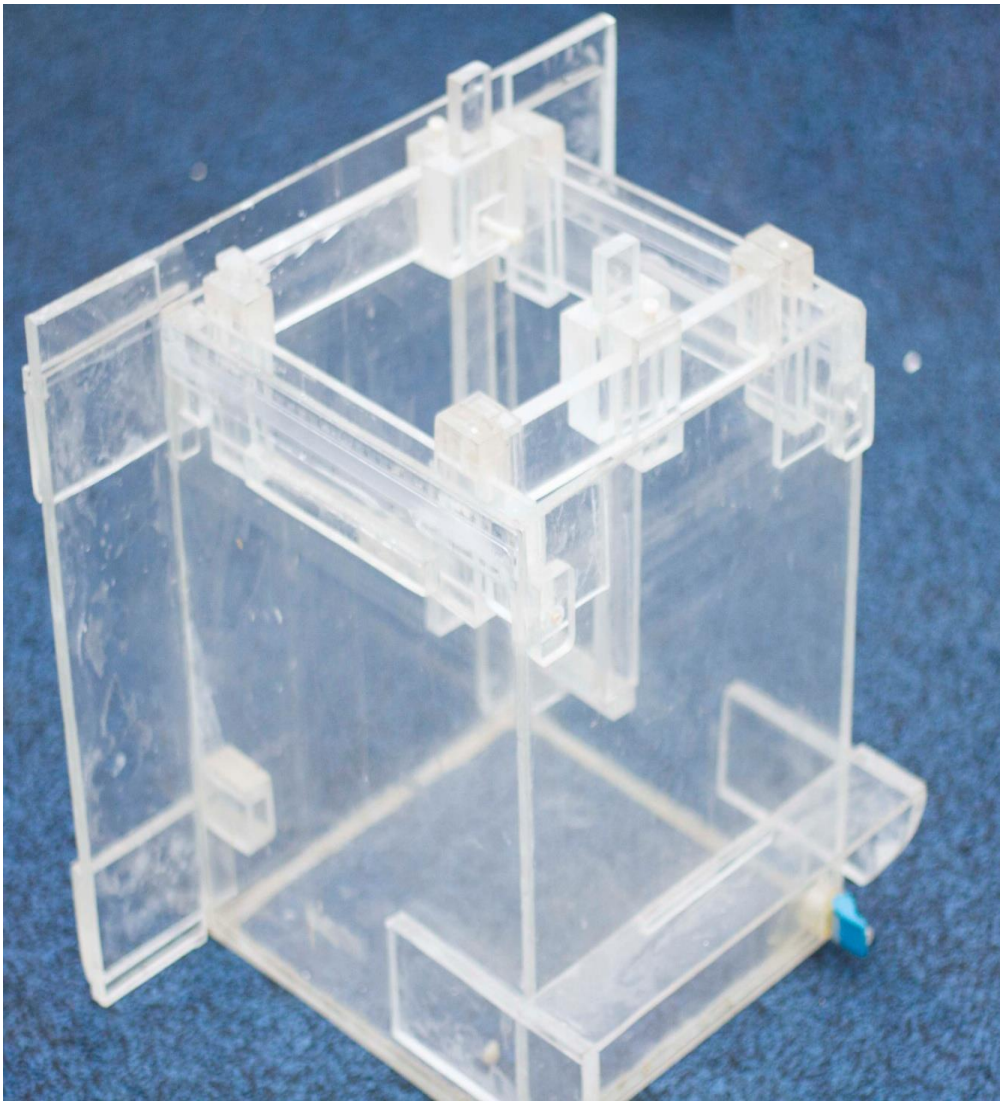

Figure 17: 3D View of the Constructed Water Phantom

Calibration of Gafchromic Film to be used as a Dosimeter

Beam Output Measurement

The beam output measurement was determined using a proposed method by the IAEA in equation 22. (IAEA, TRS 398 2000).

Beam output determination in this study was carried out using the Therathron Equinox Teletherapy treatment unit (Best Theratronics, Canada); at the reference field size of 10 × 10 cm^2 at a depth of 5 cm using the PTW 30001

ionization chamber (PTW-Freiburg, Germany) with the mini water phantom. The ionization chamber's stability was checked using with strontium-90 check source kit provided by the manufacturer (PTW-Freiburg, Germany). The mini water phantom was filled with water and pre cautionary measures were taken to eliminate air bubbles that were trapped in the phantom.

Light field congruence and radiation test was performed on the Therathron Equinox cobalt 60 machine using the MEDTEC iso-aligner and radiotherapy non-screen film to ensure the field size parameters were accurate and that of the radiation for the treatment machine. Source to surface (SSD) irradiation technique was employed during the beam calibration so that the SSD indicated by the optical distance measuring device on the gantry of the therathron Equinox machine read 80 cm on the surface of the manual water phantom (IBA Dosimetry GmbH, Germany).

The manual water phantom was then carefully placed on the couch of the therathron equinox treatment unit and a digital spirit level was placed on the surface of the phantom to check its flatness. A slight adjustment was made to the phantom to ensure that the field size on the surface of the phantom corresponds with the light field of that of the Therathron Equinox treatment unit. The dose rate of the machine was then determined using the IAEA TRS 398 procedure and verified with the TPS.

A treatment plan was created such that it had the same configurations as the research set up with a dose of 2 Gy being prescribed to the region of measurement and the treatment time was obtained. Using the TRS 398 formulas

with manual calculations, the dose rate derived from the ion chamber was used to calculate the treatment time for the prescribed dose using equation 26.

$$T = \left(\frac{D}{PDD/_{100} \times \dot{D} \times \lambda} \right) - t_s \quad (27)$$

where PDD is the percentage depth dose,

D is the prescribed dose

$\dot{D}$ is the dose rate

λ is the decay factor

The treatment time for the prescribed doses ranged from 0 – 1000 cGy with a variation of 20 cGy to a treatment depth of 5 cm for SAD irradiation technique, using the iso-centre as the dose normalization point. The values for the parameters have been indicated in Table 5 of Appendix C.

Calibration of Gafchromic EBT3 Films

Ten (10) strips of Gafchromic EBT3 films with the same lot number were cut to dimensions of 2.6 cm × 3.2 cm and inserted in the manual water phantom. This was done such that the strip of film was at a depth of 5 cm from the radioactive source within the phantom. The film was then inserted in a perspex flab in the phantom. The phantom was aligned in a way that it was central to a field size of 10 cm ×10 cm towards the direction of propagation of the beam whilst the gantry was kept at 0º. The rest of the films were then exposed perpendicularly one after the other from 0 cGy to 1000 cGy to the cobalt 60 beams and the duration of exposure recorded (treatment time). The films were stored for 24 hours to allow the colorization to reach its peak and

also for the stabilization of post exposure density growth (Shima et al, 2000) before being scanned and analyzed.

An EPSON scanner (Stylus C×5900, USA) was used to scan all the irradiated films in a transmission mode. The films were arranged in the centre of the scanner and positioned in such a way that the longest side was perpendicular to the scanning direction according to the manufacturer's specification. The EBT3 films were split into (Red-Green-Blue Channels) (RGB). The images were then converted to a depth of 16 bits per color channel of spatial resolution of 72 dpi corresponding to a pixel size of 0.35×0.35 mm^2 and saved in a Tagged Image File Format (TIFF).

The scanned images of the film were then imported into the ImageJ software (National Institute of Health, USA) for analysis. In using the ImageJ, the images were split into Red-Green-Blue Channels. Image measurements were performed on the point of interest which was the centre of each image of the irradiated film. Film intensity values were obtained from the ImageJ. The film intensities were then converted into net optical densities (OD) using equation 21.

A graph of prescribed dose as a function of optical density was plotted to determine the calibration curve or sensitometric curve of the Gafchromic EBT3 films for all three-color channels (RGB). From Figure 38, the Green channel gave the best regression. The equation from the Green Channel was then used to calculate the optical density of the film to the absorbed dose measured by the film.

A reproducibility test was performed on the EPSON Scanner. This was done by scanning a film repeatedly at different times. The film non-uniformity and film-to-film variations determined from eight films selected randomly from the same film lot number using the method proposed by Saur et al (Sar & Frengen, 2008).

Using the method proposed by Van Battum, Piersma & Heukelom, 2008 (Van Battum, Piersma & Heukelom, 2008), the overall accuracy of the Gafchromic EBT3 films was determined. This takes in consideration the most pronounced sources of uncertainties in dose determination when using the film (scanner, lateral correction, fit accuracy, intra-batch variation, background and intrinsic film inhomogeneity). An overall uncertainty was obtained using the error propagation analysis. The experimental set up for the beam calibration is shown in Figure 18.

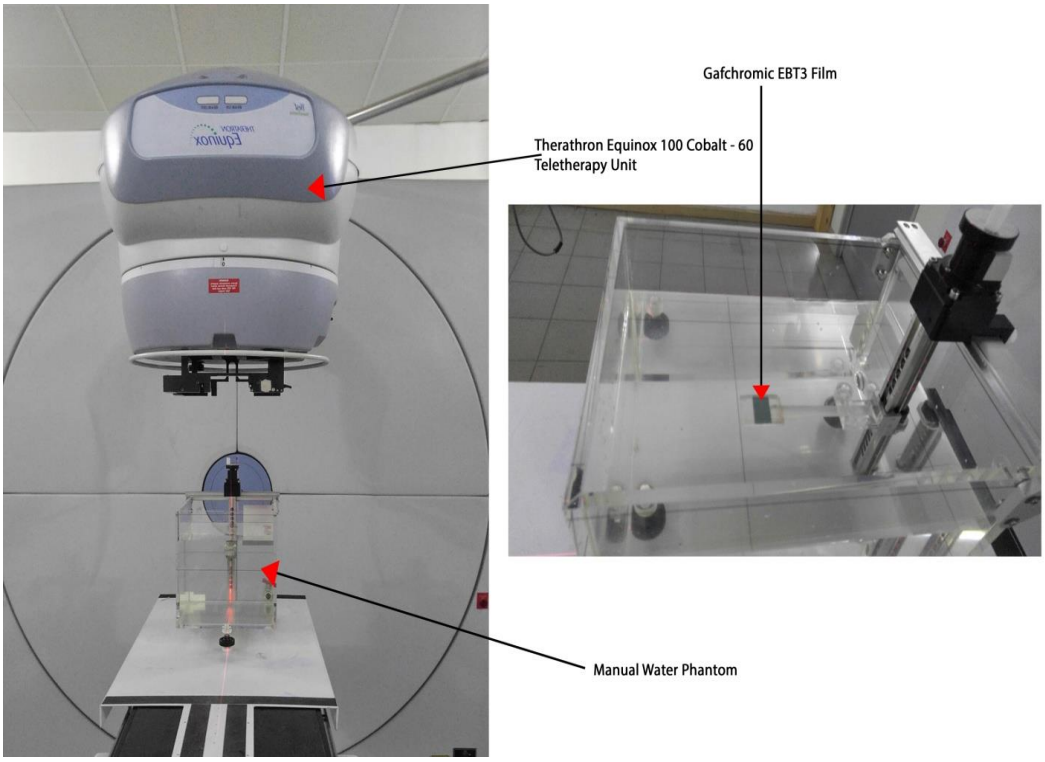

Figure 18: A Set-Up for Beam Output Measurement and Calibration of the Gafchromic EBT3 Film

Quality Assurance (QA) for HDR Treatment Unit.

The daily QA check for the Multisource HDR afterloader was performed before the dose measurements were carried out. The set up for this measurement is depicted in Figure 19. During the QA procedure the following safety test were performed: door interlock, radiation condition indicator lights, emergency stop button, console check and audio-visual device. The door interlocks were checked to ensure that when the source is out, and the door is opened, the source must not move from the HDR unit. The radiation indicator lights indicate red light when the exposure is ongoing and green when the there is no irradiation. The emergency stop button is triggered when the treatment is either interrupted

or the HDR unit encounters a technical problem. The console enables the controlling of treatment procedure. The audio-visual device manufactured by Axis communications enables the monitoring and communication with patients during treatment. Operational test is the second test performed on the unit. In this test the Visual test which aids patient and treatment monitoring must be ±1 mm and the timer check must be ≤3 sec; all these were ensured before measurements were carried out to ensure accuracy.

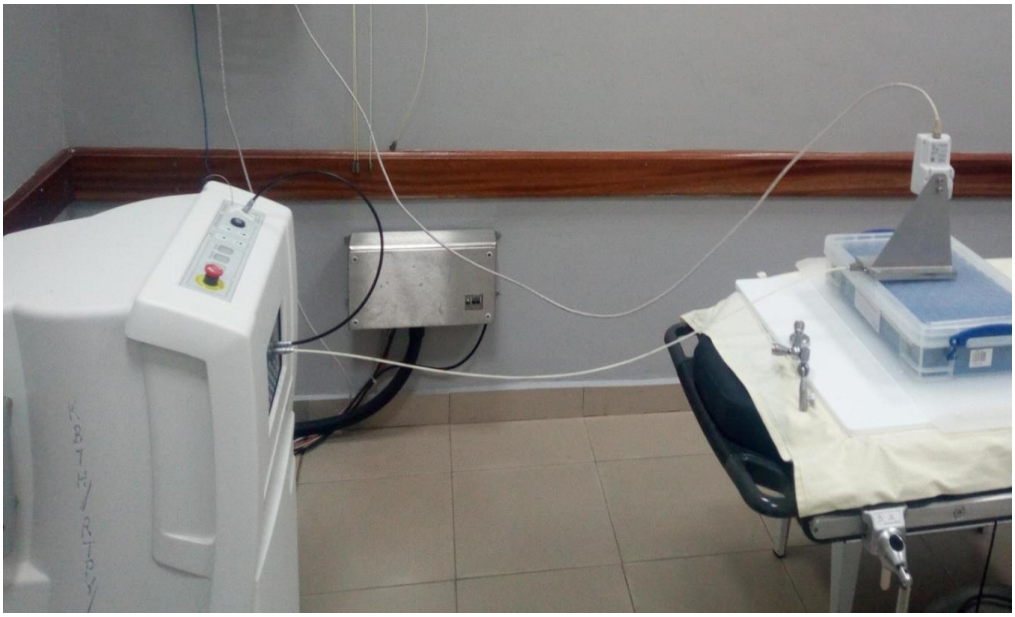

Figure 19: An Experimental Set-Up for QA

Bladder and Rectal Dose (Phantom Measurements)

During HDR BT of the cervix, the bladder and the rectum are the two main organs at risk. This is because of their anatomical proximity to the cervix. The Fletcher suites of applicators were used in carrying out clinical insertions on the locally constructed phantom. Clinical protocols and procedures used at the BT unit were strictly adhered to during the insertions of the applicators into the phantom.

Clinical insertions were carried out on the fabricated phantom as shown in Figure 20 and 21. The applicators were inserted into the phantom and carefully tightened and held in place by a metallic knot to minimize applicator movements. The applicators were positioned such that they lied in between the bladder and the rectal compartment created inside the phantom. The phantom was then filled with water with the applicators held in their respective positions. In filling the phantom with water, air bubbles trapped in the compartments were allowed to move out.

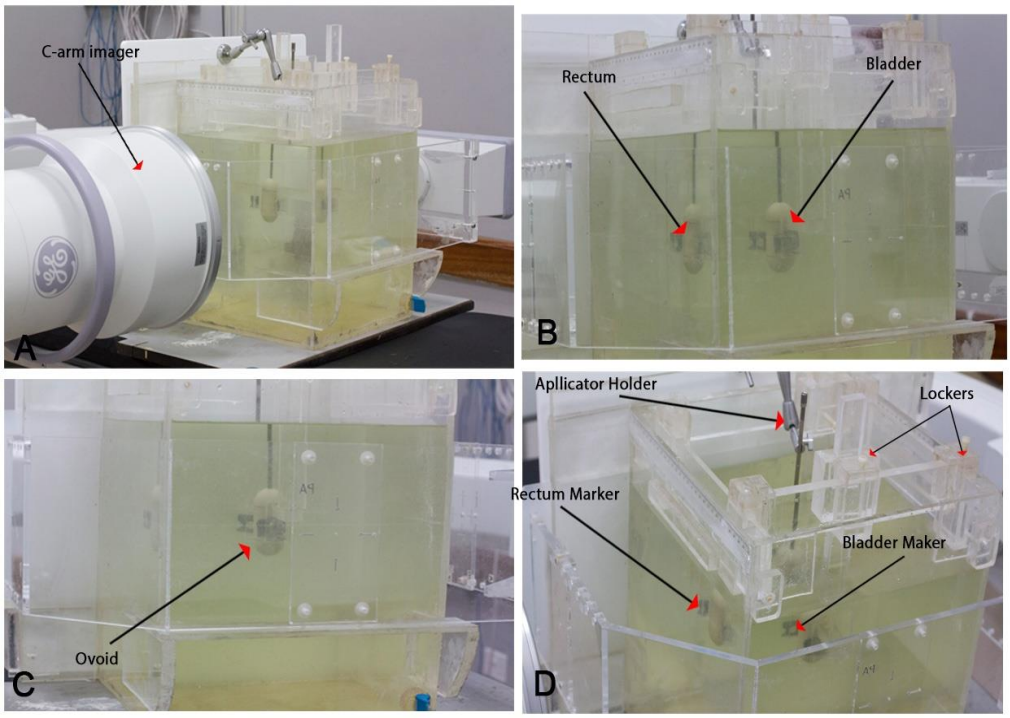

Figure 20: Phantom filled with Water showing (A) C-arm Imager (B) Rectal and Bladder Section (C) Cylinders (D) Holders, Lockers and Markers

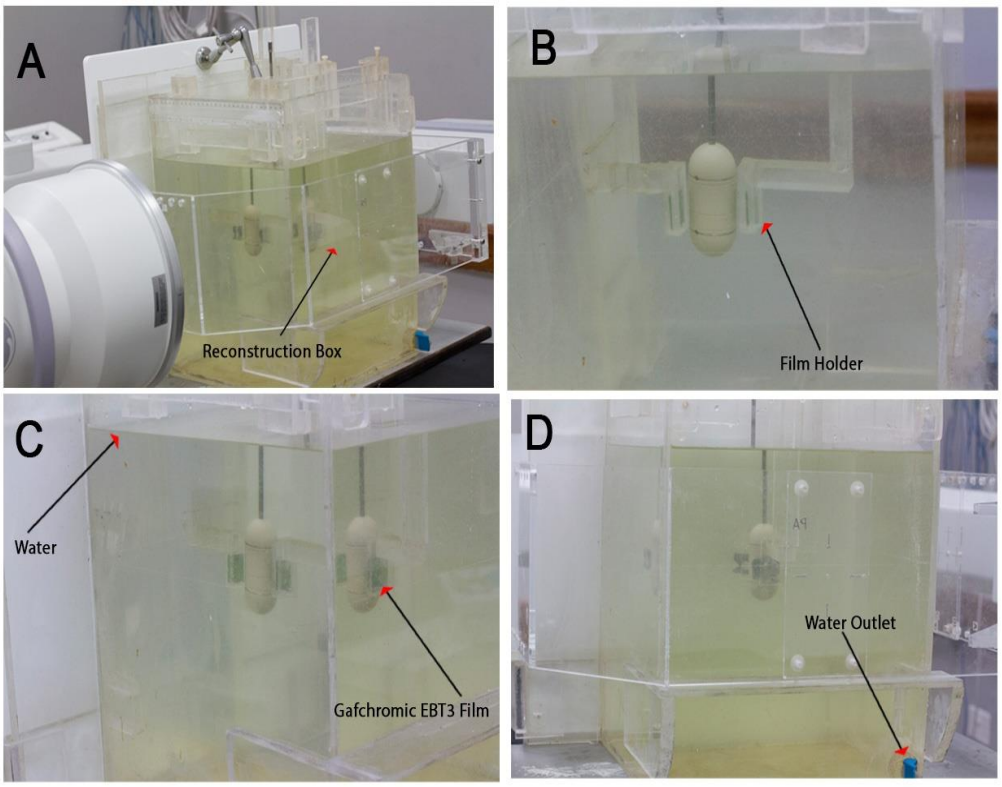

Figure 21: Phantom filled with Water for Bladder and Rectal Dose Measurements showing (A) C-arm Imager (B) Film holder (B) Gafchromic EBT3 Film

The Siemens C-arm fluoroscopic x-ray machine was positioned in two different ways to take two orthogonal images of the applicators held in place inside the phantom. The C-arm X-ray unit in a lateral position as shown in Figure 22 and the anterior-posterior position of the C-arm X-ray unit as shown in Figure 23.

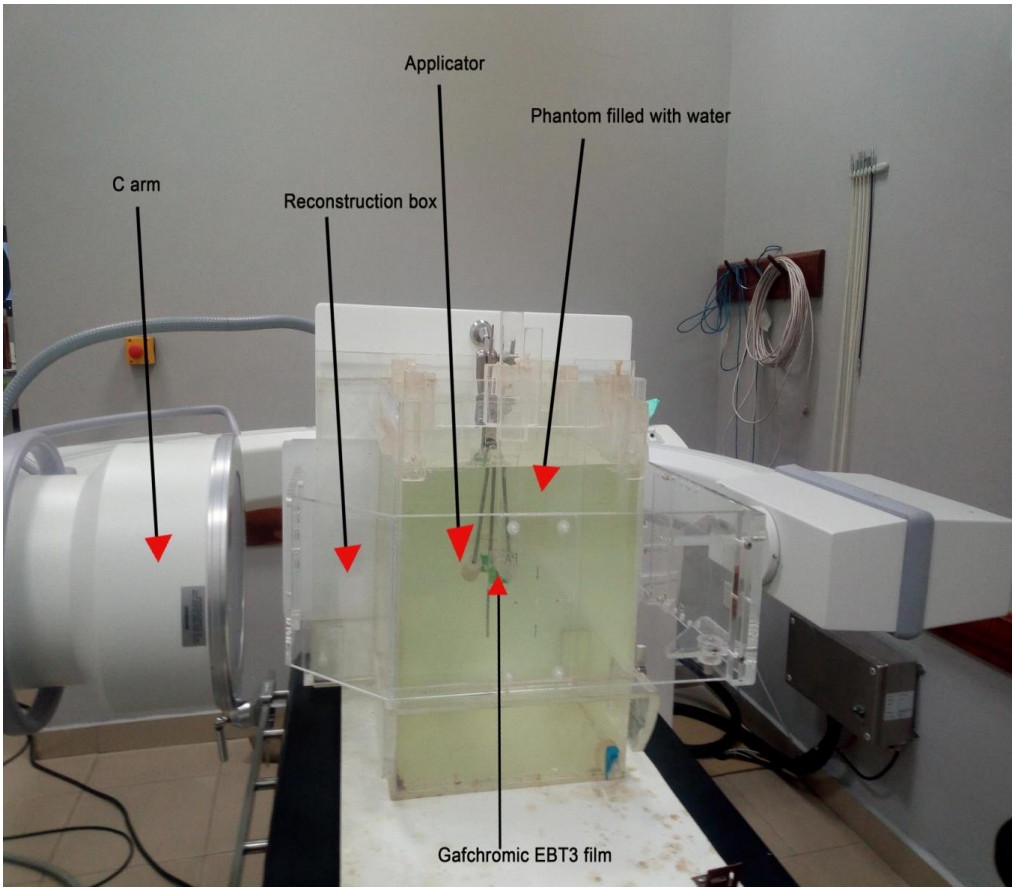

Figure 22: C-arm Fluoroscopic X-Ray Unit in a Lateral Position

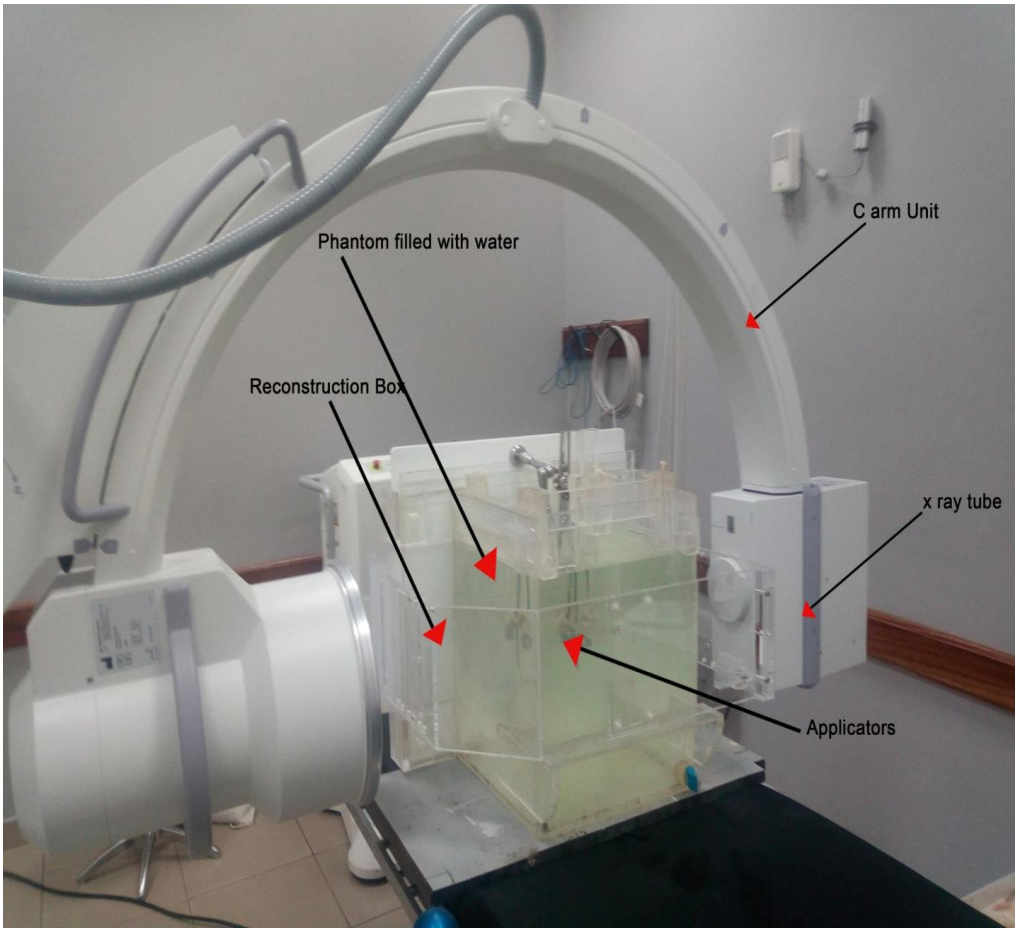

Figure 23: C-arm Fluoroscopic X-Ray Unit in an Anterior-Posterior Position.

The orthogonal image taken for anterior-posterior and lateral view for cylinders only has been shown in Figure 24 and 25. The orthogonal image taken for anterior-posterior and lateral view for Fletcher suite of applicators has been shown in Figure 26 and 27. Appendix F-1 to F-7 depicts the orthogonal images taken from the insertions performed on the phantom.

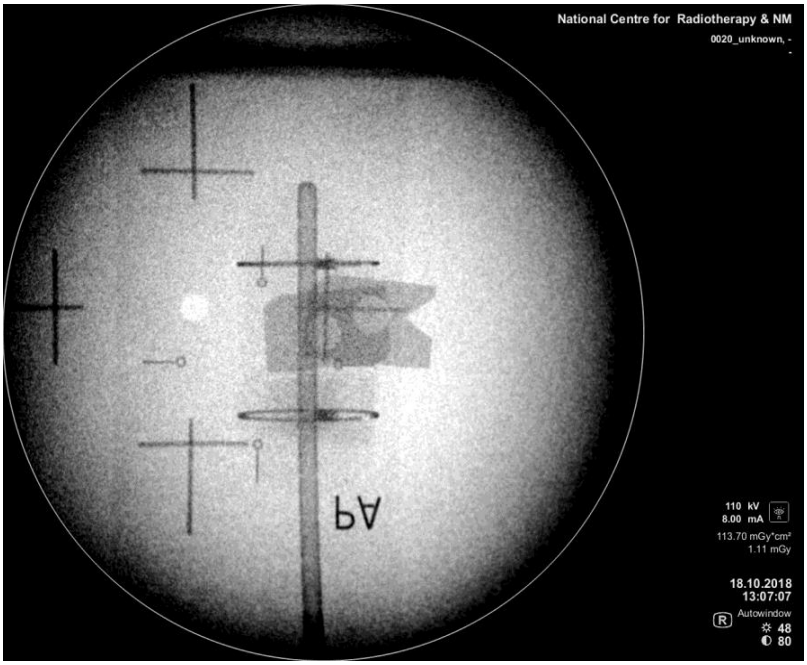

Figure 24: An Anterior – Posterior (AP) Radiograph of the Applicator (Cylinder Only) Insertions obtained from one of the Experimental Set-Ups

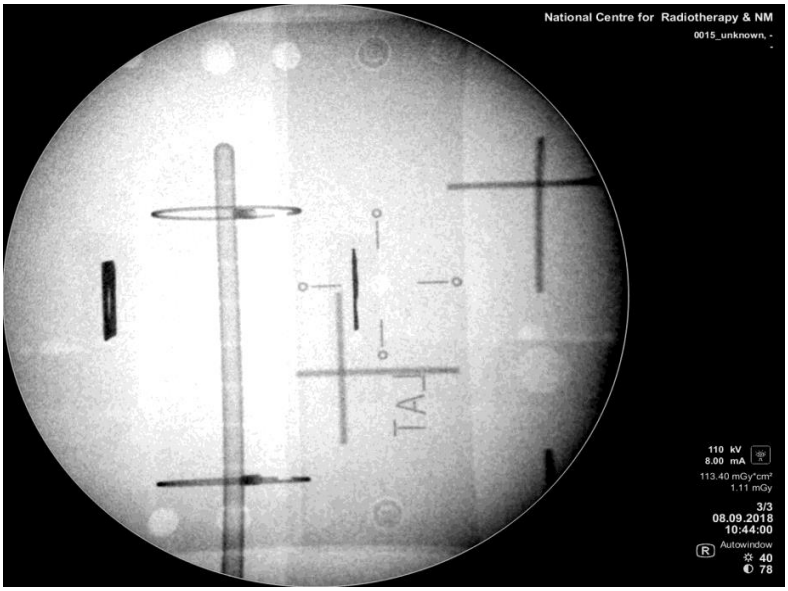

Figure 25: Lateral radiograph (LAT) of the Applicator (Cylinder only) Insertions obtained from one of the Experimental Set-Ups

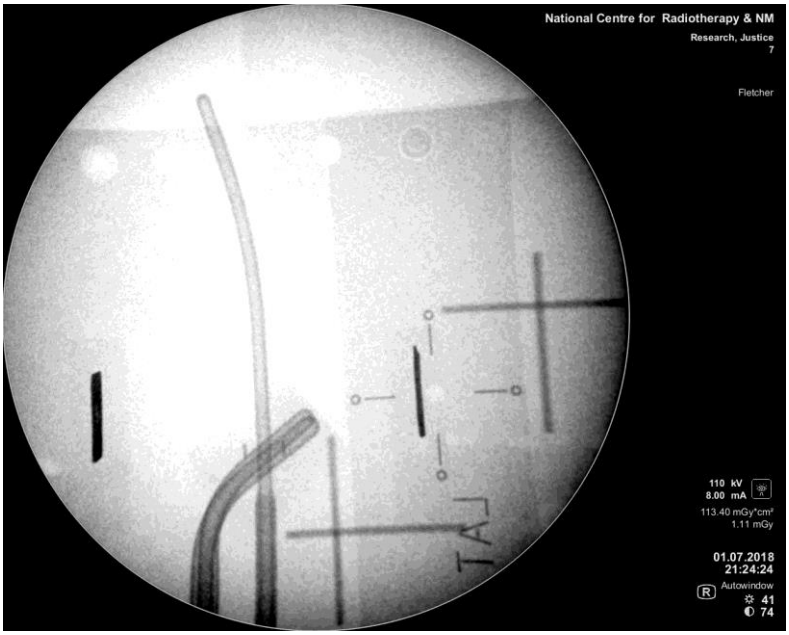

Figure 26: Lateral (LAT) Radiograph of the Fletcher Suite of Applicator Insertions obtained from one of the Experimental Set-Ups

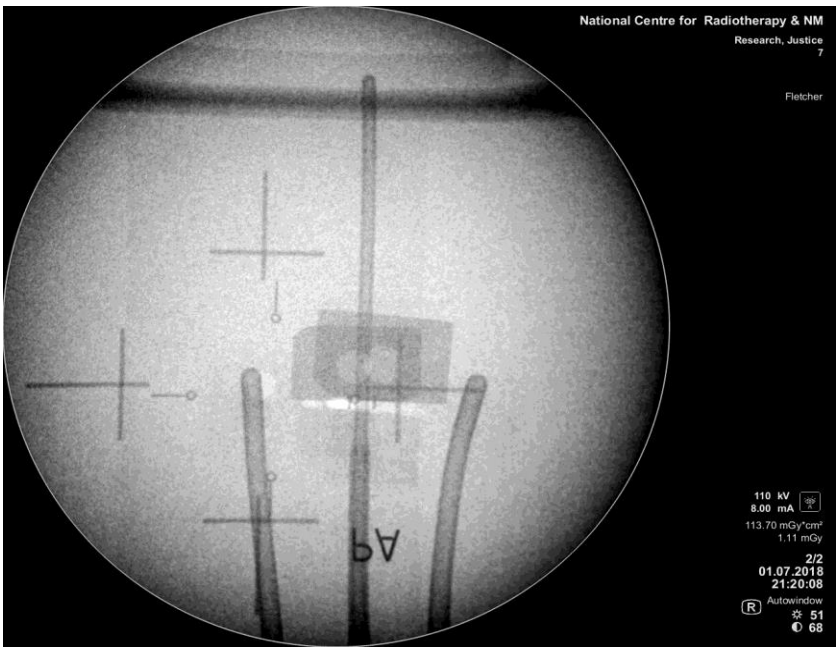

Figure 27: An Anterior – Posterior Radiograph (AP) of the Fletcher Suite of Applicator Insertions obtained from one of the Experimental Set-Ups

These orthogonal images were then imported into the TPS to determine dose to the various prescription points. For insertions that included the Fletcher suites of applicators (applicators involving tandems with the ovoids), doses were prescribed to point A, however, for insertions involving only cylinders, doses were prescribed to the surface of the voids at a depth of 0.5 *cm* from the surface of the ovoids. This is in accordance with BT treatment protocol. The BT unit at the NCRNM currently uses these prescription points. Again, doses were also varied to the bladder and the rectal points for the purposes of the research in order to assess dose measurements to these organs at risk during treatment. The orthogonal radiographs taken were then imported into the Treatment Planning System (HDR-Plus) via dicom transfer for planning. On the TPS the acquired images were reconstructed using the reconstruction box (i.e. determination of magnification and orientation of the images).

The applicators used were selected from the applicator library on the TPS and superimposed on the system. Then the dose to point A was defined as well as dose to the bladder and rectum (organs at risk). The dwell positions of the cobalt -60 sources were selected on both the tandem and the ovoids. The prescribed dose was then normalized to point A and calculated. Figure 28 depicts the TPS planning window for insertion involving Fletcher suites of applicators. For insertions where only the cylinders were used as shown in Figure 29, the doses were prescribed at 0.5 *cm* to the surface of the cylinder. The prescribed doses were then normalized and calculated. After the calculation the TPS generated a dose control point report indicating the Point A dose, minimum dose, average dose and maximum dose for both the bladder and the

rectum. Appendix G-1 to G-7 shows the TPS window for dose calculation.

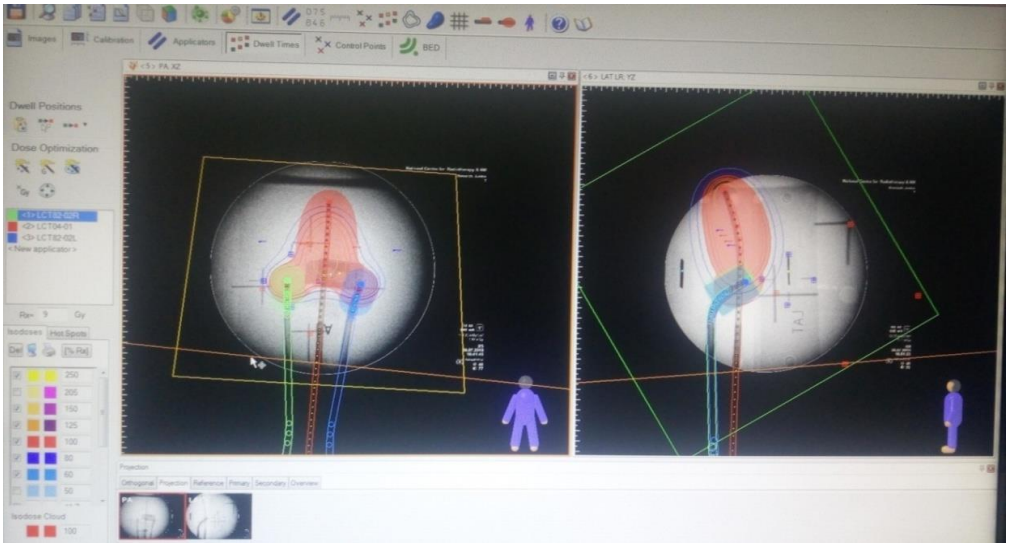

Figure 28: TPS Window showing Treatment Plan for Dose Calculation for Fletcher Suite of Applicators

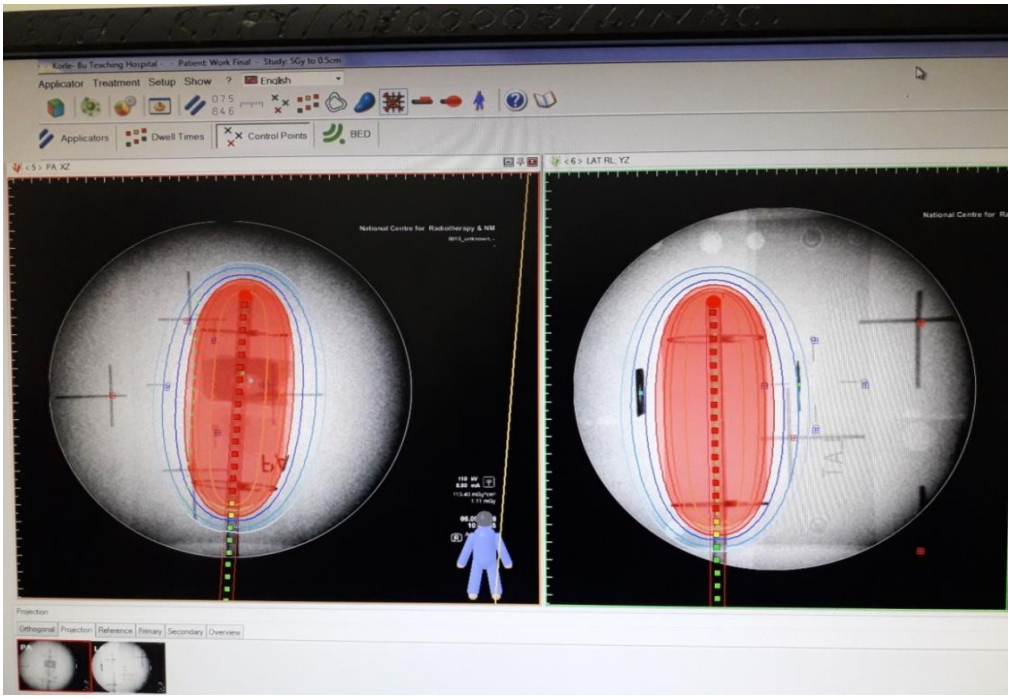

Figure 29: TPS Window showing Treatment Plan for Dose Calculation for Cylinders Only

One hundred and ninety (190) different clinical insertions were performed on the phantom. Different applicator configurations that are used in the treatment of patients at the Radiotherapy center were used in the insertions. Gafchromic EBT3 films with Lot#04201601 that had already been calibrated were cut to $2.6 \times 2.7\ cm^2$ to fit into the compartments designed in the phantom which mimics the bladder and the rectum. The films were then inserted into their various compartments; this was done cautiously to avoid the movement of the applicators. The films were held carefully to ensure there were no scratches on them. These Gafchromic EBT3 films were placed inside the phantom as shown in Figure 23 after the orthogonal images were taken.

Catheters were used in connecting the applicators to the respective channels on the HDR BT treatment unit as shown in Figure 30 and 31. After the connections the doors were locked and the treatment was initiated with the HDR brachytherapy treatment unit from the monitor in the control room. The Cameras installed in the treatment room enabled the monitoring of the entire treatment process. For each treatment, the overall time was noted and this ranged from 10 to 45 minutes depending on the prescribed dose and the type of applicators used. The films were then labeled after each irradiation and were scanned after 24 hours to allow the colorization to reach its peak. Appendix E-1 to E-2 shows strips of the irradiated films. During the scanning process, films that were not irradiated (unexposed) were placed at the end of the irradiated ones. ImageJ software was then used to determine the intensities of the irradiated films (I) and the intensities of the films that were not irradiated (I_O)

to serve as a control. The film intensities were then converted to optical density (OD) using equation 21 as discussed in chapter two.

$$Optical\ Density = \log_{10}\left(\frac{I_O}{I}\right)$$

where I_o is the intensity of the unexposed film and I is the intensity of the exposed film (irradiated).

The optical densities obtained were converted to doses using equation 29.

Doses computed by the TPS were compared with doses measured using the Gafchromic EBT3 films and the percentage difference was determined as:

$$\% \text{ difference} = \frac{TPS\ Dose - Film\ Dose}{TPS\ Dose} \times 100 \qquad (28)$$

where TPS Dose is the dose calculated by the TPS.

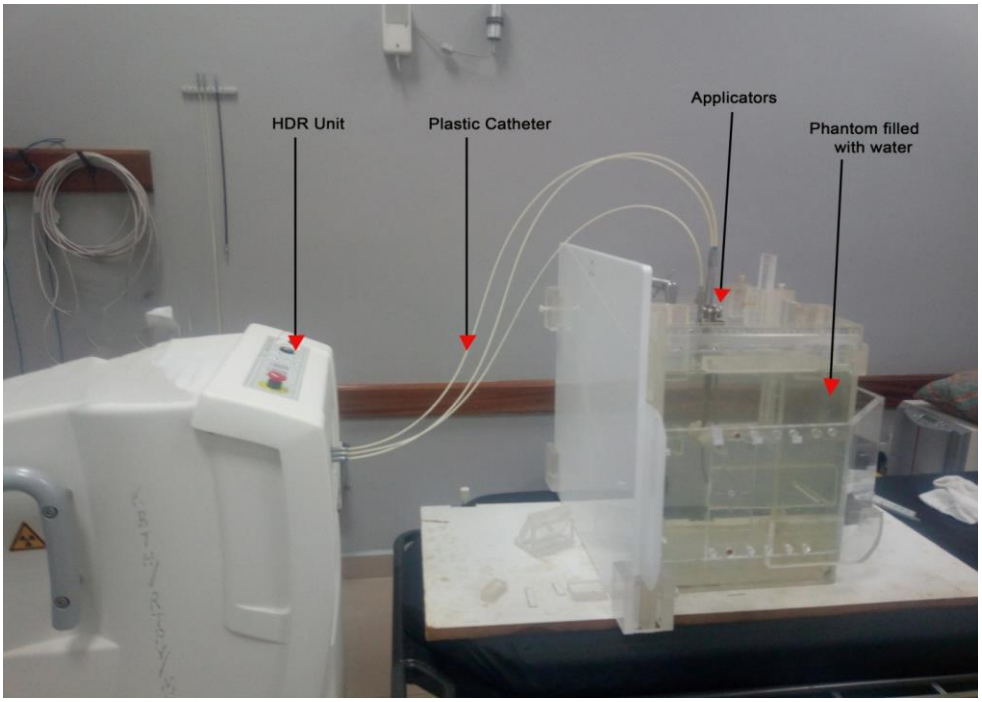

Figure 30: An Experimental Set Up showing Plastic Catheters Connected from the HDR Treatment Unit to the Fletcher Suite of Applicators in the Locally Constructed Phantom filled with Water

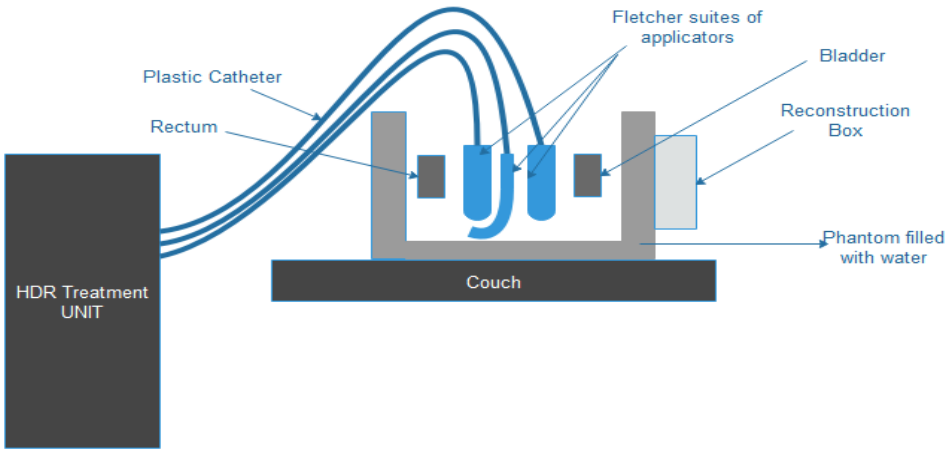

Figure 31: Schematic Diagram of the Experimental Set Up showing Plastic Catheters Connected from the HDR Treatment Unit to the Fletcher Suite of Applicators in the Phantom filled with Water

Statistical Models

The assumption in the modelling process was that the dose to the film is reflected in the corresponding Intensity of radiation extracted from the film. The statistical modeling process was based on linear approach for modeling the relationship between scalar dependent variables (dose) and independent variables (intensity of film). The relationships between the parameters were modeled using linear predictor functions whose unknown model parameters were calculated from the data in Appendix B-2. Conversely, the linear regression was focused on the conditional probability distribution based on Normal Probability Plot (NPP) of given variables.

The descriptive parameters (constants and co-efficient) of the regression equation for dose to the bladder and rectum were obtained using the normal histogram, normal probability plot based on the statistical analysis by Chambers et al (Chambers *et al.*,1983). These were the four graphical techniques for assessing whether or not a data set is approximately normally distributed. In addition, the modeled equations of all the parameters namely: dose, initial intensity and final intensity were plotted against a theoretical normal distribution in such a way that the points were evenly distributed.

Additionally, the plots were based on the residual plots which formed graphs that were used to examine the goodness-of-fit in the linear regression analysis. This helps to find out whether the ordinary least squares assumptions were being played. The assumptions satisfactorily produced unbiased coefficient estimates with the minimal variance (≤ 0.05). The four techniques used are explained as follows:

The histogram of residuals was first used to ascertain whether the data are skewed or whether outliers exist in the data. Secondly the normal probability plot of residuals, which was used to verify the assumption that the residuals are normally distributed. Furthermore, the residuals versus fits were also applied to verify the assumption that the residuals have a constant disagreement. Finally, the residual versus order of data was employed to verify the assumption that the residuals are uncorrelated with each other. For each model, there are four elements such as the model equation, the standard deviation, the predictor and the p-value. A small p-value (typically ≤ 0.05) indicates strong evidence against the null hypothesis, resulting in rejecting the null hypothesis.

Microsoft Visual Studio C++ Coding

In order to make the two models user friendly and avoid errors as a result of manual calculations, Microsoft visual studio C++ was used to write codes for the models to convert the intensity of radiation to dose (Dose Conversion Models) and installed on the computer for clinical applications. An input of film intensity into the dose conversion model will generate the corresponding dose measured. The model was designed with Microsoft visual C++. Four global variables were declared$(I_{R,}\ I_{B,}\ D_B,\ D_R)$ to represent the parameters in the model as shown below.

double $I_{R,}$;

double $I_{B,}$;

double D_B;

double D_R;

D_B= 11.520 - 0.108 * I_B ,;

D_R = 11.611 - 0.110 *I_R ,;

Where D_B is dose to the bladder and D_R is dose to the rectum.

The variables I_R and I_B are mapped or assigned to textboxes that accepts input from users.

I_R =Double::Parse(txtir->Text);

I_B =Double::Parse(txtib->Text);

When a value is entered into the textbox (txtir), the value is parsed to the variableI_R which is then used in calculating the Dose to the rectum. Also, when a value is entered into the textbox (txtib), the value is parsed to the variable I_B which is then used in calculating the Dose to the bladder. The result of the calculation is then displayed to the user.

lbldr->Text = System::Convert::ToString(Dr);

lbldb->Text = System::Convert::ToString(Db);

Chapter Summary

Perspex material was used for the construction of the water phantom for dose distribution measurement to the bladder and the rectum. The perspex material was selected because of the good radiological and physical properties it possesses. Gafchromic EBT3 was used as a dosimeter for determining the absorbed dose to the organs at risk. The Gafchromic film was used because it is easy to handle and can also measure dose in the range of 0-800 cGy and it is ten times more sensitive than its previous generation. The Gafchromic film can also withstand a temperature up to 70℃. The beam output determination was carried out using the therathron equinox teletherapy treatment unit; at the field size of 10 cm for the reference field size of 10 × 10 cm^2 at a depth of 5 cm using the PTW 30001 ionization chamber with the mini water phantom. This was done using the proposed method by the IAEA TRS 398 (IAEA, 2000). The dose rate of the machine was then determined using the IAEA TRS 398 procedure and verified with the treatment planning system. A treatment plan was created such that it had the same configurations as the research set up with a dose of 2Gy being prescribed to the region of measurement and the treatment time was obtained. Using the TRS 398 formulas with manual calculations the dose rate was used to calculate the treatment time for the prescribed dose.

Ten (10) strips of Gafchromic EBT3 films with the same lot number were cut to dimensions of 2.6 cm × 3.2 cm and inserted in the manual water phantom. The films were exposed to known range of doses using the calculated treatment time.

This was done perpendicularly one after the other to the cobalt 60 beam and their treatment times calculated. The Gafchromic films were scanned and analyzed after 24 hours to allow the film's colorization to reach its peak. Clinical insertions were performed on the locally constructed phantoms by inserting various configurations of Fletcher suite of applicator in the phantom. The C-arm imager was used to take orthogonal images which were then used for treatment planning to generate the prescribed doses for treatment and the HDR was used to measure dose distribution to the regions of interest. Doses to the bladder and rectum was measured with the strips of calibrated Gafchromic. The doses measured from the films were compared to the optimized dose from the TPS to verify the treatment system. A model was developed from the data obtained for dose to the bladder and the rectum. The results obtained from the measurements are presented and discussed in chapter four.

CHAPTER FOUR

RESULTS AND DISCUSSION

Introduction

This chapter presents the various analysis of the results obtained. The in-house water phantom constructed which mimics the radiological and physical properties of tissues was used in measuring dose distribution to the bladder and rectum. Different configurations of the Fletcher suite of applicators were used to perform clinical insertions on the locally constructed phantom and the doses measured with Gafchromic EBT3 films were compared with results from the TPS. The findings from this study have been discussed. This chapter also details the correlation between the findings of this study and other related findings.

Phantom Design and Construction

The phantom was designed to meet certain design criteria so that it can test realistic anatomic clinical situations. Computed tomography (CT) was used to obtain the relative electron density of the perspex sheet used in the entire design. It was determined to be 1.069 which is comparable to water. This makes the phantom suitable for dose measurements.

Results of Beam Output Measurement and Film Calibration

The beam output measurement was done using the IAEA calibration protocol (TRS 398). The correction factors for the dosimeter was determined. Table 1 shows readings of temperature-pressure correction factor of the dosimeter. Table 2 shows the polarity correction factor of the electrometer

readings at $+V_1$ and $-V_1$ respectively. The reference conditions have been presented in Table 3. The data in Table 4 shows the parameters of the TRS 398.

Table 1: Initial and Final Temperature and Pressure

	Temperature(℃)	Pressure (KPa)
Initial	27.3	101.3
Final	24.5	101.3
Mean	25.9	101.3

Table 2: Summary for Polarities of Electrometer Readings

Polarity	Charge (nA)
+300V	27.983
+150V	27.999
-300V	27.981

Table 3: Reference Conditions of Electrometer Readings

Reference Conditions		
Temperature (℃)	Pressure (KPa)	Calibration Factor (Gym^2/Ah)
22	101.325	4.824×10^5

Table 4: TRS 398 and treatment time Parameters for Absorbed Dose to Water Determination

Parameter	Value
$N_{d,w}(Gy/C)$	5.402×10^7
K_{TP}	1.029054832
K_{pol}	1.000547945
K_{ele}	1.0000
K_{sat}	1.000182782
$Dw(5cm)$	1.01525
$Dplastic(5cm)$	1.00408225
$Dw(Zmax)\, cGy/min$	126.30
Scaling factor	0.998
Shutter time	-0.01
Decay factor	0.9153
$PDD/100$	0.804

The output of the film was calibrated against that of the 0.6 cc ionization chamber using IAEA TRS 398 protocol. The calibration values of the three-color channels of the film was determined. This comprises of the initial intensity of the unexposed film, final intensity of the irradiated film, the duration of the irradiation and the corresponding OD determined. Table 5 shows the calibration values of the film for the Red channel. Table 6 shows the calibration values of the film for the green channel. Table 7 shows the calibration values of the film

for the Blue channel. Table 8 shows the calibration values of the film for the Green Channel which was used for calibration of the Gafchromic EBT3 Films

Table 5: Calibration Values for Red Channel

Dose (cGy)	Treatment Time(mins)	Intensity (I_o)	Intensity(I)	Optical Density
50	0.54	82.31	69.23	0.08
100	1.08	82.31	67.84	0.13
200	2.15	82.31	64.92	0.19
400	4.30	82.31	60.26	0.26
600	6.46	82.31	53.27	0.32
800	8.61	82.31	51.39	0.35
1000	10.76	82.31	48.34	0.37

Table 6: Calibration Values for Green Channel

Dose (cGy)	Treatment Time(mins)	Intensity (I_O)	Intensity(I)	Optical Density
50	0.54	117.74	69.23	0.04
100	1.08	117.74	67.84	0.08
200	2.15	117.74	64.92	0.14
400	4.30	117.74	60.26	0.23
600	6.46	117.74	53.27	0.32
800	8.61	117.74	51.39	0.37
1000	10.76	117.74	48.34	0.42

Table 7: Calibration Values for Blue Channel

Dose (cGy)	Treatment Time(mins)	Intensity (I_o)	Intensity(I)	Optical Density
50	0.54	70.82	69.23	0.01
100	1.08	70.82	67.84	0.02
200	2.15	70.82	64.92	0.04
400	4.30	70.82	60.26	0.07
600	6.46	70.82	53.27	0.12
800	8.61	70.82	51.39	0.14
1000	10.76	70.82	48.34	0.17

Table 8: Green Channel used for the Calibration of the Gafchromic EBT3 Films

Dose (cGy)	Optical Density
50	0.01
100	0.02
200	0.04
400	0.07
600	0.12
800	0.14
1000	0.17

A calibration curve was plotted to show the variation of the optical density with the dose. In Figure 32, the red, green and blue (RGB) channels were selected and plotted. The Green channel best fit the regression so this was used for the calibration as shown in Figure 33. In Figure 33, a plot of dose as a function of OD is shown for the Gafchromic EBT3 film. The Regression equation and the correlation coefficient R^2 are presented above the graph (Figure 33). After the irradiation of the Gafchromic films, a good linear correlation was obtained between the absorbed dose and the optical density of the film. The correlation coefficient of $R^2 = 0.998$, was very close to unity and this signifies that the regression equation can be used to predict the absorbed dose of the film using its optical density (OD).

Microsoft excel was used to obtain the regression equation and this is given as:

$$y = 5718.6x^3 - 94.833x^2 + 1388.7x - 3.9103 \quad (29)$$

where x is the optical density and y is the measured dose (dependent parameter). The optical densities of each irradiated Gafchromic EBT3 film in this research were converted to dose using equation 29 from the calibration curve (Figure 33).

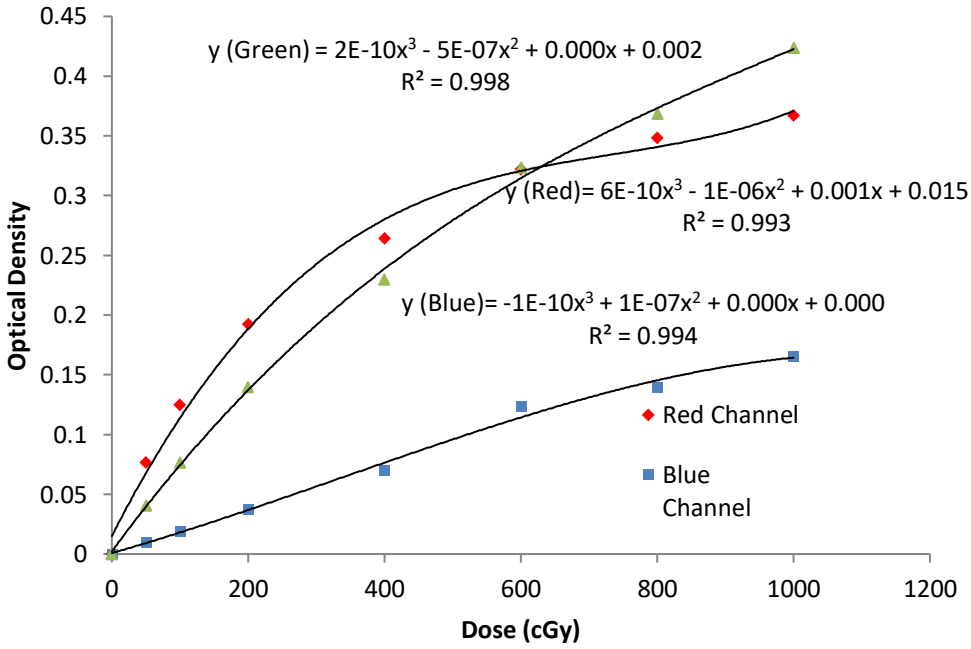

Figure 32: Calibration Curve for the Various Color Channels of the Film

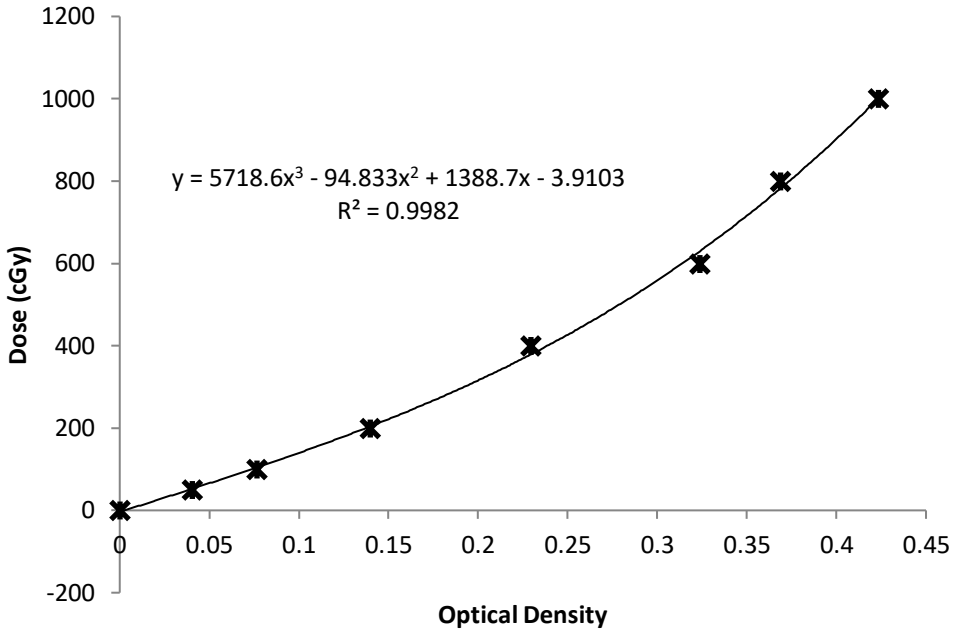

Figure 33: Calibration Curve for the Green Channel

Film Readings

The intensities of the films were measured after they have been exposed to radiation dose. The film intensities were converted to optical densities using equation 21. The optical densities were inserted into the calibration equation 29 to obtain the doses measured by the Gafchromic EBT3 film. The Appendix A-1 shows the film intensities and their corresponding optical densities measured. Appendix D-1 and D-2 shows strips of irradiated and unirradiated Gafchromic EBT3 films used for measuring doses to the bladder and rectum.

Results of Reproducibility Test on the Scanner

A reproducibility test was performed on the EPSON Scanner. This was done by scanning a film repeatedly at different times and was found to be below 0.5%. The film non-uniformity and film-to-film variations determined from

eight films selected randomly from the same film lot number using the method proposed by Saur et al (Saur & Frengen, 2008) were less than 1.2%.

Results of Overall Accuracy of the Gafchromic EBT3 Films

Using the method proposed by Van et al, 2008 (Van Battum, Piersma & Heukelom, 2008), the overall accuracy of the Gafchromic EBT3 films was determined. This takes into consideration the most pronounced sources of uncertainties in dose determination when using the film (scanner, lateral correction, fit accuracy, intra-batch variation, background, intrinsic film inhomogeneity). An overall uncertainty of less than 2.5% was obtained using the error propagation analysis.

Treatment Planning (Dose to Prescription Point)

During the clinical insertions on the phantom, doses were prescribed to Point A and the surface of the ovoids. Dose prescribed to point A represents the location where the uterine vessels cross the ureter. The tolerance of these structures is the main limiting factor in the irradiation of the uterine cervix. Doses were also prescribed to the surface of the ovoids and to 0.5 cm from the surface of the ovoids. Figure 34 shows a sample of doses calculated by the TPS when only cylinders were used to perform clinical insertions on the phantom. Figure 35 shows a sample of doses calculated by the TPS when the Fletcher suites of applicators were used to perform clinical insertions on the phantom. Appendix E-1 to E-7 shows the orthogonal radiographs imported into the TPS for planning. Appendix F-1 to F-7 shows windows of treatment plans for dose calculation. Appendix G-1 to G-11 showed dose control point reports from the TPS.

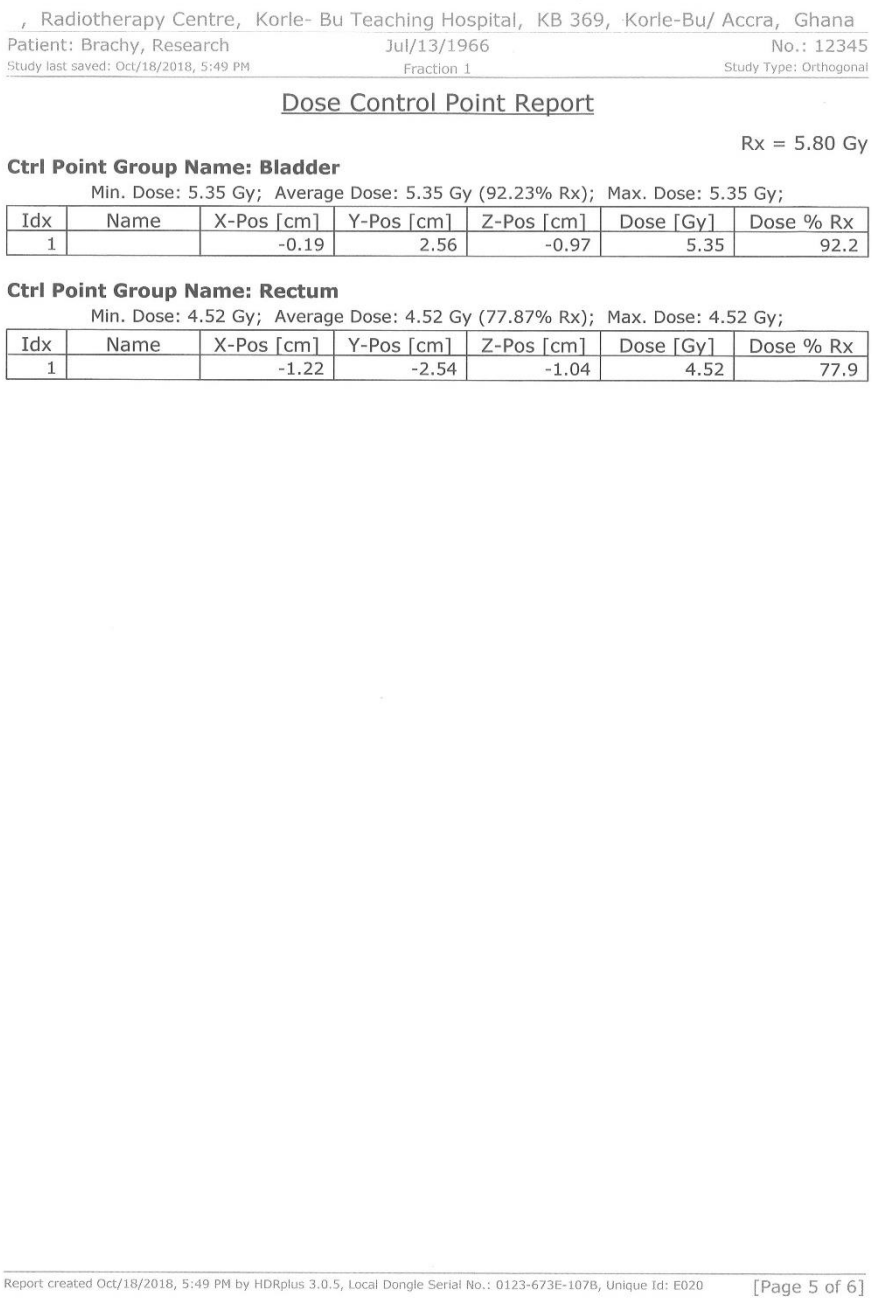

, Radiotherapy Centre, Korle- Bu Teaching Hospital, KB 369, Korle-Bu/ Accra, Ghana

Patient: Brachy, Research Jul/13/1966 No.: 12345

Study last saved: Oct/18/2018, 5:49 PM Fraction 1 Study Type: Orthogonal

Dose Control Point Report

Rx = 5.80 Gy

Ctrl Point Group Name: Bladder

Min. Dose: 5.35 Gy; Average Dose: 5.35 Gy (92.23% Rx); Max. Dose: 5.35 Gy;

Idx	Name	X-Pos [cm]	Y-Pos [cm]	Z-Pos [cm]	Dose [Gy]	Dose % Rx
1		-0.19	2.56	-0.97	5.35	92.2

Ctrl Point Group Name: Rectum

Min. Dose: 4.52 Gy; Average Dose: 4.52 Gy (77.87% Rx); Max. Dose: 4.52 Gy;

Idx	Name	X-Pos [cm]	Y-Pos [cm]	Z-Pos [cm]	Dose [Gy]	Dose % Rx
1		-1.22	-2.54	-1.04	4.52	77.9

Report created Oct/18/2018, 5:49 PM by HDRplus 3.0.5, Local Dongle Serial No.: 0123-673E-107B, Unique Id: E020 [Page 5 of 6]

Figure 34: Dose Control Point Report from the TPS for Cylinders only

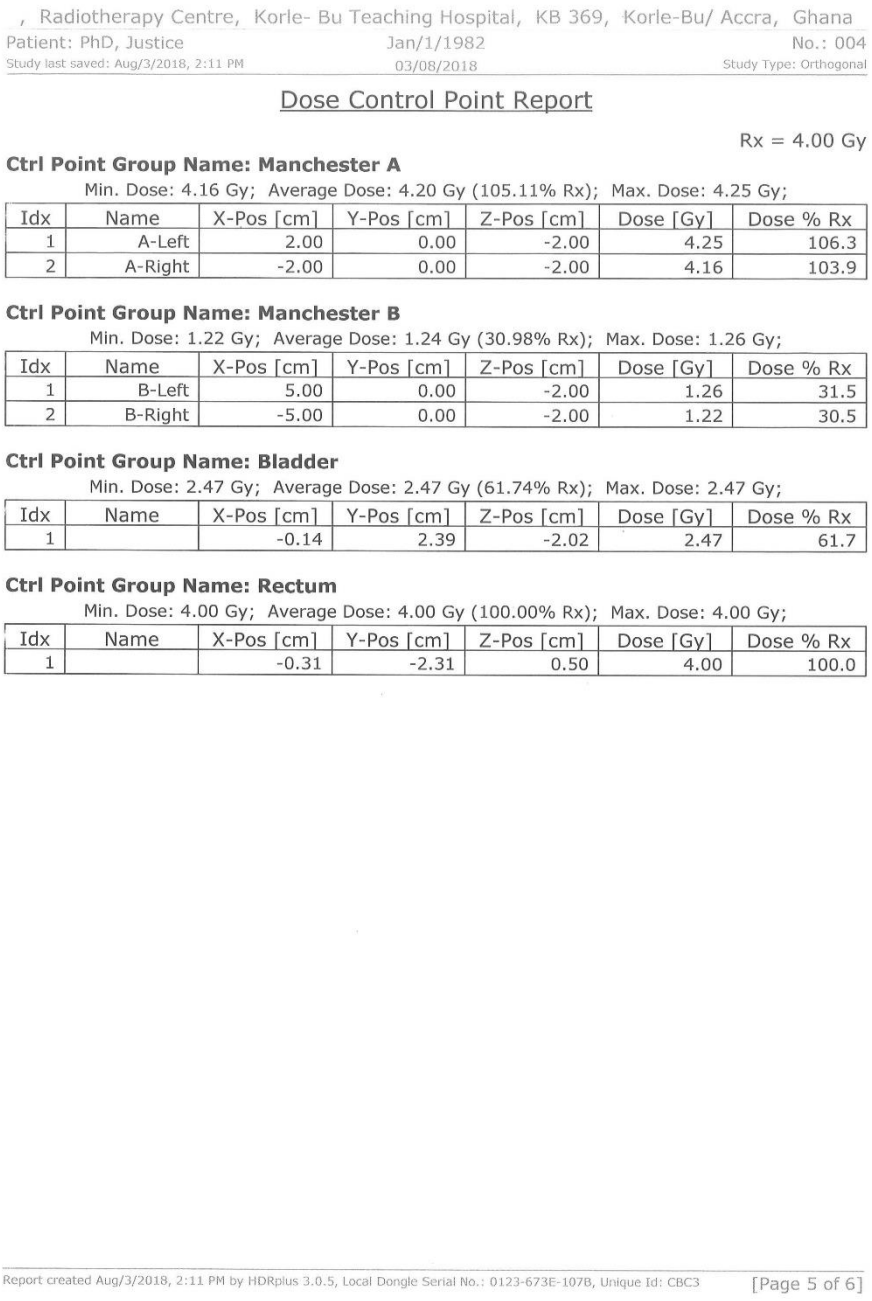

, Radiotherapy Centre, Korle- Bu Teaching Hospital, KB 369, Korle-Bu/ Accra, Ghana

Patient: PhD, Justice | Jan/1/1982 | No.: 004

Study last saved: Aug/3/2018, 2:11 PM | 03/08/2018 | Study Type: Orthogonal

Dose Control Point Report

Rx = 4.00 Gy

Ctrl Point Group Name: Manchester A

Min. Dose: 4.16 Gy; Average Dose: 4.20 Gy (105.11% Rx); Max. Dose: 4.25 Gy;

Idx	Name	X-Pos [cm]	Y-Pos [cm]	Z-Pos [cm]	Dose [Gy]	Dose % Rx
1	A-Left	2.00	0.00	-2.00	4.25	106.3
2	A-Right	-2.00	0.00	-2.00	4.16	103.9

Ctrl Point Group Name: Manchester B

Min. Dose: 1.22 Gy; Average Dose: 1.24 Gy (30.98% Rx); Max. Dose: 1.26 Gy;

Idx	Name	X-Pos [cm]	Y-Pos [cm]	Z-Pos [cm]	Dose [Gy]	Dose % Rx
1	B-Left	5.00	0.00	-2.00	1.26	31.5
2	B-Right	-5.00	0.00	-2.00	1.22	30.5

Ctrl Point Group Name: Bladder

Min. Dose: 2.47 Gy; Average Dose: 2.47 Gy (61.74% Rx); Max. Dose: 2.47 Gy;

Idx	Name	X-Pos [cm]	Y-Pos [cm]	Z-Pos [cm]	Dose [Gy]	Dose % Rx
1		-0.14	2.39	-2.02	2.47	61.7

Ctrl Point Group Name: Rectum

Min. Dose: 4.00 Gy; Average Dose: 4.00 Gy (100.00% Rx); Max. Dose: 4.00 Gy;

Idx	Name	X-Pos [cm]	Y-Pos [cm]	Z-Pos [cm]	Dose [Gy]	Dose % Rx
1		-0.31	-2.31	0.50	4.00	100.0

Report created Aug/3/2018, 2:11 PM by HDRplus 3.0.5, Local Dongle Serial No.: 0123-673E-107B, Unique Id: CBC3 [Page 5 of 6]

Figure 35: Dose Control Point Report from the TPS for Fletcher Suites of Applicators

Bladder and Rectal Dose

The doses calculated by the TPS for the bladder and the rectum have been shown in Appendix A-2. The doses measured by the film for the bladder and the rectum have been presented in Appendix A-3. The film doses were then compared with the TPS doses. The differences between the film doses and the TPS doses measured have been presented in Appendix A-4. The deviations between the film doses and the TPS doses were expressed as percentage difference of the TPS dose using equation 30. This is expressed as:

$$\%\, difference = \frac{TPS\ Dose - Film\ Dose}{TPS\ Dose} \times 100 \qquad (30)$$

Summary of Results

The summary of comparison of TPS dose with film dose for both bladder and rectum has been shown in Table 9.

Table 9: Summary of Comparison of TPS Dose with Film Dose for the Bladder and Rectum

nth insertions	Bladder Dose (Gy)	Rectal Dose (Gy)
	% Difference	% Difference
Mean	15.38	14.73
MIN	-29.03	-47.22
MAX	43.75	51.06
SD	±10.61	±12.26

Results from Modeling

The statistical modeling process was based on linear approach for modeling the relationship between scalar dependent variables and independent variables. The relationships between the parameters were modeled using linear predictor functions whose unknown model parameters were calculated from the data. Appendix B-1 contains the initial intensity of the unexposed film, the final intensity of the exposed film and the dose measured by the irradiated film. The data in Appendix B-1 was the population used in modeling the dose. The linear approach method used to model the relationship between the initial intensity I_O, final intensity I of the film and the corresponding dose measured by the film. The initial I_O, however, had had no impact on the dose calculated therefore it was not included in the model. The model enabled the calculation of dose to rectum and bladder for error detection and variation analysis during treatment. Two separate equations were developed respectively for the bladder and the rectum. The scatter plot of dose against intensity for bladder has been shown in Figure 36. Figure 37 shows the scatter plot of dose against intensity for rectum.

Regression Equation for Dose to the Bladder

$$\widehat{\text{Bladder Dose}} = 11.520 - 0.108\text{I}_\text{B} \quad (31)$$

where I_B is the intensity of the irradiated film for the bladder

Regression Equation for Dose to the Rectum

$$\widehat{\text{Rectum Dose}} = 11.611 - 0.110\text{I}_\text{R} \quad (32)$$

where I_R is the intensity of the irradiated film for the rectum

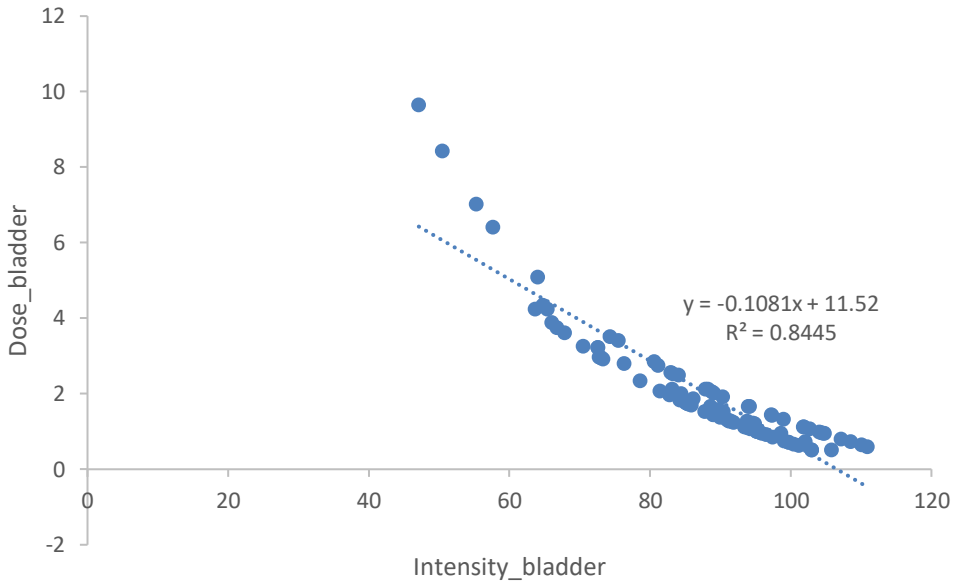

Figure 36: Scatter Plot of Dose against Intensity for Bladder

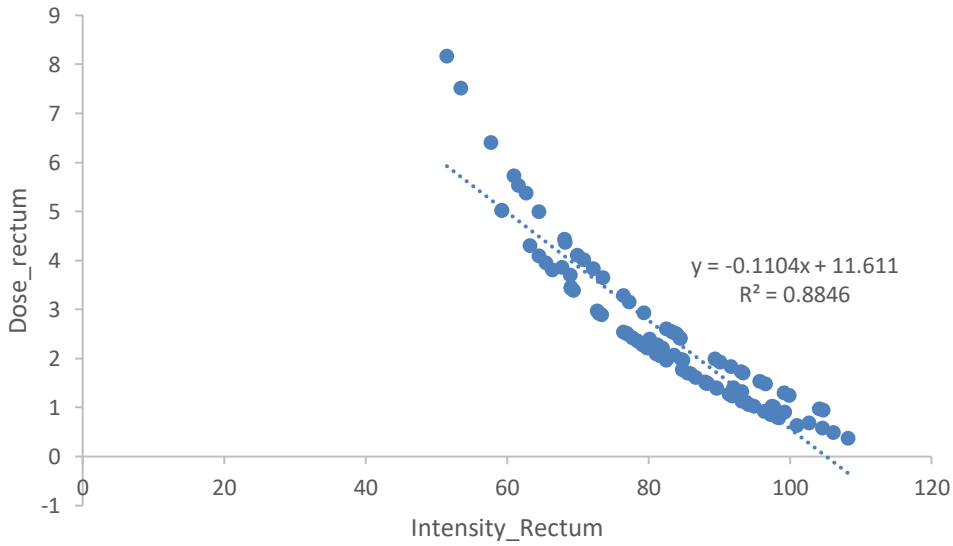

Figure 37: Scatter Plot of Dose against Intensity for Rectum

Analysis and Interpretation of the Model Developed

Model Summary (Rectum)

Table 10 illustrates the analysis of the model developed for dose calculation to the rectum. The model summary shows the strength of the association between dose to the rectum and intensity of the radiation measured by the film to the rectum(I_R). From Table 10, R indicates the correlation coefficient between rectal dose and intensity(I_R).

Table 10: Summary of Analysis of the Model Developed for Dose Calculation to the Rectum

Model Summary					
Model	R	R Square	Adjusted R Square	Std. Error of the Estimate	Durbin-Watson
1	0.941[a]	0.885	0.883	0.53066	0.682

a. Predictors: (Constant), I_R

b. Dependent Variable: Rectum Dose

This is 94.1%, which implies that there exists a strong relation between the dose to the rectum and the intensity(I_R). In addition, adjusted R-Square shows the coefficient of determination, which takes into consideration the sample size. From the table, it shows that the total variation in rectal dose is explained by 88.3% of intensity(I_R), thus, intensity(I_R) has a very good impact on dose.

Test for Independence

The Durbin-Watson test value of 0.682 in Table 10 indicates that the error terms of the regression model are dependent since it does not lie within 1.50 and 2.50, which is acceptable range.

Test of Linearity (Analysis of Variance)

The ANOVA in Table 11 shows the significance of the linearity of the model. The F-statistics of the model (regression) is 713.098 with a p-value of 0.000. The p-value of 0.000 shows that there exists a linear relation between dose to the rectum and the intensity of the rectum I_R at 5% level of significance since it is less than 0.05. Therefore, the model is a best fit.

Table 11: Test of Linearity of the Model Developed for Dose Calculation to the Rectum

ANOVA[a]

Model		Sum of Squares	Df	Mean Square	F	Sig.
1	Regression	200.807	1	200.807	713.098	0.000[b]
	Residual	26.189	93	0.282		
	Total	226.996	94			

a. Dependent Variable: Rectum Dose

b. Predictors: (Constant), I_R.

The Table 12 above shows that any change in intensity (I_R) decreases dose to the rectum by 0.110. This implies that intensity (I_R) has significant negative effect on rectum dose at 5% level of significance.

The VIF value for the unexposed film at the rectal point (I_O) and the irradiated film at the rectal point (I_R) is 1. This implies that there is no existence of inter-relation between the predictor (multicollinearity).

Table 12: Regression Coefficients Estimates of the Model Developed for Dose Calculation to the Rectum

Regression Coefficients Estimates				
Model	Unstandardized Coefficients		T	Sig.
	B	Std. Error		
(Constant)	11.611	0.346	33.528	0.00.
IR	0-.110	0.004	-26.704	0.00

a. Dependent Variable: Rectum Dose

Regression Model for Rectum Dose

$$Dose(Gy) = 11.611 - 0.110 \times I_R$$

Normality Test

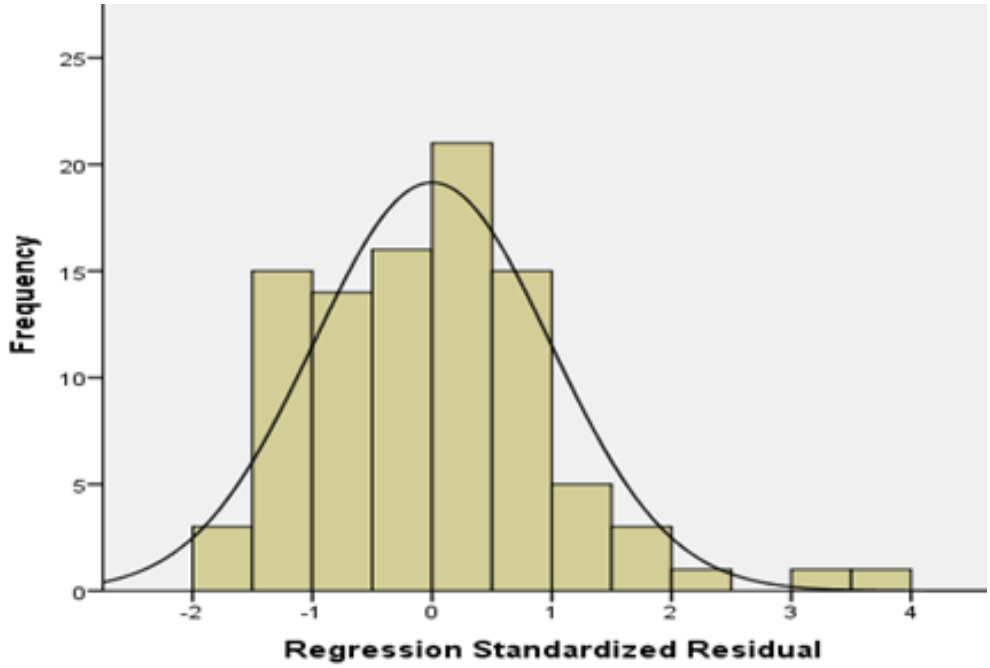

Figure 38: Histogram Showing Normality Test for the Rectum.

The histogram in Figure 38 shows the test for normality. The curve shows that the histogram is a normal curve. This meets the assumptions of normality.

Constancy in Variance (Homoscedasticity)

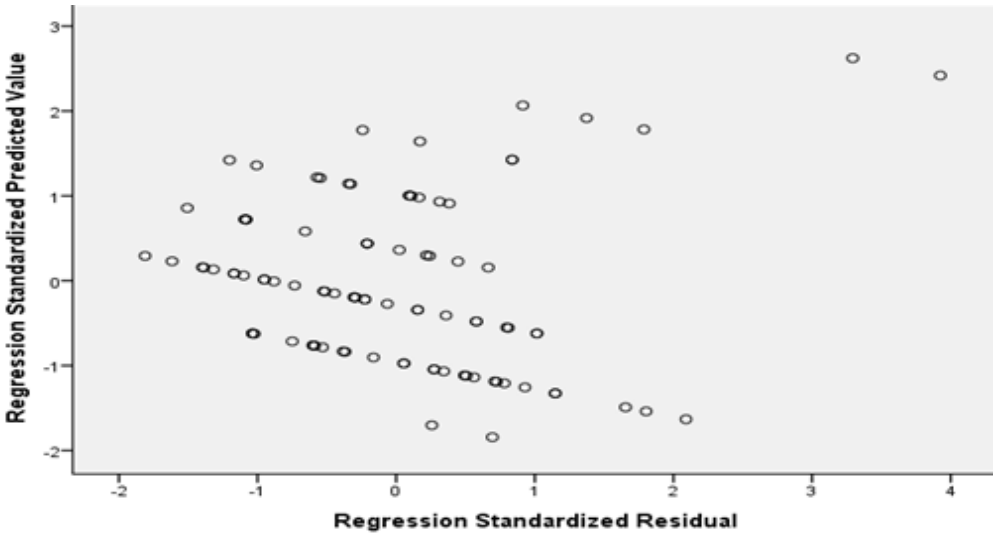

Figure 39: Scatter Plot for Constancy in Variance for the Rectum

The scatter plot in Figure 39 above shows that there is no pattern between the residuals. This indicates that the models meet the assumption of constancy in variance.

Model Summary for the Bladder

The model summary for the bladder in Table 13 shows the strength of the association between dose to bladder and the intensity of radiation measured by the film to the bladder(I_B). From Table 13, R indicates the correlation coefficient between dose to the bladder and the intensity of the bladder (I_B). This is 91.9%, which implies that there exists a strong relation between bladder dose and intensity(I_B).

In addition, adjusted R Square shows the coefficient of determination, which takes into consideration the sample size. From Table 13, it shows that the total variation in Bladder is explained by 84.3% of I_B, thus, I_B have a very good impact on Bladder.

Table 13: Summary of Analysis of the Model Developed for Dose Calculation to the Bladder

Model Summary

Model	R	R Square	Adjusted R Square	Std. Error of the Estimate	Durbin-Watson
1	0.919	0.845	0.843	0.639	0.726

a. Predictors: (Constant), I_B.
b. Dependent Variable: Bladder Dose

Test for Independence

The Durbin-Watson test value of 0.726 in Table 13 indicates that the error terms of the regression model are dependent since it does not lie within 1.50 and 2.50, which is the acceptable range.

Test of Linearity (Analysis of Variance)

The ANOVA in Table 14 shows the significance of the linearity of the model. The F-statistics of the model (regression) is 505.187 with a p-value of 0.000. The p-value of 0.000 shows that there exists a linear relation between dose to the bladder and the intensity of the bladder (I_B) at 5% level of significance since is less than 0.05. Therefore, the model is a best fit.

Table 14: Test of Linearity of the Model Developed for Dose Calculation to the Bladder

ANOVA

Model		Sum of Squares	Df	Mean Square	F	Sig.
1	Regression	206.307	1	206.307	505.187	0.000[b]
	Residual	37.979	93	0.408		
	Total	244.286	94			

a. Dependent Variable: Bladder Dose

b. Predictors: (Constant), I_B

Regression Coefficients Estimates

The Table 15 shows that any change in Intensity of the Bladder (I_B) decreases bladder dose by 0.108. This implies that I_B has significant negative effect on the bladder dose at 5% level of significance.

The VIF value for the unexposed film at the bladder point (I_O) and the irradiated film at the bladder point $(I_B)$is 1, which indicates that there is no existence of inter-relation between the predictor (multicollinearity).

Table 15: Regression Coefficients Estimates of the Model Developed for Dose Calculation to the Bladder

Regression Coefficients Estimates					
Model		Unstandardized		T	Sig.
		B	Std. Error		
	(Constant)	11.52	0.427	26.98	0
	IB	-0.108	0.005	-22.476	0

a. Dependent Variable: Bladder dose

Regression Model for Bladder Dose

$$Dose(Gy) = 11.520 - 0.108 \times I_B$$

Normality Test

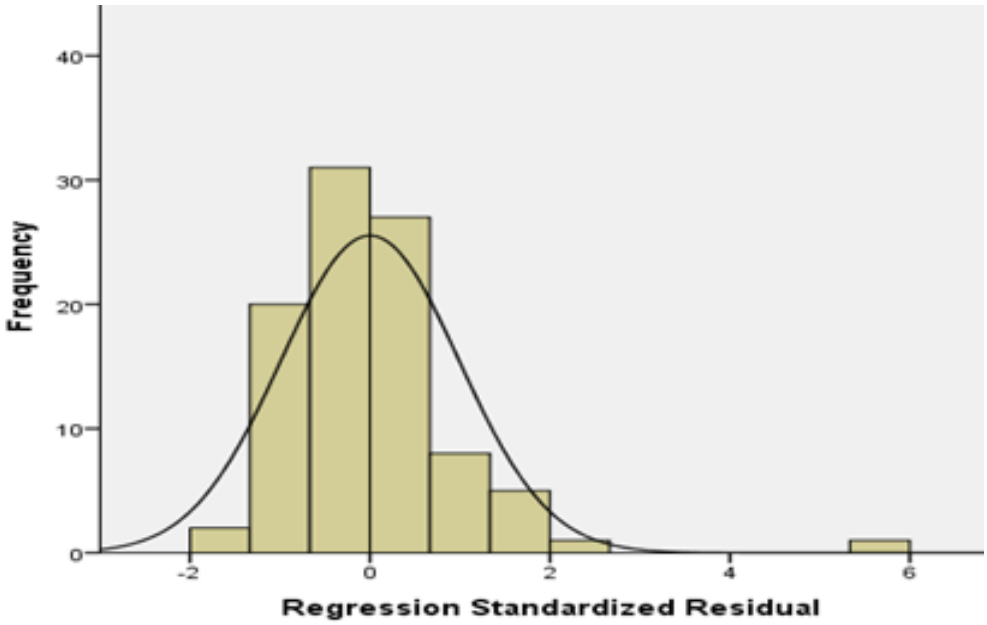

Figure 40: Histogram Showing Normality Test for the Bladder

The histogram in Figure 40 shows the test for normality for the bladder. The curve shows that the histogram is a normal curve. This meets the assumptions of normality.

Constancy in Variance (Homoscedasticity)

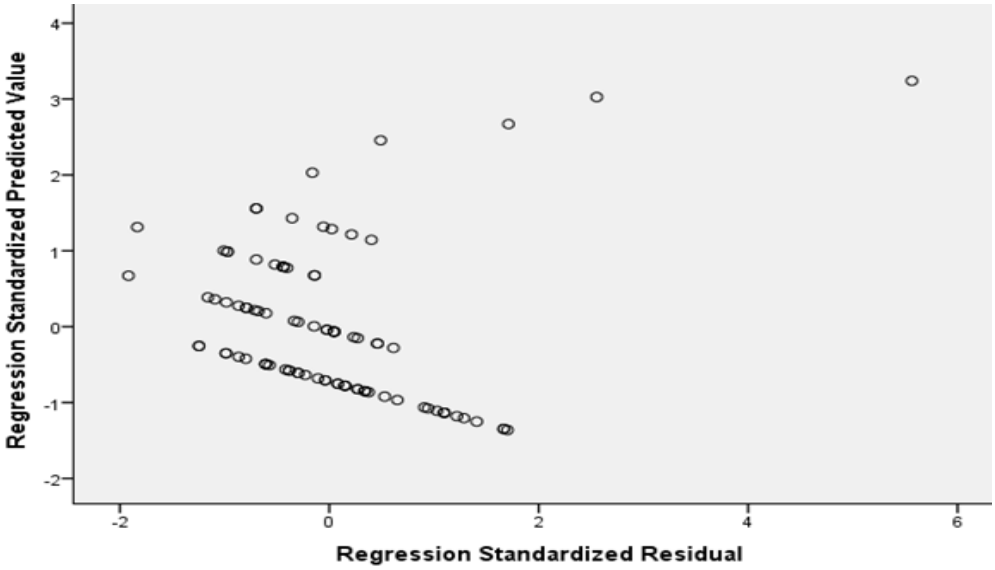

Figure 41: Scatter Plot for Constancy in Variance for the Bladder

The scatter plot for constancy in variance for the bladder depicted in Figure 41 illustrates that there is no pattern between the residuals. This indicates that the model meets the assumption of constancy in variance.

Results from Model Validation

In order to validate the model another, clinical procedure was carried out by measuring doses to the bladder and the rectum. The intensities of the irradiated films were measured for the bladder and the rectum using ImageJ. The intensities of the irradiated films for the bladder were then inserted into equation 31 to calculate dose to the bladder. The intensities of the irradiated films for the rectum were also inserted into equation 32 to calculate dose to the rectum.

The dose calculated by the model (expected) was then compared with the TPS dose (actual). The differences between the TPS dose and the dose calculated by the model have been tabulated in Appendix C-1. The deviations between the TPS dose and the dose calculated using the model was expressed as percentage difference of the TPS dose using equation 33. This is expressed as:

$$\%\, difference = \frac{TPS\ Dose - Model\ Dose}{TPS\ Dose} \times 100 \qquad (33)$$

Table 16 shows the comparison between dose calculated by the model and dose determined by the TPS. The results from the study was compared with other studies in Table 17 and 18.

Summary of Results

Table 16: Comparison of TPS Dose with Dose calculated by the Model

nth insertions	Bladder Dose (Gy)	Rectal Dose (Gy)
	% Difference	% Difference
Mean	9.53	13.57
MIN	-22.68	-34.51
MAX	22.04	26.84
SD	±8.04	±8.46

Table 17: Comparing the Results of this Study with different Investigators (Bladder)

Film	Model	Gholami et al, 2013	AAPM TG-46 (Reference)
$\pm 15.38\%$	$\pm 9.53\%$	$\pm 23.40\%$	$\pm 15.00\%$

Table 18: Comparing the Results with different Investigators (Rectum)

Film	Model	Gholami et al, 2013.	AAPM TG-46 (Reference)
$\pm 14.73\%$	$\pm 13.57\%$	$\pm 23.40\%$	$\pm 15.00\%$

Results from the Coding of the Model

Visual Studio programming tool was used to write a code for calculating dose to both the bladder and the rectum. Figure 42 shows the Dose conversion model developed which can be installed for clinical applications. Figure 43 depicts a sample of how the intensity is converted to dose. Appendix H shows the written codes for the dose conversion model.

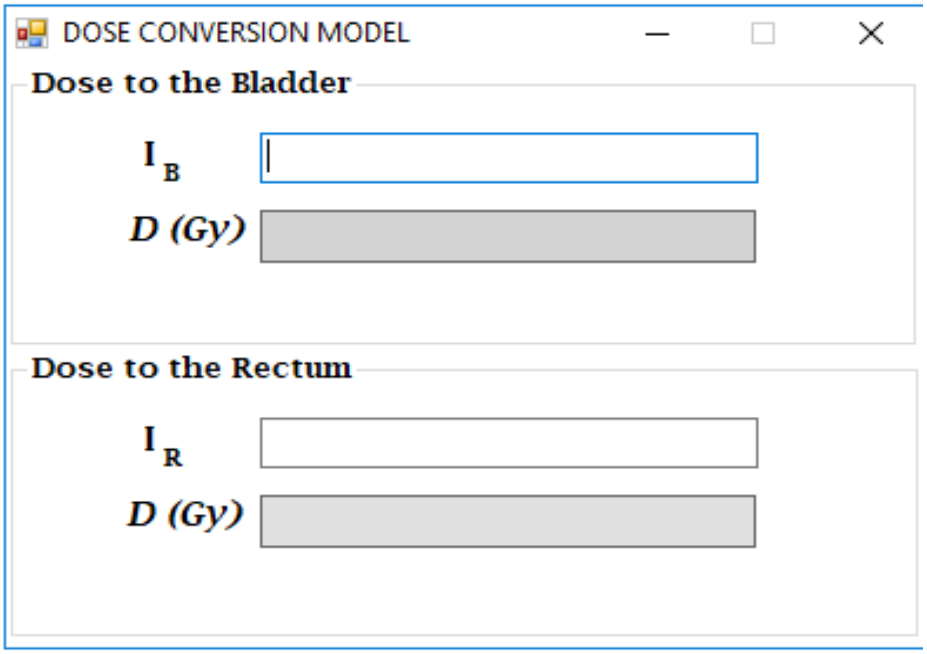

Figure 42: Interface of Dose Conversion Model Generated from the Coding

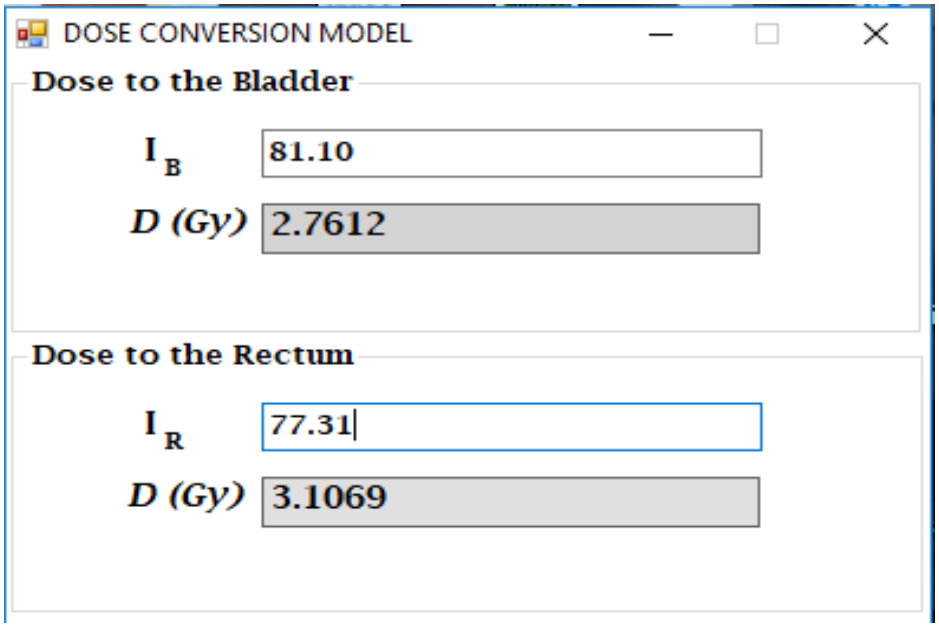

Figure 43: Interface of Dose Conversion Model Generated from the Coding

Discussions

A water phantom was locally constructed from perspex materials and its electron density was measured to be 0.96 which is closer to unity making it suitable for dose measurements. The perspex materials used mimic radiological properties when irradiated. The relative electron density of the perspex sheet used in the entire design was determined to be 1.066 which is comparable to water. This makes the phantom suitable for dose measurements. The phantom was filled with water because greater part of the human body weight is made up of water. Water was used as substitute for tissues and bones.

The human adult body is made up of 60% water. The brain and heart are composed of 73% water, and the lungs are about 83% water. The skin contains 64% water, muscles and kidneys are 79%, and even the bones are 31% (Mitchell, 2011). Water is an appropriate material because it has the advantage of conducting electricity as required for electron measurements and is universally available (Galbraith, Rawlison, & Munro, 1984). The PMMA material used in constructing the phantom and the water are homogenous; they are the only substitute for tissue and muscles in a real patient when considering BT treatment.

Dosimetry protocols require that dose measurements test be carried out using phantoms, because using human beings for experiments involving radiations could cause cancer. The phantom constructed gave reliable results which are consistent with the AAPM TG-46 recommendations and therefore, can be used for dose distribution measurements in cervical cancer treatment at

the Radiotherapy center. This will help save cost and enable the center to maximize profit.

A total of one hundred and ninety (190) clinical insertions were carried out on the locally constructed phantom using the Fletcher suite of applicators for the bladder and the rectum respectively. In cases where the patient with cervical cancer has her womb removed, only cylinders are used in the treatment so as to fit the anatomical geometry. A complete set of Fletcher suite of applicators including the tandems are used if the uterus is intact. All these configurations were carried out on the phantom during the dose measurements. The absolute values of the doses measured and calculated were used in calculating the mean.

The difference between doses calculated by the TPS and the doses measured by the Gafchromic EBT3 film at the bladder point was 15.38% (mean) ranging from -29.03% to 43.75%. The difference between doses calculated by the TPS and the doses measured by the Gafchromic EBT3 film at the rectum point was 14.73% ranging from -47.22% to 51.06%. The AAPM TG-46 has proposed ±15% (for dose measurements in phantom) deviation of prescribed dose delivery for intracavitary BT (Hanson et al., 1994). The deviation of 15.38% for the bladder is comparable to the ±15% proposed by the AAPM TG 46. Comparing the 14.73% deviation of the rectum to the acceptable limit of ±15% indicates that these deviations are within the range of deviations documented by the AAPM TG 46. The phantom used in this study is a homogenous one. However, the dose distribution measurement carried out by Hanson et al., was done with a phantom that had homogenous and heterogenous

components (Hanson et al., 1994). This could account for some level of variations in measurement done in this study. Gholami, Mirzaei, & Meigooni investigated the source of errors in Treatment Planning of HDR brachytherapy using a phantom with Gafchromic films; they reported a ±23.4% of dose deviation between the TPS and measured dose (Gholami, Mirzaei, & Meigooni, 2013). It can be seen that the deviations reported in this study compare well with other investigations carried out.

This study has shown that the doses predicted by TPS were higher than the doses measured by the film. The study has also shown that 27% of the doses measured by the film were higher than doses calculated by the TPS for the bladder. At the rectal point, 47% of the doses measured by film were higher than the doses calculated by the TPS. The deviations between TPS doses and measured doses larger than 15% occurred in 50% of the entire measurement for the bladder (Appendix A-1). There is a significant difference between the TPS and the measured dose, discrepancies in TPS dose and measured dose for the bladder larger than 30% occurred in 7% of the entire treatment. For the rectum, the discrepancies between TPS dose and measured dose that is larger than 15% occurred in 64% of the entire treatment. Deviations at rectal point larger than 30% occurred in 6% of the entire measurements (Appendix A-1)

There are numerous reports that show that deviations in clinical measurements could be as high as 50%. From the study, the maximum percentage difference between dose calculated by the TPS and dose measured by the Gafchromic EBT3 film was 43.75%, while the minimum percentage difference between dose calculated by the TPS and dose measured by the film was -29.03%. It is observed from the study that the film does not respond appreciably and quite accurately at low energy of the photons. This is due to the energy dependence characteristic of the film.

Many investigators have researched the energy dependence of the films in several applications. (Meigooni et al, 1996). The degree of energy dependence can affect the dosimetry properties of the film when an unknown spectrum of radiation energies is present. Most of these films under-respond at lower energies. Sayeg et al have suggested that the lower response of the film is due to the larger carbon content in the film relative to that in soft tissues.

The TPS used in this study employs the algorithm of AAPM TG 43 dosimetry protocol for calculation of dose. The TG 43 formalism assumes that the entire human body or any medium used as a patient is entirely water equivalent. However, this was not the case during this study or during clinical treatment. The Gafchromic EBT3 film in the phantom during measurements generates an inhomogeneous condition. This is due to the fact that the effective atomic number (Z_{eff}) for the film is 6.84 but the effective atomic number of water is 7.42. The implication is that the dose from the TPS will not correspond entirely with the dose measured by the film. It has been reported that commercially available TPS used by hospitals for treatment uses dose

calculation algorithms that do not account for the impact of the heterogeneities encountered in the film or the patient (Uniyal, Sharma & Naithan 2011).

When using the film in dose measurement, an indirect method is employed. A calibration curve is required to convert the film response or optical density (OD) values to doses. Scanning orientation and scanner uniformity are two main factors that do affect the accuracy and precision in obtaining accurate optical density values. These factors can give higher percentage difference when measuring point doses (Rink, Vitkin, & Jaffray, 2005); Saur and Frengen, 2008); Zeidan, et al, 2006); Martisikova, Ackermann and Jakel, 2008).

In this study the reproducibility of the EPSON scanner was ascertained by scanning a film repeatedly at different times. This was found to be below 0.5%. Film non-uniformity and film-to-film variations measured from six films (randomly selected) from the same film batch (or lot number), following the method proposed by Saur and Frengen (2008), were less than 1.2 %. The overall accuracy of EBT3 film measurements was derived using the method proposed by Van, Hoffmans, Piersma, & Heukelom (2008) that takes into account the most pronounced sources of uncertainties in dose determination (scanner, lateral correction, fit accuracy, intra-batch variation, background and intrinsic film inhomogeneity) and using error propagation analysis an overall uncertainty of less than 2.0 % was observed.

Another factor responsible for the discrepancies between TPS dose and measured dose is the tungsten shields provided in the rectal and bladder compartments of the Fletcher suite of applicators used in this study. The shielding in the applicators minimize dose to the critical organs. During brachytherapy treatment of cervix, clinical complications do result from high doses received by organs at risk (bladder and rectum). Reports from Meli (2002) have also shown that dose deviations as a result of the shielding at some points in these applicators could be high as 25%. Their reports have also been well documented (Meli, 2002). The deviations at points in this study are due to the shielding. The study has shown that shields in the applicators have a significant impact on the dose delivery during brachytherapy. The algorithms used by commercially available treatment planning systems (TPS) do not take into account the effect of the shielding provided in these applicators on dose delivery (Uniyal, Sharma, and Naithani, 2011). Further study can be done to account for the shielding in these applicators and inculcate it into the algorithm of the TPS.

Furthermore, potential organ movements and occasional relocation of the applicator in between imaging and treatments has contributed to the variations in the dose delivery. The position of the applicators and the dosimeter (films) during image acquisition must be the exact position during treatment delivery in order to avoid uncertainties. The measured doses can relate with the TPS dose if this is achieved. BT deals with point doses, hence, a movement of the organ and shift in applicator positions can result in a significant deviation or error.

During the insertion of the Gafchromic films into the rectal and bladder compartments of the phantom, these sections do shift at times due to the nature of the applicators and how the phantom was constructed.

Waldhäusl, Wambersie, Potter, and Georg, (2005) and Seymour, Downes, Fogarty, Izard, and Metcalfe (2011) both conducted IVD for patients undergoing HDR brachytherapy treatments. Their measurements resulted in differences in calculated and measured doses ranging from -31% to +90% for the rectum and from -27% to +26% for the bladder. They also reported that shifts in probe position of 2.5 mm for the rectal probe and 3.5mm for the bladder probe caused dose differences exceeding 10% (Waldhäusl, Wambersie, Potter, & Georg, 2005; Seymour, Downes, Fogarty, Izard, & Metcalfe 2011).

In BT treatment, most of the errors are categorized as 'human error', since it involves a lot of human handling of the procedure. In this study two mathematical algorithms (models) have been developed to enable error detection and variation analysis during HDR brachytherapy of the cervix. A sample test was done using the model to calculate the dose distribution. The mean difference between doses calculated by the TPS and the doses calculated by the model at the bladder point was 9.53% ±8.04. The mean difference between doses calculated by the TPS and the doses calculated by the model at the rectal point was 13.57% ±8.46. Dose deviation to the bladder was less but high to the rectum.

The results of the proposed model are within the ± 15% uncertainty proposed for dose delivery in radiation therapy (Hanson et al., 1994).

Chapter Summary

Dose measurement to the bladder and rectum was done using the locally fabricated water phantom. The phantom met the basic requirements which made it suitable for the dose reading. The electron density of the phantom was found to be 1.069 which is comparable to water. The Gafchromic EBT3 films were calibrated for quality assurance purposes, the films response or optical densities were converted to dose using the calibration equation obtained from the calibration. The calibration equation gave a correlation regression of $R^2 = 0.998$ which is close to unity. A reproducibility test was performed on the EPSON Scanner. This was done by scanning a film repeatedly at different times and was found to be below 0.5%. An overall uncertainty of less than 2.5% was obtained using the error propagation analysis. The doses calculated by the TPS were compared with the doses measured by the Gafchromic EBT3 films.

The difference between the dose calculated by the TPS and the dose measured by the film at the bladder point was 15.38%. This is not far from the proposed ±15% deviation of prescribed dose by the AAPM TG 46 (Hanson et al., 1994). The difference between the dose calculated by the TPS and the dose measured by the film at the rectal point was 14.73%. This is comparable to acceptable dose deviation limit. Two mathematical models were developed from the study to calculate dose to the bladder and rectum for error detection, variation analysis and verification of the HDR BT treatment system at the NCRNM.

For this model, the intensity of radiation measured by the film at the bladder and rectal compartment can be inserted into the model to determine dose

to the bladder and rectum respectively. The model establishes a relation between film intensity and dose. The model for the rectum gives a 94.1% correlation coefficient between the rectal dose and film intensity. The implication is that intensity has a strong impact on the dose. The model for the bladder gave a 91.9% correlation coefficient between the bladder dose and the film intensity. This means that film intensity has a significant impact on dose.

The model was then used to calculate doses measured by the film and compared with doses calculated by the TPS. The difference between the doses calculated by the model compared with the dose calculated by the TPS for the bladder was 9.53%. This compares very well with the proposed dose deviation limit of ±15%. The difference between the doses calculated by the model compared with the dose calculated by the TPS for the rectum was 13.53%. This is also within the acceptable limit.

Several factors might have accounted for the variations in the dose distribution measurements. The algorithm used by the TPS assumes that the human body is completely made of water and therefore disregards tissue heterogeneities; however, this is not the case in real patient treatment. An applicator movement is another contributing factor to the deviations in dose measurements. A shift in position during treatment will affect dose delivered to the treatment target.

CHAPTER FIVE

SUMMARY, CONCLUSIONS AND RECOMMENDATIONS

Overview

This final chapter provides an overview of the main findings of the study. The main objective of this study is to determine the absorbed dose to the bladder and rectum (organs at risk) in the treatment of cervical cancer using the BEBIG Multisource HDR BT treatment unit in order to establish an in-vivo dosimetric and quality assurance (QA) protocol for patient treatment. This has become necessary because, clinical complications do result from high doses received by organs at risk in BT treatment of the cervix. There is no independent verification that is independent of how the treatment progresses in the clinical workflow.

In order to address this challenge, a phantom was fabricated from perspex material and clinical insertions were carried out on the phantom using various configurations of the Fletcher suite of applicators. Gafchromic EBT3 was used as a dosimeter to measure doses to the organs at risk. The films were calibrated using the IAEA TRS 398 protocol. The doses measured by the film were then compared to the ones calculated by the TPS to verify the effectiveness of the treatment system. The data obtained from the study was used to develop a mathematical model using the SPSS for calculating dose to the bladder and rectum. The chapter ends with conclusions based on the findings and the recommendations for stakeholders and give suggestions for further research work.

Summary

Accuracy in dosimetry is crucial in BT of the cervix to increase the likelihood of desired treatment outcomes by increasing the tumor control and minimizing dose to surrounding organs that are healthy and at the same time ensuring the validity of the treatment delivery. There is a need for independent verification of the treatment flow in order to establish a highly effective treatment outcome.

Dose distribution within a patient is determined with the help of dosimetric functions and it is measured with phantoms. This is because the materials used in fabricating the phantoms mimic the anatomical properties of the human tissue. The relative electron density of the phantom must be comparable to that of water since the human adult body is made up of about 60% of water. In this study the data from the fabricated phantoms gave desirable results. The relative electron density of the perspex was 1.069.

Gafchromic EBT3 was used as a dosimeter to measure the dose to the bladder and rectal compartment created in the fabricated phantom. For QA purposes, the films were calibrated to measure the doses to the bladder and the rectum. A calibration curve was obtained to convert the film response or OD values to doses. The correlation coefficient of the curve, R^2 was 0.998. This value is close to unity and therefore was used to predict the dose measured by the film using the optical density.

When scanning the film, the scanning orientation and scanner uniformity are the main factors that can affect the accuracy and precision in reading the accurate optical density values of the film.

Therefore, a reproducibility test was performed on the scanner and was found to be below 0.5%. The film's non-uniformity and film to film variation was also found to be less than 1.2%.

In any radiation therapy process, the performance of the TPS is a major component in determining the accuracy of the treatment towards the target volume. In this study, the doses calculated by the TPS were compared to the doses measured by the Gafchromic EBT3 films for both the bladder and the rectum. The difference between the dose calculated by the TPS and the dose measured by the film for the bladder was 15.38%. The difference between the dose calculated by the TPS and the dose measured by the film for the rectum was 14.73%. These dose deviations for the bladder and the rectum are within the proposed dose variations of ±15% in phantom measurements by the AAPM TG 46 (Hanson et al., 1994)

A mathematical model was developed from study which can be used to calculate dose to the bladder and the rectum. This model will limit the numerous steps in calculating dose measured by the film. Dose measurements using the Gafchromic film is dependent on the intensity of light passing through the film. The intensity of radiation measured by the film can be inserted into the model to determine the dose for both rectum and bladder.

In order to validate the model, an insertion was carried out on the phantom and the model was used to calculate dose to bladder and rectum. The results were compared to the dose calculated by the TPS.

The deviation between the dose calculated by the TPS and the dose calculated by the model for the bladder was 9.53%. This is within the acceptable limit. The deviation between the dose calculated by the TPS and the dose calculated by the model for the rectum was 13.57%. This is also comparable to the proposed action level uncertainty for phantom measurements as documented by the AAPM TG 46 (Hanson et al., 1994). The model developed from the study can be used for further research works involving dose measurements.

There were challenges in the construction of the phantom. The distance between the bladder and the rectal compartment was very close. This resulted in the movement of the applicators when inserting the Gafchromic films into the bladder and rectal compartment of the phantom.

Conclusions

The results from this research suggested that the locally constructed phantom is suitable and can be used for dose measurements and system verification during HDR BT of the cervix. The results have shown that the fabricated phantom mimics radiological and anatomic properties of tissues hence make it suitable for dose distribution measurements and further research work relating to cervical cancer. The perspex materials mimic radiological properties and can be used for constructing any local phantom for research purposes. The electron density of the perspex materials is comparable to that of water. The Gafchromic EBT3 films are suitable and can be used as accurate and reproducible detectors for dose measurement to organs at risk during treatment.

The difference between TPS dose and the dose measured by the Gafchromic film for the bladder point is 15.38%. This signifies that it has deviated by a margin of 0.38% from the limit of ±15%. This deviation could be due to the several factors enumerated in the discussion. The difference between TPS dose and dose measured by the Gafchromic film for the rectal point is 14.73%. The rectal point measurements compare well within the dose deviation recommended. The results from the dose distribution measurement using the film are very reliable. This indicates that the method used in this study can be recommended for clinical applications.

The results from this study also highlighted the fact that films have high spatial resolution. This makes the film to have higher sensitivity for dose measurements in high dose gradient located very near to the source giving accurate results.

However, in low dose regions located away from the radiation source the film does not perform very well resulting in high discrepancies in dose measurements.

Furthermore, the inability of the TPS to account for tissue heterogeneities which creates full scatter condition during measurements in the phantom or patients could also be another factor that is responsible for very higher difference between doses measured by the film compared with dose calculated by the TPS. This can be investigated separately by other researches.

The doses measured using the developed model from this study gave results that are consistent with recommendations from the AAPM TG 46. The deviation in the TPS dose compared with the dose calculated by the model at the bladder point is 9.53%, which is within the acceptable limit of ±15%. The deviation between the TPS dose compared with the dose calculated by the model at the rectal point is 13.57%. This is also comparable to the proposed limit.

In conclusion, the phantom fabricated and the mathematical model developed from this study gave reliable results, and can therefore be utilized for the QA procedure to verify the accuracy of the dose distribution before the commissioning of a new TPS.

Recommendations

The following recommendations are made based on the findings of this study to the various stakeholders in the treatment of cervical cancer at the National Centre for Radiotherapy and Nuclear Medicine at the Korle-Bu Teaching Hospital Accra, Ghana.

Medical Physicist

(i) A mathematical model for calculating dose distribution to the bladder and rectum in HDR BT of the cervix has been developed from this study. It is recommended that the Medical Physicists use this model for IVD to determine the variations between TPS dose and measured dose for accurate system verification.

(ii) Establish a faster QA program based on the findings of this study to implement the use of the model developed for faster QA procedures. This will eliminate human interference thereby mitigation errors.

Facility Regulators

The regulatory body in charge of the facility should maintain a consistent monitoring by conducting the necessary checks on the dosimetry effectiveness of the facility at the NCRNM to ensure that patient safety is always maintained.

Further Research

It is recommended that this research is extended to develop other ways of measuring doses to the organs at risk during treatment which can aid an independent verification of the dosimetry system. This research made use of the films for dose measurement; researches can also develop customized TLDs and other detectors to measure the doses to the bladder and rectum for comparison to observe the effectiveness of the dosimeters as well.

REFERENCES

Aldelaijan, S., Mohammed, H., Tomic, N., Liang, L. H., Beblois, F., Sarfehnia, A., Abdel- Rahman, W., Seuntjens, J. & Devic, S. (2011). Radiochromic film dosimetry of HDR 192Ir source radiation fields. *Medical Physics*. 38(11): 6074-6083.

American Association of Physicists in Medicine (AAPM). (1998). Report Report No. 63: *Radiochromic Film Dosimetry Recommendations of AAPM. Radiation Therapy Committee.* Task Group No. 55:6-9.

Ashton, L. P., Cosset, J-M, Levin, V., Martinez, A., Nag, S. (2004). Prevention of high-dose-rate brachytherapy accidents. ICRP Publications 97, Annals of the ICRP. New York, NY: Permagon; 2004.

Attix, F. H. (1998). Introduction to radiological *Physics and Radiation Dosimetry*. John Wiley & Sons, New York.

Avevor, J., Tagoe S. N. A., Amuasi J. H., & Fletcher J. J., (2017). "Dose assessment of the rectum during brachytherapy of cervix using Gafchromic films", *International Journal of Scientific Research in Science, Engineering and Technology (IJSRSET), Online ISSN*: 2394-4099, Print ISSN: 2395-1990, Volume 3 Issue 5, (3)5: 651-659, July-August 2017. Available at www.ijsrset.com. Journal URL: http://ijsrst.com/IJSRSET173487

Avevor, J., Tagoe S. N. A., Amuasi J. H., & Fletcher J. J., (2017). "Dose assessment to the bladder during brachytherapy of the cervix using Gafchromic films", *International Journal of Scientific Research in*

Science, Engineering and Technology (IJSRSET), Online ISSN: 2394-4099, Print ISSN: 2395-1990, 3(6): 97-105, September-October 2017. Available at www.ijsrset.com. Journal URL: http://ijsrst.com/IJSRSET173486

Bahena, J. H, Martinez A, Yan D, Mele E, Edmunson G, Brown D, (1998). Spatial reproducibility of the ring and tandem high-dose rate cervix applicator. Int J RadiatOncolBiolPhys; 41: 13–19.

Beaulieu, L., CarlssonTedgren A, Carrier J-F, Davis SD, Mourtada F, & Rivard MJ. (2012). Report of the Task Group 186 on modelbased dose calculation methods in brachytherapy beyond the TG-43 formalism: current status and recommendations for clinical implementation. Med Phys; 39: 6208–36. doi: 10.1118/1.4747264.

Best® medical international. Best® Theratronics. (2009). Equinox external beam therapy system brochure, Best® medical international.

Brahme, A., Chavauradra, J., & Landberg, T. (1998). Accuracy requirements and quality assurance of external beam therapy with photons. Acta Oncol Supply 1.

Butson, M. J., Yu K. N., Cheung T., & Metcalfe, P. E. (2003). *Radiochromic film for Medical Radiation Dosimetry*, Mater. Sci. Eng., R. 41, 61–120.

Canadian Nuclear Safety Commission. (2012). *Certified Transport Packages and Special Form Radioactive Material*. Canadian Nuclear Safety Commission.

CarlssonTedgren, A., & Grindborg, J. E. (2008). Radiother. Oncol86, 126-30.

Chambers, J. M. (1983). Graphical methods for data analysis. Boston: Duxbury Press.

Chambrette, V., Hardy, S., & Nenot J-C. (2001). Irradiation accidents. Establishment of a data base "ACCIRAD" at the IPSN [in French]. Radioprotection; 36: 477–510. 7.

Cherpak, A. J., Cygler J. E., Perry, G. (2013). Real time measurement of urethral dose and position during permanent seed implantation for prostate brachytherapy. Brachytherapy 2013; 13: 169–77. doi: 10.1016/j. brachy.2013.11.004.

Cunningham, J., Coffey, M., Knoos, T., & Holmberg, O. (2010). *Radiation Oncology Safety Information System (ROSIS)–profiles of participants and the first 1074 incident reports.* RadiotherOncol 2010; 97: 601–7. doi: 10.1016/j.radonc.2010.10.023 8.

Datta, N. R., Kumar, S., Das, K. J., Pandey, C. M., Halder, S., & Ayyagari, S. (2001). Variations of intracavitary applicator geometry during multiple HDR brachytherapy insertions in carcinoma cervix and its influence on reporting as per ICRU report 38. Radiother. Oncol; 60: 15–24.

De Leeuw, A. A., Moerland, M. A., Nomden, C., Tersteeg, R. H., Roesink, J. M., & Jürgenliemk-Schulz, I. M. (2009). "Applicator reconstruction and applicator shifts in 3D MR-based PDR brachytherapy of cervical cancer," Radiother. Oncol. 93, 341–346.

De Leeuw, A. A., Moerland, M. A., Nomden, C., Tersteeg, R. H., Roesink, J. M., & J¨urgenliemkSchulz, I.M. (2009). Applicator reconstruction and applicator shifts in 3D MR-based PDR brachytherapy of cervical cancer. Radiother. Oncol 2009; 93: 341–6. doi: 10.1016/j. radonc.05.003.

DeWerd, L. A, Ibbott, G.S., Meigooni, A.S., Mitch, M.G., Rivard, M. J., & Stump, K. E. (2011). A dosimetric uncertainty analysis for photon-emitting brachytherapy sources: report of AAPM Task Group No. 138 and GEC-ESTRO. Med Phys 2011; 38: 782–801.

Dewerd, L. A., Kissick M. (Eds). (2014). *The Phantoms of Medical and Health Physics: Devices for Research and development*. New York, Springer.

Dimopoulos, J. C. A., Petrow, P., Tanderup, K, Petric P., Berger D., & Kirisits C. (2012) Recommendations from Gynaecological (GYN) GEC-ESTRO Working Group (IV): basic principles and parameters for MR imaging within the frame of image based adaptive cervix cancer brachytherapy. Radiother. Oncol; 103: 113–22.

Elfrink, R. J. Met. (2001). Radiotherapy and Oncology. chapter 59297-306 Retrieved from www.iopscience.iop.org

Fragoso, M. (2004). Application of Monte Carlo Techniques for the Calculation of Accurate Brachytherapy Dose Distributions., University of London, London,UK.

Fragoso, M., Love, P. A., Verhaegen, F., Nalder, C., Bidmead, A. M., & Leach, M. (2004). The dose distribution of low dose rate Cs-137 in intracavitary brachytherapy: comparison of Monte Carlo simulation, treatment planning calculation and polymer gel measurement. Phys Med Biol, 49 (24), 5459-5474.

Galbraith, D. M., Rawlison, J. A., & Munro, P. (1984). Dose errors due to charge storage in electron irradiated plastic phantoms. Med. Physics., 21, 1605-9.

Gholami, S., Mirzaei, H., Meigooni, A., (2013). "Investigation about source of errors in Treatment Planning of HDR brachytherapy by using a New Phantom Design combined with Gafchromic Films and TG-43 calculation". Med. Phys. 40:285-286.

Haack, S., Nielsen, S. K., Lindegaard, J.C., Gelineck, J., & Tanderup, K. (2009). Applicator reconstruction in MRI 3D image-based dose planning of brachytherapy for cervical cancer. RadiotherOncol ; 91: 187–93. doi: 10.1016/j.radonc.2008.09.002.

Haie-Meder, C., P¨otter, R., Van Limbergen, E., Briot, E, De Brabandere M, & Dimopoulos J. (2005). Recommendations from Gynaecological (GYN) GEC-ESTRO Working Group (I): concepts and terms in 3D image-based 3D treatment planning in cervix cancer brachytherapy with emphasis on MRI assessment of GTV and CTV. RadiotherOncol; 74: 235–45.

Hanson, W., F., Kutcher, G., J., Coia, L., Gillin, M., Leibel, S., Morton, R., J. (1994). "Comprehensive QA for radiation oncology, AAPM task group Number 46". Med. Phys. 21(4):581-618.

Hass, J. S., Dean, R. D., & Mansfield, C. M., (1980). Evaluation of a new Fletcher applicator using cesium-137.Int J Radiat.Oncol Bio Phys;6.

Hellebust, T. P, Kirisits C., Berger, D., P´erezCalatayud, J., De Brabandere, M., & De Leeuw, A. (2010). Recommendations from Gynaecological (GYN) GEC-ESTRO Working Group: considerations and pitfalls in commissioning and applicator reconstruction in 3D image-based treatment planning of cervix cancer brachytherapy. RadiotherOncol; 96: 153–60.

Hellebust, T. P., Dale, E., Skjønsberg, A., Rune, D. R., (2001). Inter fraction variations in rectum and bladder volumes and dose distributions during high dose rate brachytherapy treatment of the uterine cervix investigated by repetitive CT-examinations. RadiotherOncol; 60: 273–80.

Hellebust, T. P., Tanderup, K., Lerv˚ag, C., Fidarova, E., Berger, D., Malinen, E. (2013). Dosimetric impact of interobserver variability in MRI-based delineation for cervical cancer brachytherapy. Radiother.Oncol; 107: 13–19. doi: 10.1016/j.

Hellebust, T. P., Tanderup, K., Bergstrand, E. S., Knutsen, B. H., Røislien, J., & Olsen, D. R. (2007). Reconstruction of a ring applicator using CT imaging: impact of the reconstruction method and applicator

orientation. Phys Med Biol; 52: 4893–904. doi: 10.1088/ 0031-9155/52/16/012.

Holloway, C.L., Racine, M.L., Cormack, R. A., O'Farrell, D. A., Viswanathan, A. N. (2009). Sigmoid dose using 3D imaging in cervical-cancer brachytherapy. Radiother.Oncol; 93: 307–10. doi: 10.1016/j. radonc.2009.06.032.

Holmberg, O., Malone, J., Rehani, M., McLean, D., Czarwinski, R. (2010). Current issues and actions in radiation protection of patients. Eur J Radiol; 76: 15–19. doi: 10.1016/j.ejrad.2010.06.033.

Hoskin, P. J., Bownes, P. J., Ostler, P., Walker, K., Bryant, L. (2003). High dose rate afterloading brachytherapy for prostate cancer: catheter and gland movement between fractions. Radiother. Oncol; 68: 285–8.

Hoskin, P. J., Cook, M., Bouscale, D., Cansdale, J. (1996). Changes in applicator position with fractionated high dose rate gynaecological brachytherapy. Radiother. Oncol; 40: 59–62.

International Atomic Energy Agency (IAEA). (2000). Safety Report Series 17. Lessons learned from accidental exposures in radiotherapy. Vienna, Austria: IAEA. IAEA Safety Reports Series.

International Atomic Energy Agency (IAEA). (2000). Technical report series 398. *Absorbed dose determination in external beam radiotherapy*. IAEA, Vienna.

International Atomic Energy Agency (IAEA). (2005). Radiation Oncology Physics: A handbook for Teachers and Students, Vienna, 45-60,81, 164.

International Atomic Energy Agency (IAEA). (2017). Radiation protection of patients (RPOP). Accident Prevention [Internet] [cited 2 August 2017]. Available from: https://rpop.iaea.org/RPOP/RPoP/Content/ Information For/Health Professionals/ 2_Radiotherapy/Accident Prevention.htm

International Atomic Energy Agency (IAEA). (2017). Radiation protection of patients (RPOP). Safety in Radiation Oncology SAFRON [cited 15 August 2017]. Available from: https://rpop.iaea.org/RPOP/ RPoP/ Modules/login/safron-register.htm

International Atomic Energy Agency. (IAEA). (2014). Radiation protection and safety of radiation sources: international basic safety standards. International Atomic Energy Agency, Vienna. Pp. 16-27.

International Commission on Radiation Units and Measurements, (ICRU). Report 24. (1976). *Determination of absorbed dose in a patient irradiated by beams of X or gamma rays in radiation therapy procedures.* Washington D.C.

International Commission on Radiation Units and Measurements, (ICRU). (2011). International Commission on Radiation Units and Measurements. Report No. 85.

International Specialty Products Advanced Materials. (ISP). (2011) New Jersey, USA Gafchromic EBT3 brochure 2011 Retrieved from www.iopscience.iop.org

International Specialty Products. (ISP) (2009). *GAFCHROMIC® EBT2, self-developing film for radiotherapy dosimetry*. (Revision 1). ISP,1361 Alps Road Wayne, NJ 07470, Pp. 3- 16.

Jamema, S. V., Mahantshetty, U., Tanderup, K., Malvankar, D., Sharma, S., Engineer, R., et al., (2013). Inter-application variation of dose and spatial location of D(2 cm^3) volumes of OARs during MR image based cervix brachytherapy. RadiotherOncol 2013; 107: 58–62. doi: 10.1016/j.radonc.2013.01.011.

Kertzscher, G., Andersen, C. E., Tanderup, K., (2014). Adaptive error detection for HDR/PDR brachytherapy: guidance for decision making during real-time in-vivo point dosimetry. Med Phys; 41: 1–11.

Kertzscher, G., Rosenfeld, A., Beddar, S., Tanderup, K., Cygler, J. E. (2014). In vivo dosimetry: trends and prospects for brachytherapy. Britsih jounal of Radiol: 87-206.

Khan, F. M. (2010). *The Physics of Radiation Therapy* (4th ed.). Lippincott Williams and Wilkins.

Kim, R. Y., Meyer, J. T., Spencer, S. A., Meredith, R. F, Jennelle, R. L. S., Salter, M. M. (1996). Major geometric variations between intracavitary applications in carcinoma of the cervix: high dose rate vs. low dose rate. Int J RadiatOncol; 35: 1035–8.

Kirisits, C., Rivard, M. J., Baltas, D., Ballester, F., De Brabandere, M., Van der Laarse, R. (2014). Review of clinical brachytherapy uncertainties: analysis guidelines of GECESTRO and the AAPM. RadiotherOncol; 110: 199–212. doi: 10.1016/j. radonc.2013.11. 002.

Kirisits, C., Siebert, F. A., Baltas, D., De Brabandere, M., Hellebust, T. P., & Berger, D. (2007). Accuracy of volume and DVH parameters determined with different brachytherapy treatment planning systems. RadiotherOncol; 84: 290–7. doi: 10.1016/j.radonc..06. 010.

Larry, A., DeWerd A., Mark, J., Rivard, & Hans-Joachim Selbach. (2012). Uncertainties associated with clinical aspects of brachytherapy. Comprehensive brachytherapy pp 225-228.

Liu, L., Prasad, S.C., & Bassano, D.A. (2004). Determination of 137Cs dosimetry parameters according to the AAPM TG-43 formalism. Med Phys, 31 (3), 477-483.

Lliso, F. (2011). *Journal of Contemporary Brachytherapy*. 3: 32-35 Retrieved from www.iopscience.iop.org.

Lopez, P. O., Andreo, P., Cosset, J-M, Dutreix, A., & Landberg, T. (2000). Prevention of accidental exposures to patients undergoing radiation therapy. ICRP Publications 86, Annals of the ICRP. New York, NY: Permagon.

Markman, J., Williamson, J. F., Dempsey, J. F., & Low, D. A. (2001). On the validity of the superposition principle in dose calculations for

intracavitary implants with shielded vaginal colpostats. Med Phys, 28 (2), 147-155.

Martisikova, M., Ackermann, B., & Jakel, O. (2008). Analysis of uncertainties in Gafchromic film dosimetry of photon beams. Physics in Medicine and Biology. 53(24): 7013-7027.

Mayles, P., Nahum, A., & Rosenwald, J. C. (Eds). (2007). Handbook of Radiotherapy Physics: Theory and Practice (5th edition); 1094.

Meigooni, A. S., Rachabatthula, V., Awan, S. B. & Koona, R. A. (2005). Comment on "Update of AAPM Task Group no. 43 report: A revised AAPM protocol for brachytherapy dose calculations". Med Phys, 32 (6), 1820-1821; author reply 1822-1824.

Meigooni, A. S., Sanders, M. S, Ibbott, G. S., & Szeglin, G. (1996), Dosimetric characteristics of improved radiochromic film, Med. Phys. 23, 1883-1888.

Meigooni, A. S., Zhang, H., Perry, C., Dini, S. A. & Koona, R. A. (2003). Theoretical and experimental determination of dosimetric characteristics for brachyseed Pd-103, model Pd-1, source. Appl Radiat Isot, 58 (5), 533-541.

Melhus, C. S. & Rivard, & M. J. (2006). Approaches to calculating AAPM TG-43 brachytherapy dosimetry parameters for 137Cs, 125I, 192Ir, 103Pd, and 169Yb sources. Med Phys, 33 (6), 1729-1737.

Meli, J. A. (2002). Dosimetry for interstitial and intracavitary sources and their applaicators. 185-207.

Mijnheer, B. J., Battermann, J. J., & Wambersie, A. (1987). What degree of accuracy is required and can be achieved in photon and neutron therapy. Radiotherapy Oncol 8:237-52.

Nag, S., Abitbol, A., & Anderson, L. L. (1993). Consensus Guidelines for High Dose Rate Remote Brachytherapy (HDR) in Cervical, Endometrial, and Endobronchial Tumors. Int. J. Radiat. Oncol. Biol. Phys. 27, 1241–1244.

Nag, S., Erickson, B., Thomadsen, B., Orton, C., Demanes, J. D., & Petereit, D. (2000). The American Brachytherapy Society Recommendations for HDR Brachytherapy of the Cervix. Int. J. Radiat. Oncol. Biol. Phys. 48, 201–211.

Nag, S., Samsami, N. (2000). Pitfalls of inappropriate optimization, Journal of Brachytherapy International. 16:187-198.

Nath, R., Anderson, L. L., Luxton, G., Weaver, K. A., Williamson, J. F., and Meigooni, A. S. (1995). Dosimety of interstitial brachytherapy sources: Recommendations of the AAPM Radiation Therapy Commitee Task Group No. 43. Med Phys 22:209-34.

Nath, R., Anderson, L. L., Luxton, G., Weaver, K. A., Williamson, J. F. & Meigooni, A. S. (1995). Dosimetry of interstitial brachytherapy sources: recommendations of the AAPM Radiation Therapy Committee Task Group No. 43. American Association of Physicists in Medicine. Med Phys 22 (2), 206-234.

Nesvacil, N., Tanderup, K., Hellebust, T. P., De Leeuw, A., Lang, S., & Mohamed, S. (2013). A multicentre comparison of the dosimetric

impact of inter- and intra-fractional anatomical variations in fractionated cervix cancer brachytherapy. RadiotherOncol; 107: 20–5.

P¨otter, R., Haie-Meder, C., Van Limbergen, E., Barillot, I., De Brabandere, M, & Dimopoulos, J. (2006). Recommendations from gynaecological (GYN) GEC ESTRO working group (II): concepts and terms in 3D image-based treatment planning in cervix cancer brachytherapy-3D dose volume parameters and aspects of 3D image-based anatomy, radiation physics, radiobiology. RadiotherOncol; 78: 67–77.

Palmer, A. L., Nisbet, A. & Bradley, A. (2013). Semi -3D dosimetry of high dose rate brachytherapy using a novel Gafchromic EBT3 film array water phantom. 7th International Conference on 3D Radiation Dosimetry (IC3DDose) *Journal of Physics: Conference Series 444* (2013) 012101 doi:10.1088/1742-6596/444/1/012101.

Palmer, A., Bradley, D., & Nisbet, A. (2012). Physics-aspects of dose accuracy in high dose rate (HDR) brachytherapy: source dosimetry, treatment planning, equipment performance and in-vivo verification techniques. *Journal of Contemporary Brachytherapy. 4*(2):81-91. Retrieved from www. researchgate. com

Parsai, E. I., Zhang, Z. & Feldmeier, J. J. (2009). A quantitative three-dimensional dose attenuation analysis around Fletcher-Suit-Delclos due to stainless steel tube for high dose-rate brachytherapy by Monte Carlo calculations. Brachytherapy, 8 (3), 318-323.

Perez-Calatayud, J., Granero, D., & Ballester, F. (2004). Phantom size in brachytherapy source dosimetric studies. Med Phys, 31 (7), 2075-2081.

Perez-Calatayud, J., Granero, D., Ballester, F., & Lliso, F. (2005). A Monte Carlo study of intersource effects in dome-type applicators loaded with LDR Cs-137 sources. Radiother Oncol, 77 (2), 216-219.

Petriˇc, P., Hudej, R., Rogelj, P., Blas, M., Tanderup, K., & Fidarova, E. (2013). Uncertainties of target volume delineation in MRI guided adaptive brachytherapy of cervix cancer: a multi-institutional study. RadiotherOncol; 107: 6–12. Retrieved from www.iopscience.iop.org

Richley, L., John, A. C., Coomber, H. & Fletcher, S. (2012). Evaluation and optimization of the new EBT2 radiochromic film dosimetric system for patient dose verification in radiotherapy. Physics in Medicine and Biology. 55(9): 2601.

Rink, A., Vitkin, I. A., & Jaffray, & D. A., (2005). Characterisation and real time optical measurements of the ionising radiation dose response for a new radiochromic medium. Medical Physics. 32(8):2510-2516.

Rivard, M. J., Coursey, B. M., DeWerd, L. A., Hanson, W. F., Huq, M.S., & Ibbott, G. S. (2004). Update of AAPM Task Group No. 43 Report: A revised AAPM protocol for brachytherapy dose calculations. Med Phys, 31 (3), 633-674.

Rivard, M. J., Coursey, B. M., DeWerd, L. A., Hanson, W. F., SaifulHuq, M, & Ibbott, G. S. (2004). Update of AAPM Task Group No. 43 Report: a revised AAPM protocol for brachytherapy dose calculations. Med Phys; 31: 633–74.

Rivard, M. J., Venselaar, J. L. & Beaulieu, L. (2009). The evolution of brachytherapy treatment planning. Med Phys, 36 (6), 2136-2153.

Rivard, M. J., Venselaar, J. L., & Beaulieu, L. (2009). The evolution of brachytherapy treatment planning. Med Phys; 36: 2136–53.

Rivard, M. J.; Butler, W. M., DeWerd, L. A., Huq, M. S., Ibbott, G. S., Meigooni. (2007). Supplement to the 2004 update of the AAPM Task Group No. 43 Report. Med Phys, 34 (6), 2187-2205.

Saur, S. & Frengen, J. (2008). Gafchromic EBT film dosimetry with flatbed CCD scanner:a novel background correction method and full dose uncertainty analysis. Medical Physics. 35(7): 3094-3101.

Seymour, E. L., Downes, S. J., Fogarty, G. B., Izard, M. A., & Metcalfe, P. (2011). “In vivo real-time dosimetric verification in high dose rate prostate brachytherapy,” Med. Phys. 38, 4785–4794.

Shima, K., Tateoka, K., Saitoh, Y., Suzuki, J., Yaegashi, Y., Fujimoto, K., Nakazawa, T., Nakata, A., Abe, T., Imai, S., Sakata, K., & Hareyama, M. (2012). Analysis of post-exposure density growth in radiochromic film with respect to the radiation dose.*J Radiat Res,53(2),* 301-305.

Sina, S. (2007). Simulation and Measurement of Dosimetric Parameters for 137Cs Brachytherapy Source, Based on TG-43 Protocol by TLD and Monte Carlo. Shiraz univercity, Shiraz.

Sina, S., Faghihi, R., Meigooni, A. S., Mehdizadeh, S., Mosleh, Shirazi, M. A., & Zehtabian, M. (2011a). Impact of the vaginal applicator and dummy pellets on the dosimetry parameters of Cs-137 brachytherapy source. *Journal of Applied Clinical Medical Physics, 12* (3), 183-193.

Sina, S., Faghihi, R., Meigooni, A. S., Mehdizadeh, S., Zehtabian, M. & Mosleh Shirazi, M. A. (2009). Simulation of the shielding effects of an applicator on the AAPM TG-43 parameters of CS-137 Selectron LDR brachytherapy sources. Iran. J. Radiat. Res, 7 (3), 135-140.

Siwek, R. A., Obrien, P. F., & Leung, P. M. K. (1991). Shielding effects of Selectron applicator and pellets on isodose Distributions. Radiother. Oncol., 20, 132–138.

Song, G., & Wu, Y. (2008). In A Monte Carlo Interstitial Brachytherapy Study for AAPM TG-43 Dose Calculation Formalism in Heterogeneous Media. Paper presented at the 2nd International Conference on Bioinformatics and Biomedical Engineering, 2008. ICBBE 2008.

Sureka, C. S. & Armpilia, C. (2007). Radiation Biology for Medical Physicists. Phys. Med. Bio (52); 525-37.

Tanderup, K., Hellebust, T. P., Lang, S., Granfeldt, J., P¨otter, R., & Lindegaard, J. C. (2008). Consequences of random and systematic reconstruction uncertainties in 3D image-based brachytherapy in cervical cancer. Radiother Oncol 2008; 89: 156–63. doi:10.101 6/j.radonc.06.010.

Tanderup, K., Nesvacil, N., P¨otter, R., & Kirisits, C. (2013). Uncertainties in image guided adaptive cervix cancer brachytherapy: impact on planning and prescription. RadiotherOncol; 107: 1–5.

Uniyal, S. C., Sharma, S. D., & Naithani, U. C. (2011). Evaluation of Gafchromic EBT2 film for the measurement of anisotropy function for HDR 192Ir brachytherapy source with respect to thermoluminescent dosimetry. Reports of Practical Oncology and Radiotherapy. 16(1): 14-20.

Van Battum, L. J., Hoffmans, D., Piersma, H., & Heukelom, S. (2008). Accurate dosimetry with Gafchromic EBT film of a 6 MV photon beam in water: what level is achievable? Med Phys.; 35(2):704–16.

Waldhäusl, C. A. Wambersie, R. Potter, & Georg, D. (2005) "In-vivo dosimetry for gynaecological brachytherapy: Physical and clinical considerations," Radiother. Oncol. 77, 310–317.

Willaimson, J. F., Meigooni A. S. (1995). Quantitative dosimetry methods in brachytherapy, 887-133.

Williamson, J. F. (1990). *Dose calculations about shielded gynecological colpostats*. Int. Journal Radiation Oncology BiolPhys; 19:167-178.

Wills, R., Lowe, G., Inchley, D., Anderson, C., Beenstock, V., & Hoskin, P. (2010). Applicator reconstruction for HDR cervix treatment planning using images from 0.35 T open MR scanner. RadiotherOncol; 94: 346–52.

World Health Organisation. (WHO). (2008). Radiotherapy risk profile. Geneva, Switzerland.

World Health Organization. (WHO). (2017). Data on Cervical Cancer ICO Information Centre on HPV and related cancers, Fact sheet. Retrieved from retrieved from www.hpvcentre.net/statistics/reports/GHA_FS.pd

Wulf, J., Popp, K., Oppitz, U., Baier, K., & Flentje, M. (2004). Positional variability of a tandem applicator system in HDR brachytherapy for primary treatment of cervix cancer. Analysis of the anatomic pelvic position and comparison of the applicator positions during five insertions. StrahlentherOnkol; 180: 216–24.

Zaman, Z. K. Ung, N. M., Malik, R. A.G. .F., Ho, V. C. E. Phua, Z. Jamalludin, M. T. H. Baharuldin, K. H. Ng (2014), Comparison of planned and measured rectal dose in-vivo during high dose rate Cobalt-60 brachytherapy of cervical cancer, PhysicaMedica Venselaar, J., Pérez-; 15: 76-82.

Zehtabian, M., Faghihi, R., Sina, S., & Noorizadeh, A. (2010). Investigation of the Effects of Tissue Inhomogeneities on the Dosimetric Parameters of a Cs-137 Brachytherapy Source using the MCNP4C Code. Iran. J. of Med. Physics, 7 (3 (28)), 15-20.

Zeidan, O., Stephen, S., Meeks, S., Wagner, T., Willoughby, T., Kupelian, P. & Langen, K. (2006). Characterization and use of EBT radiochromic film for IMRT dose verification. Medical Physics. 33(11): 4064-4072.

APPENDICES

APPENDIX A-1: THE INTENSITIES AND OPTICAL DENSITIES MEASURED BY THE GAFCHROMIC EBT3 FILMS FOR BLADDER AND RECTUM

Cal Point	Dwell Time($mins$)	Film Intensity(I)			Optical Density(OD)	
		I_O	Bladder	Rectum	Bladder	Rectum
1.	29:42	122.49	81.10	77.31	0.18	0.20
2.	38:12	122.49	74.30	68.19	0.22	0.25
3.	21:13	122.49	87.88	84.40	0.14	0.16
4.	18:56	122.49	88.79	82.51	0.14	0.17
5.	26:31	122.49	82.96	79.32	0.17	0.19
6.	34:05	122.49	50.48	64.49	0.38	0.28
7.	12:29	122.49	64.00	69.92	0.28	0.24
8.	38:58	122.49	47.11	53.46	0.41	0.36
9.	31:10	122.49	55.23	57.68	0.35	0.33
10.	11:41	122.49	83.22	84.55	0.17	0.16
11.	27:18	122.49	57.63	61.63	0.33	0.30
12.	08:26	122.49	90.29	90.08	0.13	0.13
13.	09:27	122.49	89.04	89.37	0.14	0.14
14.	18:22	122.99	84.04	68.12	0.17	0.26
15.	15:27	122.99	88.22	73.56	0.14	0.22
16.	25:01	122.99	75.49	60.94	0.21	0.30
17.	03:08	122.99	110.03	104.72	0.05	0.07
18.	03:05	122.99	110.90	104.15	0.04	0.07
19.	05:00	122.99	104.63	96.51	0.07	0.11
20.	03:52	122.99	107.17	99.92	0.06	0.09
21.	06:15	122.99	104.81	93.07	0.07	0.12
22.	04:38	122.99	108.55	99.16	0.05	0.09
23.	07:30	122.99	104.08	91.64	0.07	0.13

Cal Point	Dwell Time($mins$)	Film Intensity(I)			Optical Density(OD)	
		I_O	Bladder	Rectum	Bladder	Rectum
24.	06:11	122.99	104.31	95.76	0.07	0.11
25.	10:00	122.99	98.97	83.97	0.09	0.17
26.	06:57	122.99	101.85	93.41	0.08	0.12
27.	11:15	122.99	97.35	76.47	0.10	0.21
28.	08:06	122.99	101.79	83.74	0.08	0.17
29.	13:08	122.99	93.99	72.19	0.12	0.23
30.	08:53	122.99	102.71	83.28	0.08	0.17
31.	14:23	122.99	97.23	70.84	0.10	0.24
32.	17:22	122.99	94.13	62.69	0.12	0.29
33.	29:09	122.99	80.56	51.49	0.18	0.38
34.	15:17	115.86	72.59	81.28	0.20	0.15
35.	15:20	115.86	72.59	82.01	0.20	0.15
36.	06:07	115.86	93.78	102.74	0.09	0.05
37.	07:39	115.86	90.42	97.68	0.11	0.07
38.	04:35	115.86	98.60	106.15	0.07	0.05
39.	02:27	115.86	105.81	108.26	0.04	0.03
40.	03:40	115.86	102.05	104.57	0.06	0.04
41.	04:54	115.86	94.63	97.41	0.09	0.08
42.	07:02	115.86	94.84	99.26	0.09	0.07
43.	05:30	115.86	89.65	93.15	0.11	0.09
44.	08:15	115.86	88.55	92.06	0.12	0.10
45.	13:46	115.86	76.26	80.12	0.18	0.16
46.	21:24	115.86	64.77	68.90	0.25	0.23
47.	22:56	115.86	65.35	67.78	0.25	0.23
48.	10:05	115.86	84.37	84.89	0.14	0.13
49.	10:42	115.86	83.15	84.69	0.14	0.14
50.	11:19	115.86	86.08	83.63	0.13	0.14
51.	04:15	112.86	101.11	98.13	0.05	0.06

Cal Point	Dwell Time($mins$)	Film Intensity(I)			Optical Density(OD)	
		I_O	Bladder	Rectum	Bladder	Rectum
52.	05:18	112.86	99.04	94.94	0.06	0.08
53.	06:22	112.86	95.44	91.87	0.07	0.09
54.	07:04	112.86	93.79	89.55	0.08	0.10
55.	08:08	112.86	85.41	85.93	0.12	0.12
56.	08:51	112.86	85.88	81.58	0.12	0.14
57.	09:33	112.86	85.03	78.40	0.12	0.16
58.	10:15	112.86	84.23	76.99	0.13	0.17
59.	10:37	112.86	82.72	76.94	0.13	0.17
60.	11:19	112.86	81.41	79.00	0.14	0.15
61.	12:13	112.86	73.01	72.77	0.19	0.19
62.	13:26	112.86	78.56	69.39	0.16	0.21
63.	14:51	112.86	72.74	69.05	0.19	0.21
64.	14:09	112.86	73.25	69.04	0.19	0.21
65.	15:55	112.86	72.98	66.40	0.19	0.23
66.	16:59	112.86	67.86	64.52	0.22	0.24
67.	17:41	112.86	66.78	65.48	0.23	0.24
68.	18:24	112.86	70.49	63.28	0.20	0.25
69.	5.50	112.86	65.99	59.28	0.23	0.28
70.	20:31	112.86	63.65	59.26	0.25	0.28
71.	04:49	112.86	91.24	88.07	0.09	0.11
72.	04:27	112.86	96.48	91.42	0.07	0.09
73.	03:02	112.73	102.97	100.97	0.04	0.05
74.	03:47	112.73	99.70	98.45	0.05	0.06
75.	04:33	112.73	100.43	94.22	0.05	0.08
76.	05:41	112.73	97.41	93.20	0.06	0.08
77.	06:49	112.73	95.52	93.17	0.07	0.08
78.	07:34	112.73	94.19	89.63	0.08	0.10
79.	08:20	112.73	95.88	88.14	0.07	0.11

Cal Point	Dwell Time($mins$)	Film Intensity(I)			Optical Density(OD)	
		I_O	Bladder	Rectum	Bladder	Rectum
80.	9.28	112.73	91.23	84.78	0.09	0.12
81.	10:36	112.73	90.91	86.67	0.09	0.11
82.	11:21	112.73	93.40	85.50	0.08	0.12
83.	12:07	112.73	91.47	82.47	0.09	0.14
84.	13:15	112.73	91.82	81.08	0.10	0.14
85.	14:23	112.73	89.92	79.76	0.10	0.15
86.	15:08	112.73	89.03	79.13	0.10	0.15
87.	15:54	112.73	88.94	77.74	0.10	0.16
88.	17:02	112.73	87.75	76.49	0.11	0.17
89.	18:10	112.73	85.44	73.38	0.12	0.19
90.	18:56	112.73	85.21	73.05	0.12	0.19
91.	06:53	112.73	95.47	94.10	0.07	0.08
92.	05:09	112.73	99.65	96.35	0.05	0.07
93.	07:43	112.73	95.15	88.31	0.07	0.11
94.	03:58	112.73	102.97	97.30	0.04	0.06
95.	06:22	112.73	95.15	88.31	0.07	0.11

Appendix A- 2: DOSE CALCULATED BY THE TPS FOR THE BLADDER AND RECTUM

Cal Point	Dwell Time(mins)	Prescribed Dose (Gy)		Dose Calculated by TPS(Gy)	
		Point A	Surface of Ovoids	Rectum	Bladder
1.	29:42	7.00	X	2.87	3.19
2.	38:12	9.00	X	3.69	4.10
3.	21:13	5.00	X	2.05	2.28
4.	18:56	5.00	X	1.93	2.17
5.	26:31	7.00	X	2.70	3.04
6.	34:05	9.00	X	3.47	3.91
7.	12:29	5.00	X	4.62	4.12
8.	38:58	10.00	X	9.24	8.24
9.	31:10	8.00	X	7.39	6.60
10.	11:41	3.00	X	2.77	2.47
11.	27:18	X	10.00	6.48	5.78
12.	08:26	X	2.00	2.00	1.78
13.	09:27	X	2.00	2.24	2.00
14.	18:22	X	5.00	2.94	4.76
15.	15:27	4.00	X	2.47	4.00
16.	25:01	6.81	X	4.00	6.48
17.	03:08	X	X	0.50	0.81
18.	03:05	X	X	0.49	0.80
19.	05:00	1.36	X	0.80	1.30
20.	03:52	1.05	X	0.62	1.00
21.	06:15	1.70	X	1.00	1.62
22.	04:38	1.26	X	0.74	1.20
23.	07:30	2.04	X	1.20	1.94
24.	06:11	1.68	X	0.99	1.60
25.	10:00	2.72	X	1.60	2.59

Cal Point	Dwell Time(mins)	Prescribed Dose (Gy)		Dose Calculated by TPS(Gy)	
		Point A	Surface of Ovoids	Rectum	Bladder
26.	06:57	1.89	X	1.11	1.80
27.	11:15	3.06	X	1.80	2.92
28.	08:06	2.21	X	1.30	2.10
29.	13:08	3.58	X	2.10	3.40
30.	08:53	2.42	X	1.42	2.30
31.	14:23	3.92	X	2.30	3.73
32.	17:22	4.73	X	2.02	4.50
33.	29:09	7.66	X	4.50	7.29
34.	15:17	X	5.00	2.99	3.53
35.	15:20	X	3.00	3.00	3.54
36.	06:07	X	2.00	1.20	1.41
37.	07:39	X	2.50	1.50	1.77
38.	04:35	X	1.50	0.90	0.82
39.	02:27	X	0.80	0.48	0.57
40.	03:40	X	1.20	0.72	0.85
41.	04:54	X	1.60	0.96	1.13
42.	07:02	X	2.30	1.38	1.63
43.	05:30	X	1.80	1.34	1.27
44.	08:15	X	2.70	1.61	1.91
45.	13:46	X	4.50	2.69	3.18
46.	21:24	X	7.00	4.19	4.95
47.	22:56	X	7.50	4.49	5.30
48.	10:05	X	3.30	1.97	2.33
49.	10:42	X	3.50	2.09	2.47
50.	11:19	X	3.70	2.21	2.61
51.	04:15	X	1.20	0.73	0.93
52.	05:18	X	1.50	1.22	1.17

Cal Point	Dwell Time(mins)	Prescribed Dose (Gy)		Dose Calculated by TPS(Gy)	
		Point A	Surface of Ovoids	Rectum	Bladder
53.	06:22	X	1.80	1.66	1.40
54.	07:04	X	2.00	1.84	1.56
55.	08:08	X	2.30	2.12	1.79
56.	08:51	X	2.50	2.31	1.95
57.	09:33	X	2.70	2.49	2.10
58.	10:15	X	2.90	2.18	2.26
59.	10:37	X	3.00	2.77	2.34
60.	11:19	X	3.20	2.95	2.49
61.	12:13	X	3.50	3.23	2.73
62.	13:26	X	3.80	3.50	2.96
63.	14:51	X	4.20	3.87	3.27
64.	14:09	X	4.00	3.69	3.11
65.	15:55	X	4.50	4.15	3.50
66.	16:59	X	4.80	4.43	3.74
67.	17:41	X	5.00	4.61	3.89
68.	18:24	X	5.20	4.80	3.68
69.	5.50	X	5.50	5.07	4.28
70.	20:31	X	5.80	5.35	4.52
71.	04:49	X	1.36	1.25	1.06
72.	04:27	X	1.26	1.16	0.98
73.	03:02	0.80	X	0.49	0.48
74.	03:47	1.00	X	0.61	0.60
75.	04:33	1.20	X	0.73	0.72
76.	05:41	1.50	X	0.92	0.90
77.	06:49	1.80	X	1.10	1.08
78.	07:34	2.00	X	1.22	1.20
79.	08:20	2.20	X	1.34	1.32

Cal Point	Dwell Time(mins)	Prescribed Dose (Gy)		Dose Calculated by TPS(Gy)	
		Point A	Surface of Ovoids	Rectum	Bladder
80.	9.28	2.50	X	1.53	1.50
81.	10:36	2.80	X	1.71	1.69
82.	11:21	3.00	X	1.47	1.81
83.	12:07	3.20	X	1.49	1.93
84.	13:15	3.50	X	1.53	2.11
85.	14:23	3.80	X	1.95	2.29
86.	15:08	4.00	X	1.53	2.41
87.	15:54	4.20	X	2.56	2.53
88.	17:02	4.50	X	1.83	2.71
89.	18:10	4.80	X	2.43	2.89
90.	18:56	5.00	X	2.63	3.01
91.	06:53	0.53	X	1.11	1.09
92.	05:09	1.36	X	0.83	0.82
93.	07:43	2.04	X	1.25	1.23
94.	03:58	1.05	X	0.64	0.63
95.	06:22	1.68	X	1.03	1.23

Appendix A-3: DOSES MEASURED BY GAFCHROMIC FILM FOR BLADDER AND RECTUM.

Cal Point	Dwell Time(mins)	Dose Measured by Film (Gy)	
		Bladder	Rectum
1.	29:42	2.74	3.15
2.	38:12	3.51	4.37
3.	21:13	2.11	2.42
4.	18:56	2.04	2.60
5.	26:31	2.56	2.93
6.	34:05	8.43	4.99
7.	12:29	5.08	4.11
8.	38:58	9.64	7.51
9.	31:10	7.02	6.40
10.	11:41	2.53	2.41
11.	27:18	6.41	5.53
12.	08:26	1.92	1.93
13.	09:27	2.02	1.99
14.	18:22	2.49	4.43
15.	15:27	2.12	3.65
16.	25:01	3.41	5.73
17.	03:08	0.64	0.95
18.	03:05	0.59	0.98
19.	05:00	0.95	1.48
20.	03:52	0.80	1.25
21.	06:15	0.94	1.73
22.	04:38	0.72	1.30
23.	07:30	0.98	1.84
24.	06:11	0.97	1.53
25.	10:00	1.31	2.50

Cal Point	Dwell Time(mins)	Dose Measured by Film (Gy)	
		Bladder	Rectum
26.	06:57	1.12	1.70
27.	11:15	1.42	3.29
28.	08:06	1.12	2.52
29.	13:08	1.66	3.83
30.	08:53	1.07	2.56
31.	14:23	1.43	4.02
32.	17:22	1.65	5.37
33.	29:09	2.84	8.17
34.	15:17	3.22	2.28
35.	15:20	3.22	2.22
36.	06:07	1.27	0.69
37.	07:39	1.52	1.01
38.	04:35	0.95	0.49
39.	02:27	0.51	0.37
40.	03:40	0.73	0.58
41.	04:54	1.21	1.03
42.	07:02	1.20	0.91
43.	05:30	1.57	1.32
44.	08:15	1.66	1.40
45.	13:46	2.79	2.40
46.	21:24	4.33	3.70
47.	22:56	4.23	3.86
48.	10:05	2.00	1.96
49.	10:42	2.11	1.98
50.	11:19	1.86	2.07
51.	04:15	0.63	0.81
52.	05:18	0.75	1.02
53.	06:22	0.99	1.23

Cal Point	Dwell Time(mins)	Dose Measured by Film (Gy)	
		Bladder	Rectum
54.	07:04	1.10	1.40
55.	08:08	1.73	1.69
56.	08:51	1.69	2.06
57.	09:33	1.76	2.36
58.	10:15	1.83	2.50
59.	10:37	1.96	2.51
60.	11:19	2.07	2.30
61.	12:13	2.94	2.97
62.	13:26	2.34	3.39
63.	14:51	2.97	3.43
64.	14:09	2.91	3.45
65.	15:55	2.94	3.81
66.	16:59	3.60	4.09
67.	17:41	3.75	3.95
68.	18:24	3.25	4.30
69.	5.50	3.87	5.02
70.	20:31	4.24	5.02
71.	04:49	1.28	1.52
72.	04:27	0.92	1.27
73.	03:02	0.51	0.63
74.	03:47	0.71	0.79
75.	04:33	0.66	1.06
76.	05:41	0.85	1.13
77.	06:49	0.98	1.14
78.	07:34	1.07	1.39
79.	08:20	0.95	1.50
80.	9.28	1.27	1.77
81.	10:36	1.30	1.62

Cal Point	Dwell Time(mins)	Dose Measured by Film (Gy)	
		Bladder	Rectum
82.	11:21	1.12	1.71
83.	12:07	1.26	1.97
84.	13:15	1.23	2.10
85.	14:23	1.37	2.22
86.	15:08	1.43	2.28
87.	15:54	1.44	2.42
88.	17:02	1.53	2.54
89.	18:10	1.72	2.89
90.	18:56	1.74	2.92
91.	06:53	0.98	1.07
92.	05:09	0.71	0.92
93.	07:43	1.00	1.49
94.	03:58	0.51	0.86
95.	06:22	1.00	1.49

APPENDIX A-4: COMPARISON OF TPS DOSE WITH FILM DOSE FOR BLADDER AND RECTUM

Cal Point	TPS Dose (Gy)		Film Dose (Gy)		% Difference	
	Bladder	Rectum	Bladder	Rectum	Bladder	Rectum
1.	2.87	3.19	2.74	3.15	4.53	1.25
2.	3.69	4.10	3.51	4.37	4.88	-6.59
3.	2.05	2.28	2.11	2.42	-2.93	-6.14
4.	1.93	2.17	2.04	2.60	-5.70	-19.82
5.	2.70	3.04	2.56	2.93	5.19	3.62
6.	3.47	3.91	3.45	4.99	0.58	-27.62
7.	4.62	4.12	5.08	4.11	-9.96	0.24
8.	9.24	8.24	9.64	7.51	-4.33	8.86
9.	7.39	6.60	7.02	6.40	5.01	3.03
10.	2.77	2.47	2.53	2.41	8.66	2.43
11.	6.48	5.78	6.41	5.53	1.08	4.33
12.	2.00	1.78	1.92	1.93	4.00	-8.43
13.	2.24	2.00	2.02	1.99	9.82	0.50
14.	2.94	4.76	2.49	4.43	15.31	6.93
15.	2.47	4.00	2.12	3.65	14.17	8.75
16.	4.00	6.48	3.41	5.73	14.75	11.57
17.	0.50	0.81	0.64	0.95	-28.00	-17.28
18.	0.49	0.80	0.59	0.98	-20.41	-22.50
19.	0.80	1.30	0.95	1.48	-18.75	-13.85
20.	0.62	1.00	0.80	1.25	-29.03	-25.00
21.	1.00	1.62	0.94	1.73	6.00	-6.79
22.	0.74	1.2	0.72	1.3	2.70	-8.33
23.	1.2	1.94	0.98	1.84	18.33	5.15
24.	0.99	1.6	0.97	1.53	2.02	4.38
25.	1.6	2.59	1.31	2.50	18.13	3.47
26.	1.11	1.80	1.12	1.70	-0.90	5.56

Cal Point	TPS Dose (Gy)		Film Dose (Gy)		% Difference	
	Bladder	Rectum	Bladder	Rectum	Bladder	Rectum
27.	1.80	2.92	1.42	3.29	21.11	-12.67
28.	1.30	2.10	1.12	2.52	13.85	-20.00
29.	2.10	3.40	1.66	3.83	20.95	-12.65
30.	1.42	2.30	1.07	2.56	24.65	-11.30
31.	2.30	3.73	1.43	4.02	37.83	-7.77
32.	2.02	4.50	1.65	5.37	40.65	-19.33
33.	4.50	7.29	2.84	8.17	36.89	-12.07
34.	2.99	3.53	3.22	2.28	-7.69	35.41
35.	3.00	3.54	3.22	2.22	-7.33	37.29
36.	1.20	1.41	1.27	0.69	-5.83	51.06
37.	1.50	1.77	1.52	1.01	-1.33	42.94
38.	0.90	0.82	0.95	0.49	-5.56	40.24
39.	0.48	0.57	0.51	0.37	-6.25	35.09
40.	0.72	0.85	0.73	0.58	-1.39	31.76
41.	0.96	1.13	1.21	1.03	-26.04	8.85
42.	1.38	1.63	1.20	0.91	13.04	44.17
43.	1.34	1.27	1.57	1.32	-17.16	-3.94
44.	1.61	1.91	1.66	1.40	-3.11	26.70
45.	2.69	3.18	2.79	2.40	-3.72	24.53
46.	4.19	4.95	4.33	3.70	-3.34	25.25
47.	4.49	5.30	4.23	3.86	5.79	27.17
48.	1.97	2.33	2.00	1.96	-1.52	15.88
49.	2.09	2.47	2.11	1.98	-0.96	19.84
50.	2.21	2.61	1.86	2.07	15.84	20.69
51.	0.73	0.93	0.52	0.81	28.77	12.90
52.	1.02	1.17	0.75	1.02	26.47	12.82
53.	1.66	1.4	0.99	1.23	40.36	12.14
54.	1.22	1.56	1.10	1.40	9.84	10.26

Cal Point	TPS Dose (Gy)		Film Dose (Gy)		% Difference	
	Bladder	Rectum	Bladder	Rectum	Bladder	Rectum
55.	2.12	1.79	1.73	1.69	18.40	5.59
56.	2.31	1.95	1.69	2.06	26.84	-5.64
57.	2.49	2.10	1.76	2.36	29.32	-12.38
58.	2.18	2.26	1.83	2.50	16.05	-10.62
59.	2.77	2.34	1.96	2.51	29.24	-7.26
60.	2.95	2.49	2.07	2.30	29.83	7.63
61.	3.23	2.73	2.94	2.97	8.98	-8.79
62.	3.50	2.96	2.34	3.39	33.14	-14.53
63.	3.87	3.27	2.97	3.43	23.26	-4.89
64.	3.69	3.11	2.91	3.45	21.14	-10.93
65.	4.15	3.50	2.94	3.81	29.16	-8.86
66.	4.43	3.74	3.60	4.09	18.74	-9.36
67.	4.61	3.89	3.75	3.95	18.66	-1.54
68.	4.80	3.68	3.25	4.30	11.68	-6.17
69.	5.07	4.28	3.87	5.02	23.67	-17.29
70.	5.35	4.52	4.24	5.02	20.75	-11.06
71.	1.25	1.06	1.28	1.52	-2.40	-43.40
72.	1.16	0.98	0.92	1.27	20.69	-29.59
73.	0.49	0.48	0.51	0.63	-4.08	31.25
74.	0.61	0.60	0.71	0.79	-16.39	-31.67
75.	0.73	0.72	0.66	1.06	9.59	-47.22
76.	0.92	0.90	0.85	1.13	7.61	-25.56
77.	1.1	1.08	0.98	1.14	10.91	-5.56
78.	1.22	1.20	1.07	1.39	12.30	-15.83
79.	1.34	1.32	0.95	1.50	29.10	-13.64
80.	1.53	1.50	1.27	1.77	16.99	-18.00
81.	1.71	1.69	1.30	1.62	23.98	4.14
82.	1.47	1.81	1.12	1.71	23.81	5.52

Cal Point	TPS Dose (Gy)		Film Dose (Gy)		% Difference	
	Bladder	Rectum	Bladder	Rectum	Bladder	Rectum
83.	1.49	1.93	1.26	1.97	15.44	-2.07
84.	1.53	2.11	1.23	2.10	19.61	0.47
85.	1.95	2.29	1.37	2.22	29.74	3.06
86.	1.53	2.41	1.43	2.28	6.53	5.39
87.	2.56	2.53	1.44	2.42	43.75	4.35
88.	1.83	2.71	1.53	2.54	16.39	6.27
89.	2.43	2.92	1.72	2.89	29.22	1.03
90.	2.63	3.01	1.74	2.92	33.84	2.99
91.	1.11	1.09	0.98	1.07	11.71	1.83
92.	0.83	0.82	0.71	0.92	14.46	-12.20
93.	1.25	1.23	1.00	1.49	20.00	-21.14
94.	0.64	0.63	0.51	0.86	20.31	-36.51
95.	1.03	1.23	1.00	1.49	2.91	-21.14

APPENDIX B-1: FILM INTENSITY VALUES AND THE CORRESPONDING DOSES MEASURED BY THE FILM USED FOR THE DOSE MODELING.

Cal Point	Initial Intensity(I_o)	Film Intensity		Dose Calculated by Film(Gy)	
		Bladder(I_B)	Rectum(I_R)	Rectum	Bladder
1.	122.49	81.10	77.31	2.74	3.15
2.	122.49	74.30	68.19	3.51	4.37
3.	122.49	87.88	84.40	2.11	2.42
4.	122.49	88.79	82.51	2.04	2.60
5.	122.49	82.96	79.32	2.56	2.93
6.	122.49	50.48	64.49	8.43	4.99
7.	122.49	64.00	69.92	5.08	4.11
8.	122.49	47.11	53.46	9.64	7.51
9.	122.49	55.23	57.68	7.02	6.40
10.	122.49	83.22	84.55	2.53	2.41
11.	122.49	57.63	61.63	6.41	5.53
12.	122.49	90.29	90.08	1.92	1.93
13.	122.49	89.04	89.37	2.02	1.99
14.	122.99	84.04	68.12	2.49	4.43
15.	122.99	88.22	73.56	2.12	3.65
16.	122.99	75.49	60.94	3.41	5.73
17.	122.99	110.03	104.72	0.64	0.95
18.	122.99	110.90	104.15	0.59	0.98
19.	122.99	104.63	96.51	0.95	1.48
20.	122.99	107.17	99.92	0.80	1.25
21.	122.99	104.81	93.07	0.94	1.73
22.	122.99	108.55	99.16	0.72	1.30
23.	122.99	104.08	91.64	0.98	1.84
24.	122.99	104.31	95.76	0.97	1.53

Cal Point	Initial Intensity(I_o)	Film Intensity		Dose Calculated by Film(Gy)	
		Bladder(I_B)	Rectum(I_R)	Rectum	Bladder
25.	122.99	98.97	83.97	1.31	2.50
26.	122.99	101.85	93.41	1.12	1.70
27.	122.99	97.35	76.47	1.42	3.29
28.	122.99	101.79	83.74	1.12	2.52
29.	122.99	93.99	72.19	1.66	3.83
30.	122.99	102.71	83.28	1.07	2.56
31.	122.99	97.23	70.84	1.43	4.02
32.	122.99	94.13	62.69	1.65	5.37
33.	122.99	80.56	51.49	2.84	8.17
34.	115.86	72.59	81.28	3.22	2.28
35.	115.86	72.59	82.01	3.22	2.22
36.	115.86	93.78	102.74	1.27	0.69
37.	115.86	90.42	97.68	1.52	1.01
38.	115.86	98.60	106.15	0.95	0.49
39.	115.86	105.81	108.26	0.51	0.37
40.	115.86	102.05	104.57	0.73	0.58
41.	115.86	94.63	97.41	1.21	1.03
42.	115.86	94.84	99.26	1.20	0.91
43.	115.86	89.65	93.15	1.57	1.32
44.	115.86	88.55	92.06	1.66	1.40
45.	115.86	76.26	80.12	2.79	2.40
46.	115.86	64.77	68.90	4.33	3.70
47.	115.86	65.35	67.78	4.23	3.86
48.	115.86	84.37	84.89	2.00	1.96
49.	115.86	83.15	84.69	2.11	1.98
50.	115.86	86.08	83.63	1.86	2.07
51.	112.86	101.11	98.13	0.63	0.81
52.	112.86	99.04	94.94	0.75	1.02

Cal Point	Initial Intensity(I_o)	Film Intensity		Dose Calculated by Film(Gy)	
		Bladder(I_B)	Rectum(I_R)	Rectum	Bladder
53.	112.86	95.44	91.87	0.99	1.23
54.	112.86	93.79	89.55	1.10	1.40
55.	112.86	85.41	85.93	1.73	1.69
56.	112.86	85.88	81.58	1.69	2.06
57.	112.86	85.03	78.40	1.76	2.36
58.	112.86	84.23	76.99	1.83	2.50
59.	112.86	82.72	76.94	1.96	2.51
60.	112.86	81.41	79.00	2.07	2.30
61.	112.86	73.01	72.77	2.94	2.97
62.	112.86	78.56	69.39	2.34	3.39
63.	112.86	72.74	69.05	2.97	3.43
64.	112.86	73.25	69.04	2.91	3.45
65.	112.86	72.98	66.40	2.94	3.81
66.	112.86	67.86	64.52	3.60	4.09
67.	112.86	66.78	65.48	3.75	3.95
68.	112.86	70.49	63.28	3.25	4.30
69.	112.86	65.99	59.28	3.87	5.02
70.	112.86	63.65	59.26	4.24	5.02
71.	112.86	91.24	88.07	1.28	1.52
72.	112.86	96.48	91.42	0.92	1.27
73.	112.73	102.97	100.97	0.51	0.63
74.	112.73	99.70	98.45	0.71	0.79
75.	112.73	100.43	94.22	0.66	1.06
76.	112.73	97.41	93.20	0.85	1.13
77.	112.73	95.52	93.17	0.98	1.14
78.	112.73	94.19	89.63	1.07	1.39
79.	112.73	95.88	88.14	0.95	1.50
80.	112.73	91.23	84.78	1.27	1.77

Cal Point	Initial Intensity(I_o)	Film Intensity		Dose Calculated by Film(Gy)	
		Bladder(I_B)	Rectum(I_R)	Rectum	Bladder
81.	112.73	90.91	86.67	1.30	1.62
82.	112.73	93.40	85.50	1.12	1.71
83.	112.73	91.47	82.47	1.26	1.97
84.	112.73	91.82	81.08	1.23	2.10
85.	112.73	89.92	79.76	1.37	2.22
86.	112.73	89.03	79.13	1.43	2.28
87.	112.73	88.94	77.74	1.44	2.42
88.	112.73	87.75	76.49	1.53	2.54
89.	112.73	85.44	73.38	1.72	2.89
90.	112.73	85.21	73.05	1.74	2.92
91.	112.73	95.47	94.10	0.98	1.07
92.	112.73	99.65	96.35	0.71	0.92
93.	112.73	95.15	88.31	1.00	1.49
94.	112.73	102.97	97.30	0.51	0.86
95.	112.73	95.15	88.31	1.00	1.49

APPENDIX C-1: RESULTS FOR VALIDATION OF THE MODEL DEVELOPED

TPS Dose (Gy)		Film Intensity		Model Dose (Gy)		% difference	
Bladder	Rectum	Bladder	Rectum	Bladder	Rectum	Bladder	Rectum
1.11	1.09	95.47	94.10	1.21	1.26	-8.94	-15.60
2.95	2.49	81.41	79.00	2.73	2.92	7.53	-17.31
2.21	2.61	86.08	83.63	2.22	2.41	-0.60	7.60
2.77	2.34	82.72	76.94	2.59	3.15	6.63	-34.51
2.12	1.79	85.41	85.93	2.30	2.16	-8.29	-20.60
5.35	4.52	63.65	59.26	4.65	5.09	13.16	-12.66
1.71	1.91	90.91	86.67	1.70	2.08	0.48	-8.76
0.92	1.21	97.41	93.20	1.00	1.36	-8.67	-12.31
3.69	3.51	73.25	69.04	3.61	4.02	2.20	-14.43
4.62	4.12	64.00	69.92	4.61	3.92	0.26	4.86
2.00	1.78	90.29	90.08	1.77	1.70	11.57	4.37
2.05	2.28	87.88	84.40	2.03	2.33	1.03	-2.06
4.49	4.91	65.35	67.78	4.46	4.16	0.62	15.37
2.69	3.18	76.26	80.12	3.28	2.80	-22.08	12.02
2.32	2.29	89.92	79.76	1.81	2.84	22.04	-23.90
2.95	2.49	81.41	79.00	2.73	2.92	7.53	-17.31
4.61	3.89	66.78	65.48	4.31	4.41	6.56	-13.32
3.00	3.54	72.59	82.01	3.68	2.59	-22.68	26.84
0.49	0.48	102.97	100.97	0.40	0.50	18.52	-5.06
1.97	2.33	84.37	84.89	2.41	2.27	-22.24	2.44

APPENDIX D-1: STRIPS OF GAFCHROMIC EBT3 FILMS USED FOR MEASURING DOSES TO THE BLADDER AND THE RECTUM.

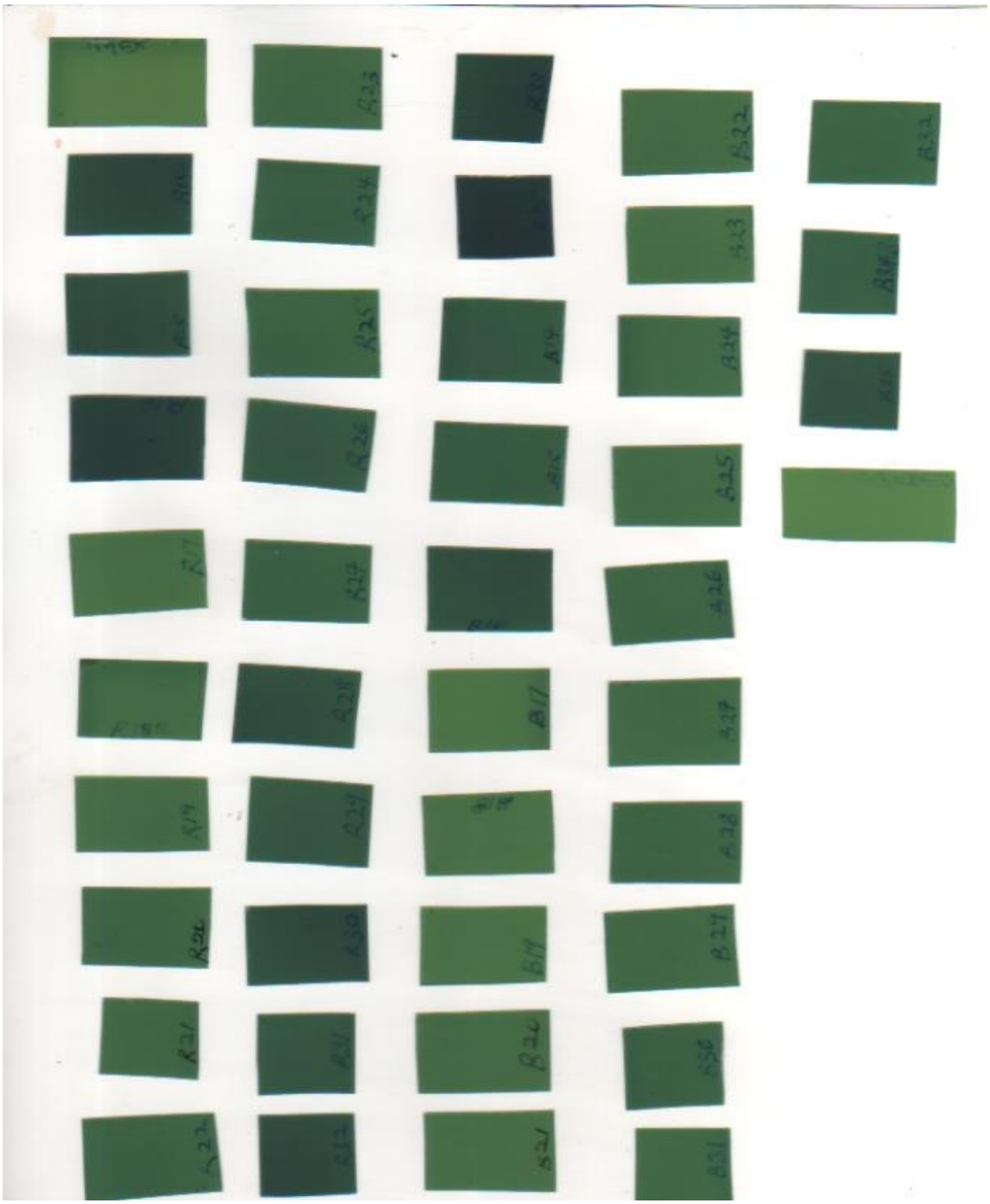

APPENDIX D-2: SUMMARY (SAMPLES) OF STRIPS OF GAFCHROMIC EBT3 FILMS USED FOR MEASURING DOSES TO THE BLADDER AND RECTUM.

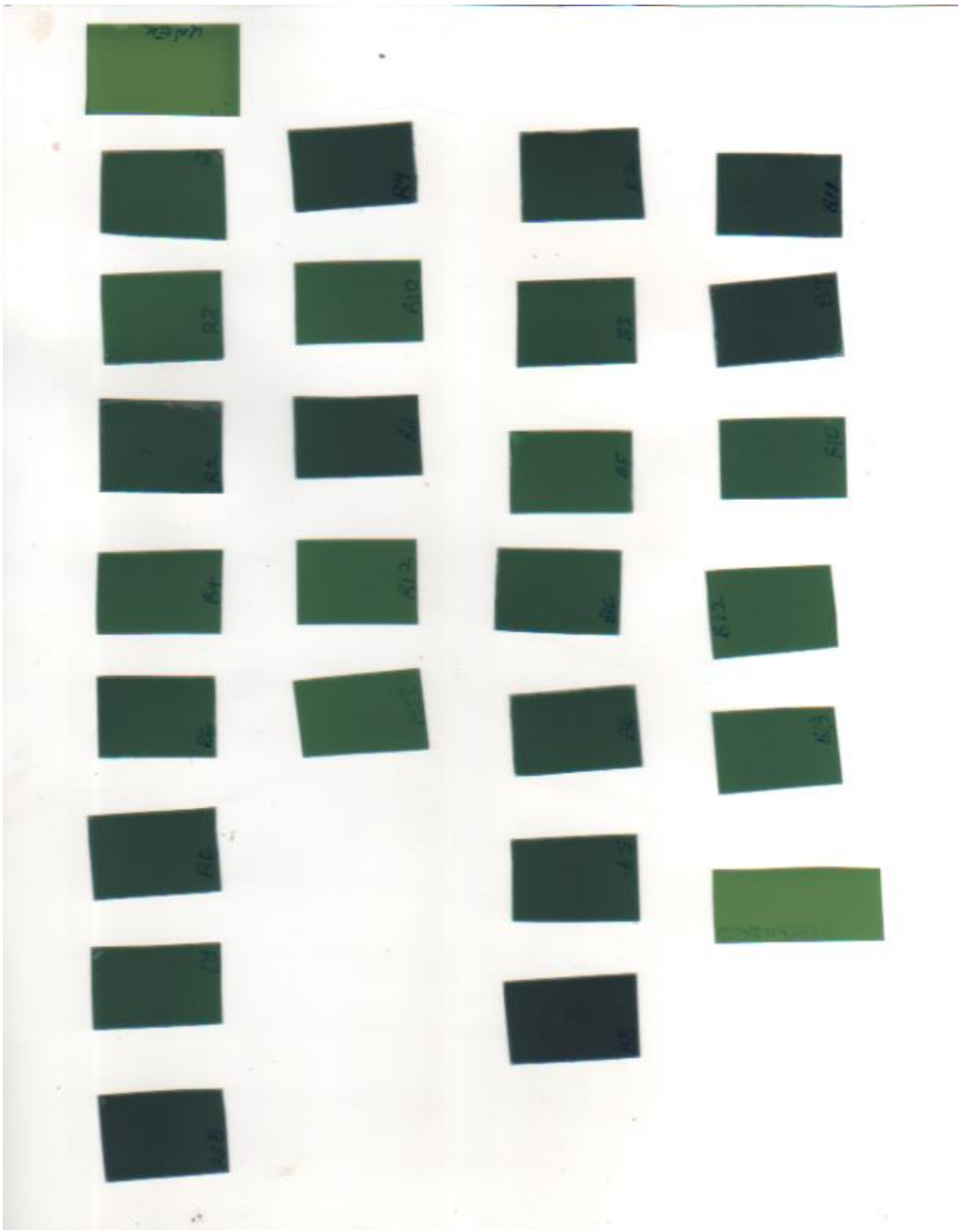

APPENDIX E-1: AN ANTERIOR – POSTERIOR (AP) RADIOGRAPH OF THE APPLICATOR (CYLINDER ONLY) INSERTIONS OBTAINED FROM ONE THE EXPERIMENTAL SET-UPS.

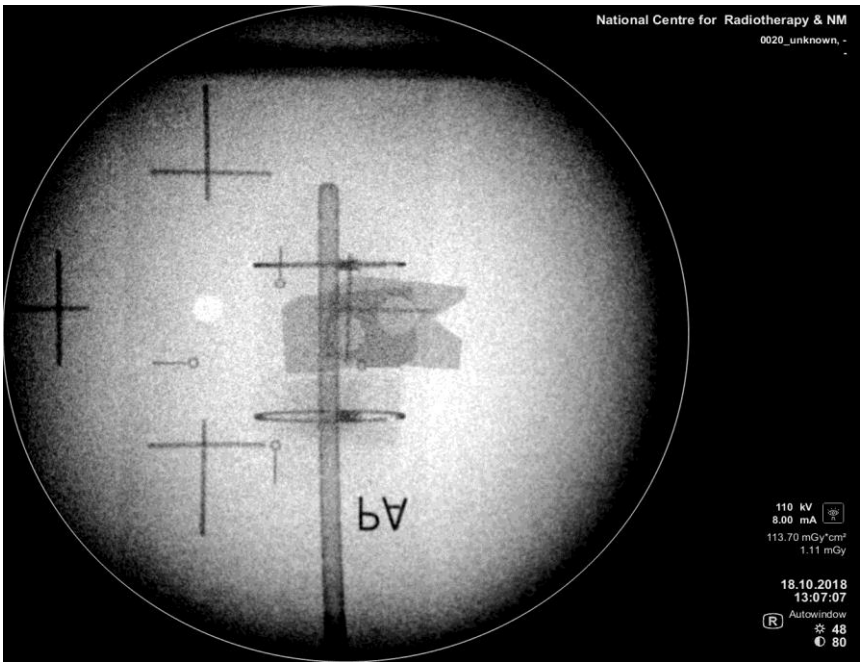

APPENDIX E-2: LATERAL RADIOGRAPH (LAT) OF THE APPLICATOR (CYLINDER ONLY) INSERTIONS OBTAINED FROM ONE OF THE EXPERIMENTAL SET-UPS.

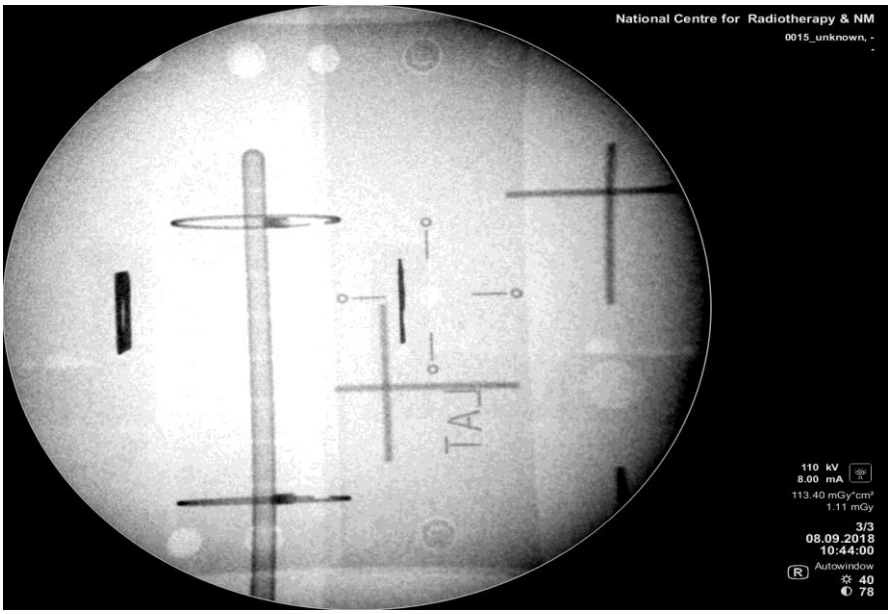

APPENDIX E- 3: AN ANTERIOR – POSTERIOR RADIOGRAPH (AP) OF THE FLETCHER SUITE OF APPLICATOR INSERTIONS OBTAINED FROM ONE OF THE EXPERIMENTAL SET-UPS.

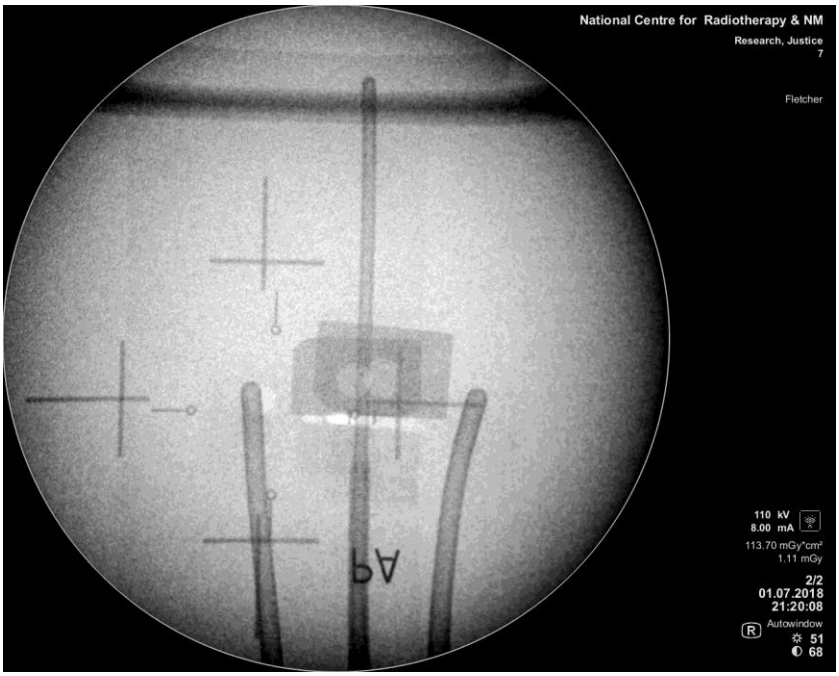

APPENDIX E-4: LATERAL RADIOGRAPH (LAT) OF THE FLETCHER SUITE OF APPLICATOR INSERTIONS OBTAINED FROM ONE OF THE EXPERIMENTAL SET-UPS.

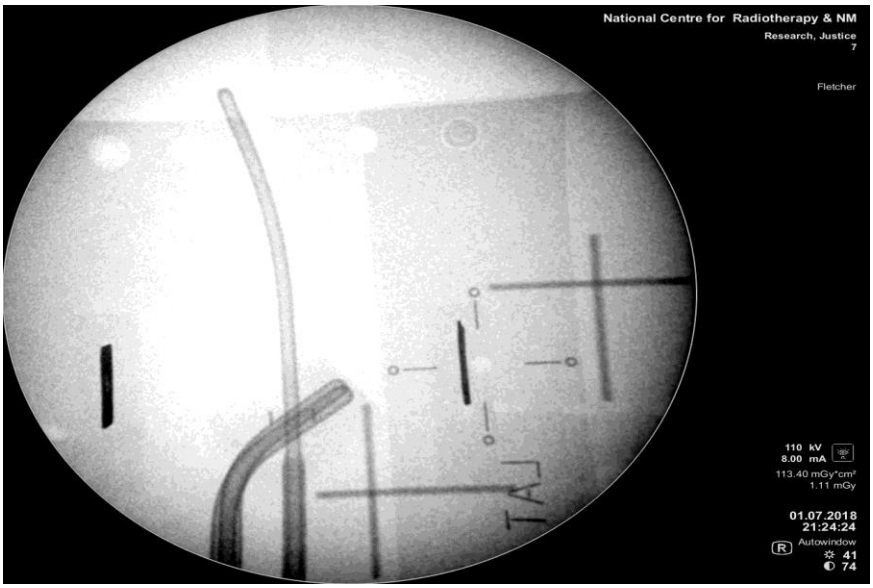

APPENDIX E-5: AN ANTERIOR – POSTERIOR RADIOGRAPH (AP) OF THE FLETCHER SUITE OF APPLICATOR INSERTIONS OBTAINED FROM ONE OF THE EXPERIMENTAL SET-UPS.

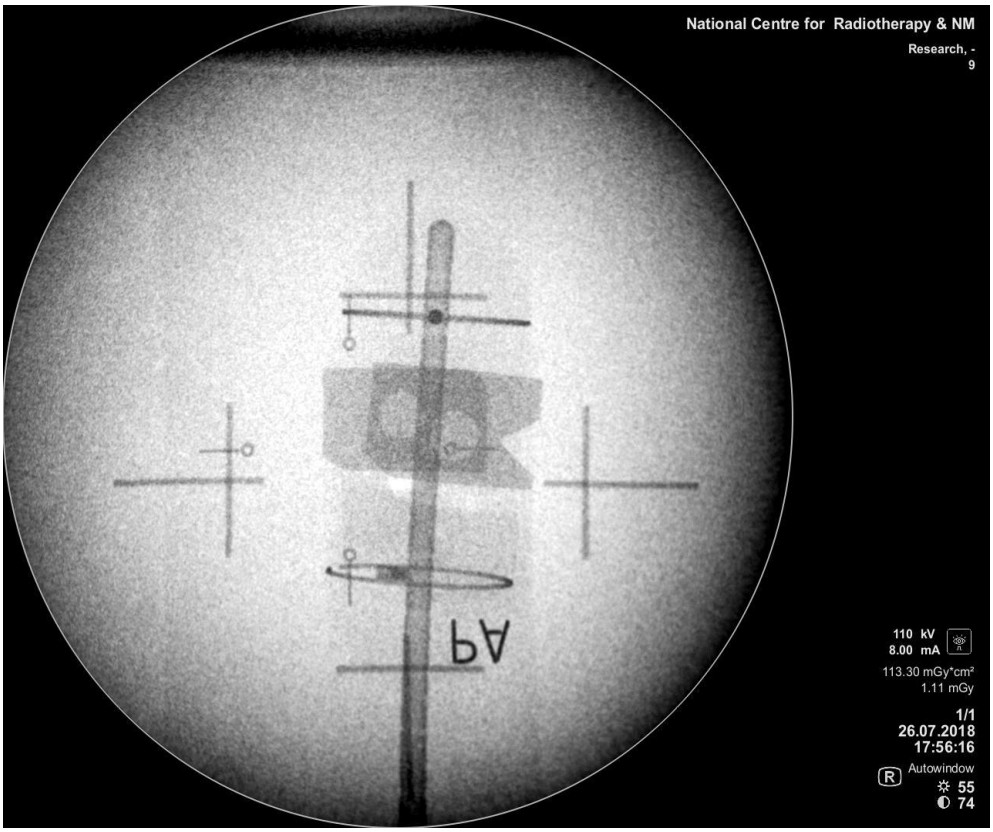

APPENDIX E-6: LATERAL RADIOGRAPH (LAT) OF THE FLETCHER SUITE OF APPLICATOR INSERTIONS OBTAINED FROM ONE OF THE EXPERIMENTAL SET-UPS.

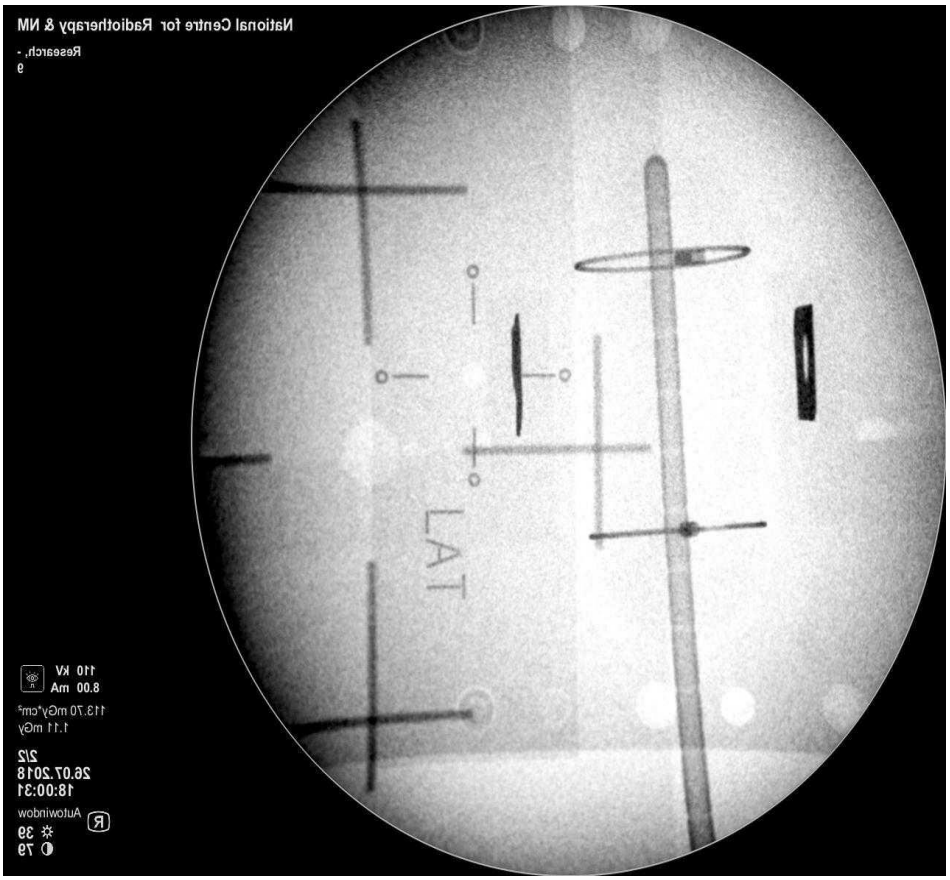

APPENDIX E-7: LATERAL RADIOGRAPH (LAT) OF THE FLETCHER SUITE OF APPLICATOR INSERTIONS OBTAINED FROM ONE OF THE EXPERIMENTAL SET-UPS.

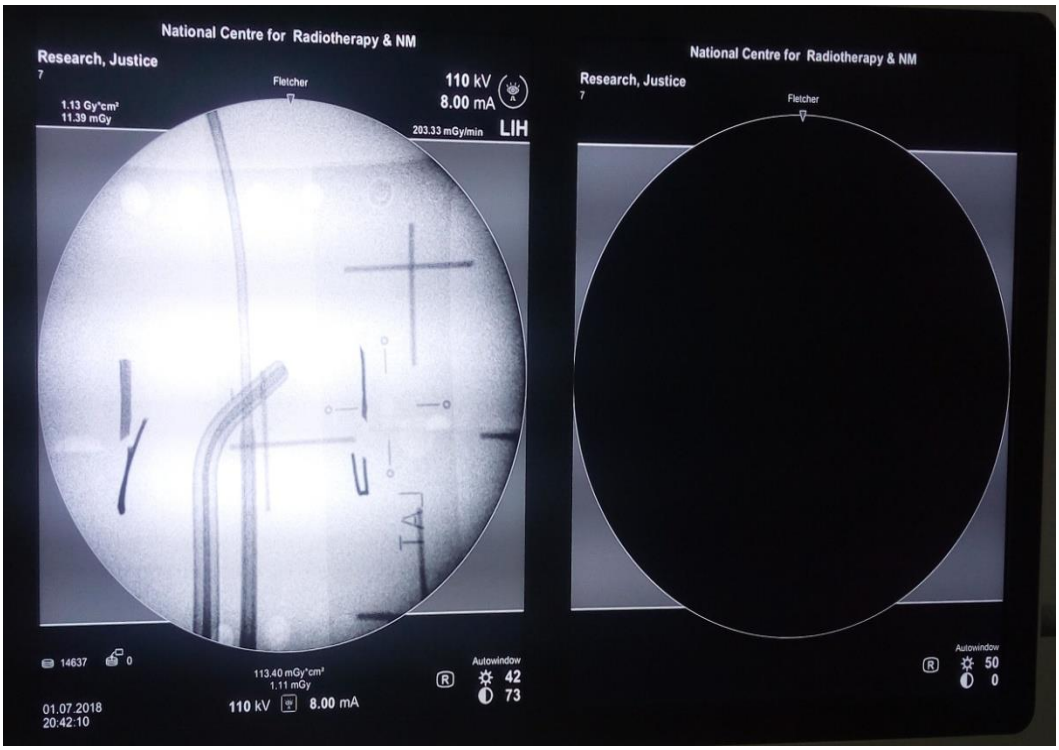

APPENDIX F-1: TPS WINDOW SHOWING PLANS FOR DOSE CALCULATION (FOR FLETCHER SUITE OF APPLICATORS INCLUDING THE TANDEM).

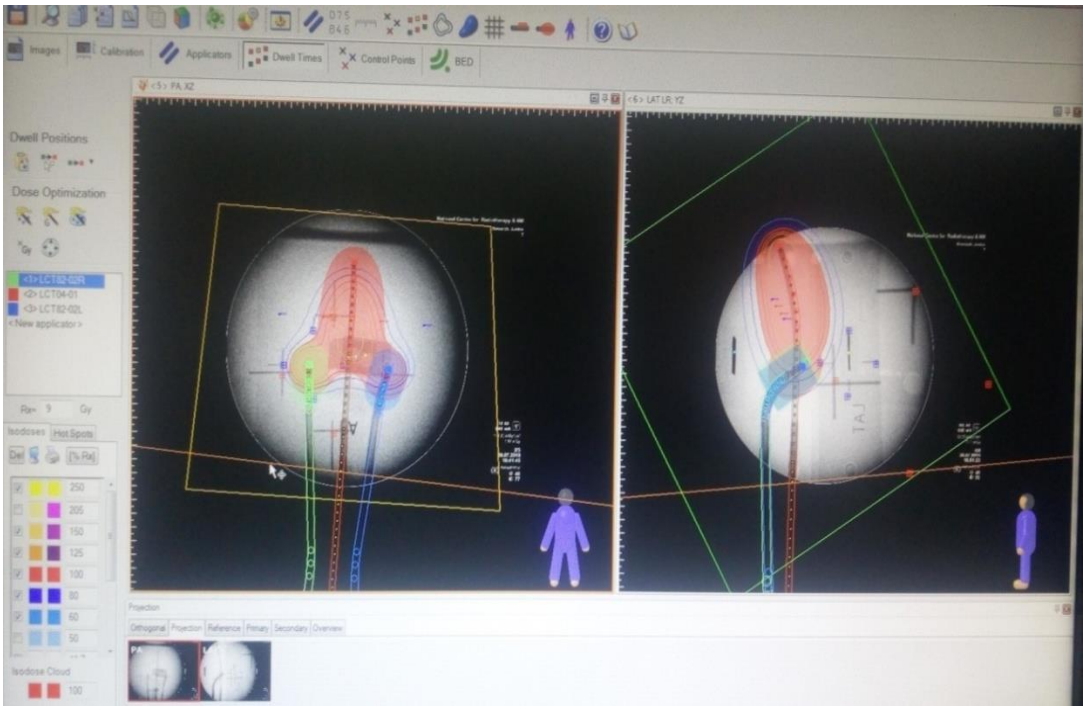

APPENDIX F-2: TPS WINDOW SHOWING PLANS FOR DOSE CALCULATION (CYLINDERS ONLY).

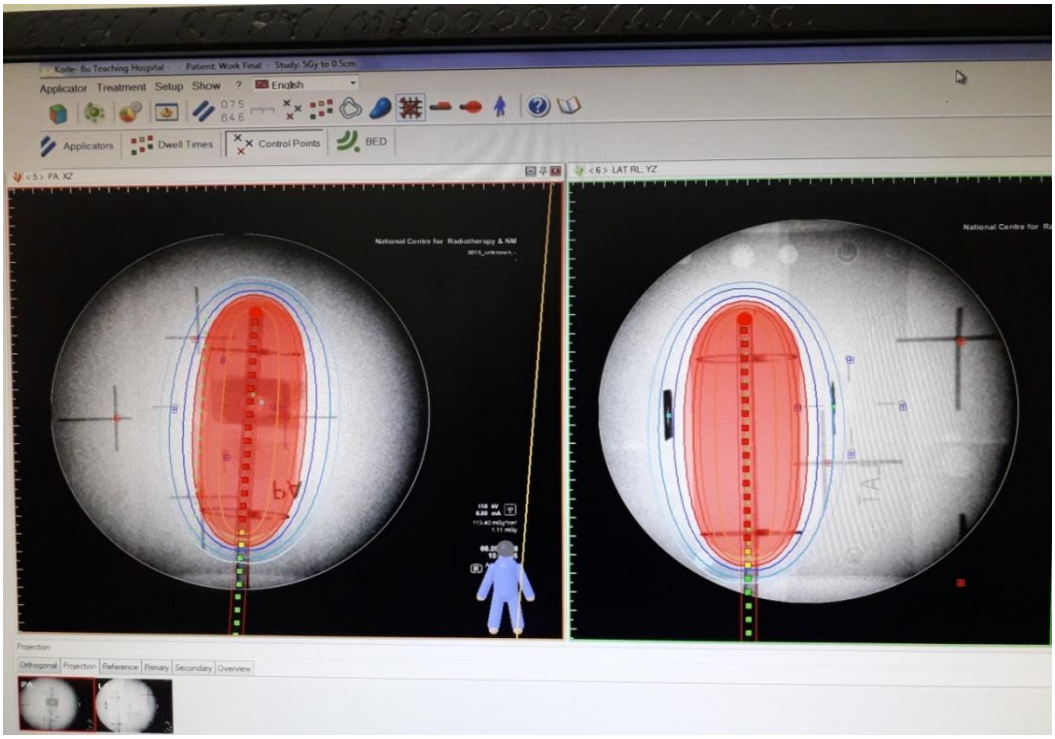

APPENDIX F-3: TPS WINDOW SHOWING PLANS FOR DOSE CALCULATION (FOR FLETCHER SUITE OF APPLICATORS INCLUDING THE TANDEM).

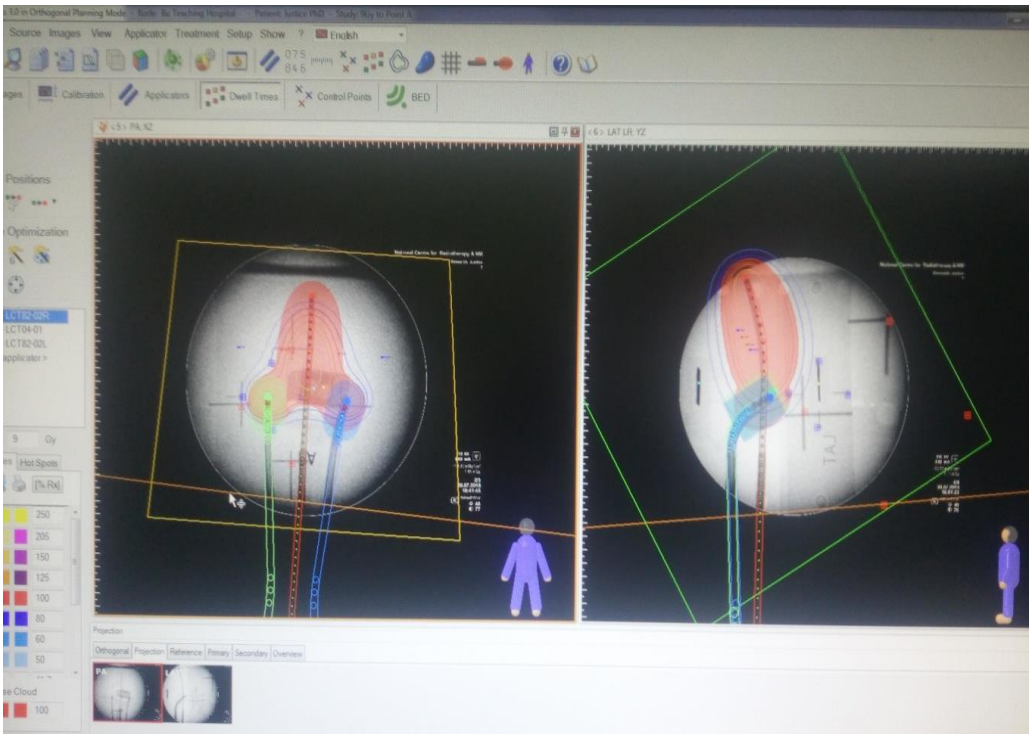

APPENDIX F-4: TPS WINDOW SHOWING PLANS FOR DOSE CALCULATION (FOR FLETCHER SUITE OF APPLICATORS INCLUDING THE TANDEM).

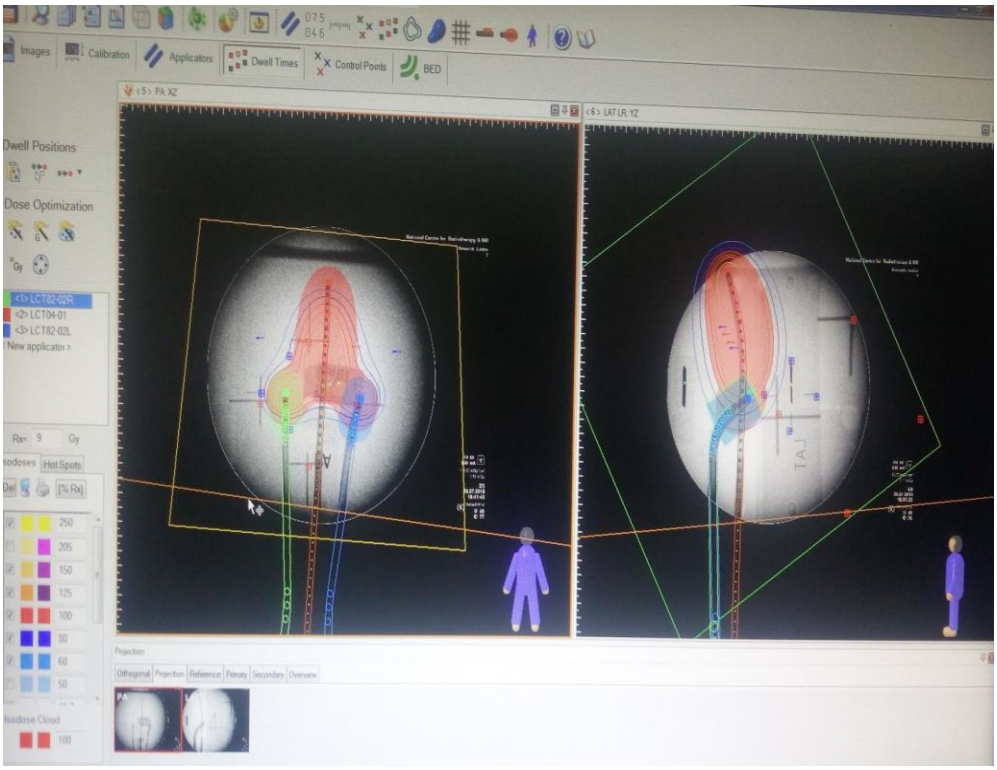

APPENDIX F-5: TPS WINDOW SHOWING PLANS FOR DOSE CALCULATION (FOR FLETCHER SUITE OF APPLICATORS INCLUDING THE TANDEM).

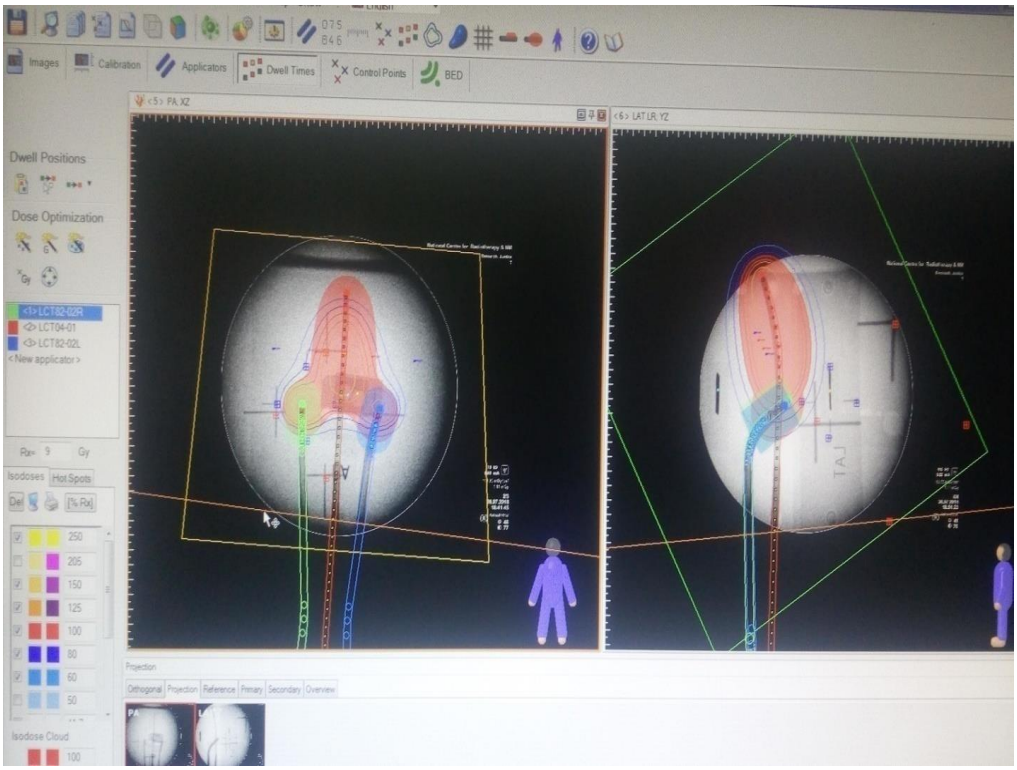

APPENDIX F-6: TPS WINDOW SHOWING PLANS FOR DOSE CALCULATION (FOR FLETCHER SUITE OF APPLICATORS INCLUDING THE TANDEM).

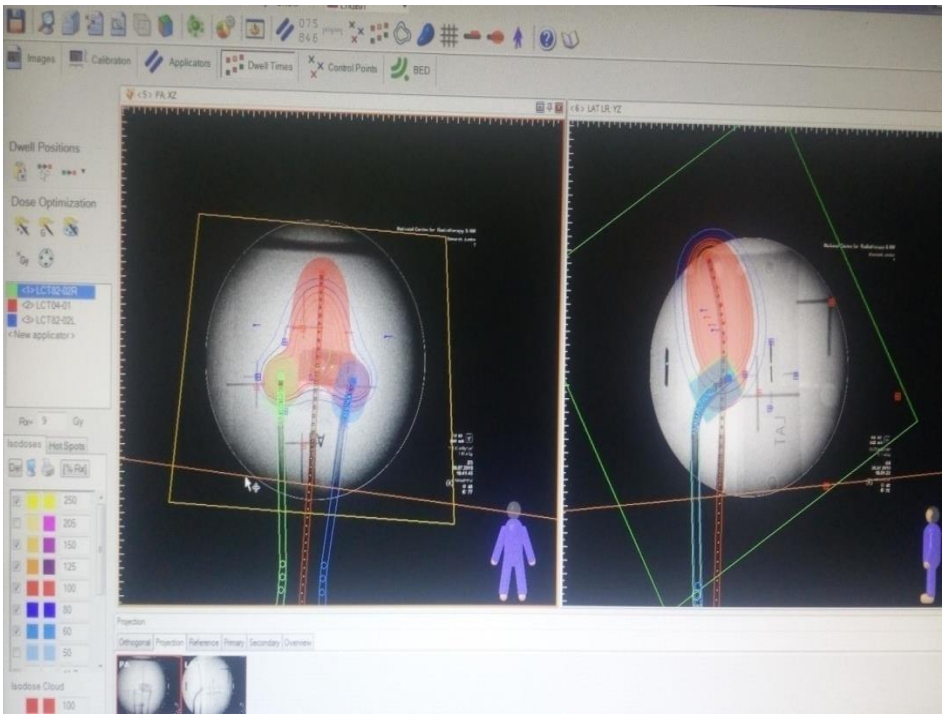

APPENDIX F-7: TPS WINDOW SHOWING PLANS FOR DOSE CALCULATION (FOR CYLINDERS ONLY).

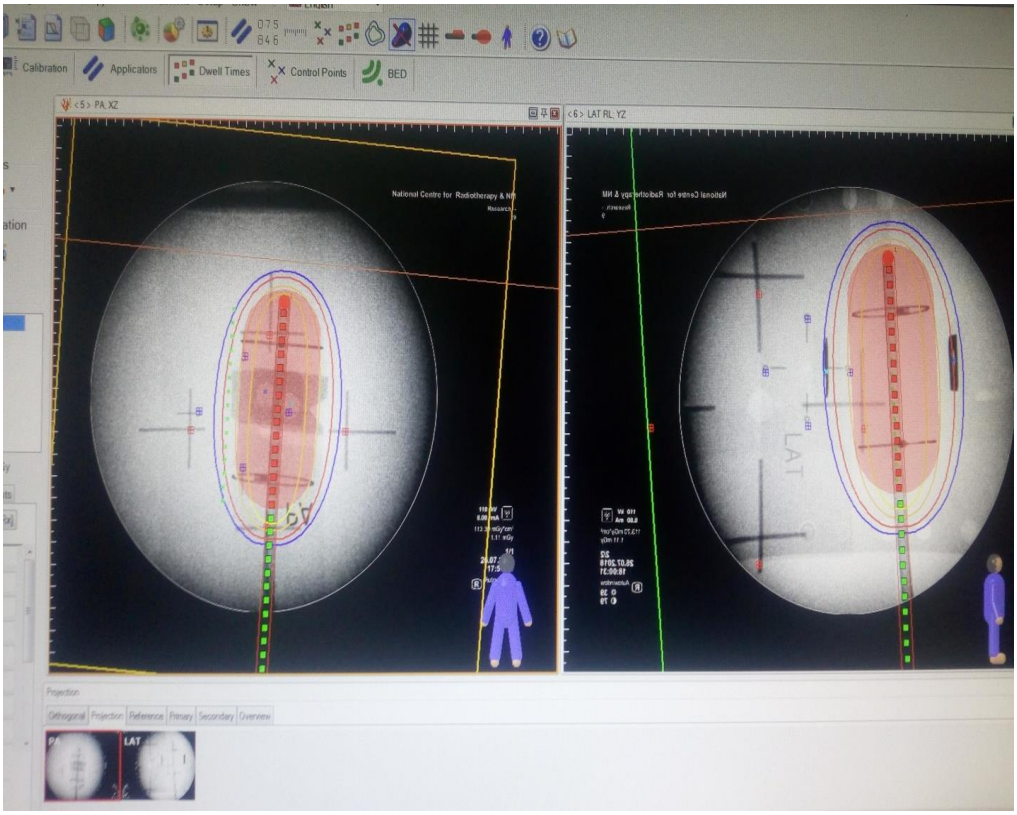

APPENDIX G-1: DOSE CONTROL POINT REPORT OF THE TREATMENT PLAN FROM THE TPS SHOWING DOSE CALCULATION (CYLINDERS ONLY).

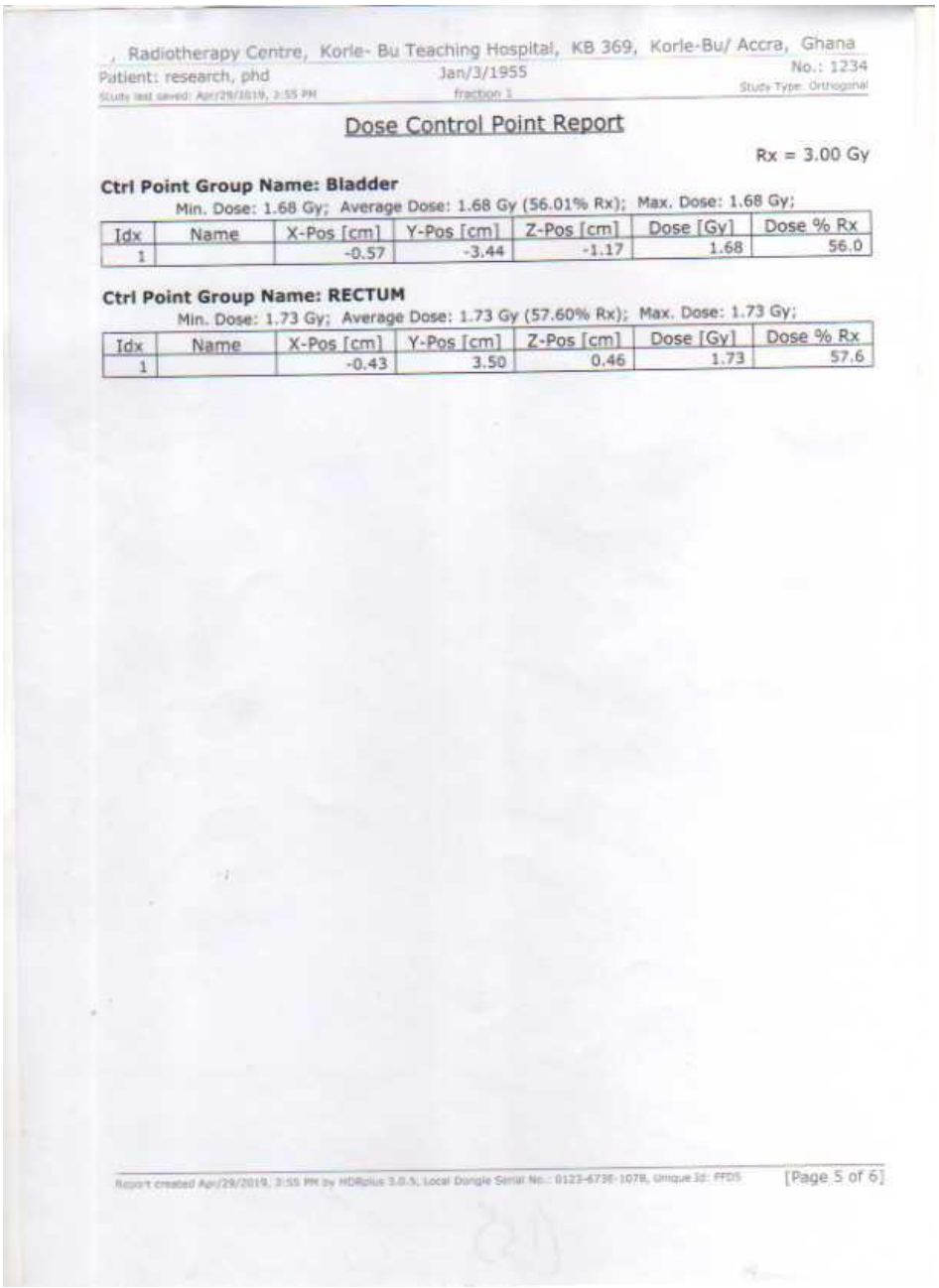

, Radiotherapy Centre, Korle- Bu Teaching Hospital, KB 369, Korle-Bu/ Accra, Ghana

Patient: research, phd — Jan/3/1955 — No.: 1234

Study last saved: Apr/29/2019, 3:55 PM — fraction 1 — Study Type: Orthogonal

Dose Control Point Report

Rx = 3.00 Gy

Ctrl Point Group Name: Bladder

Min. Dose: 1.68 Gy; Average Dose: 1.68 Gy (56.01% Rx); Max. Dose: 1.68 Gy;

Idx	Name	X-Pos [cm]	Y-Pos [cm]	Z-Pos [cm]	Dose [Gy]	Dose % Rx
1		-0.57	-3.44	-1.17	1.68	56.0

Ctrl Point Group Name: RECTUM

Min. Dose: 1.73 Gy; Average Dose: 1.73 Gy (57.60% Rx); Max. Dose: 1.73 Gy;

Idx	Name	X-Pos [cm]	Y-Pos [cm]	Z-Pos [cm]	Dose [Gy]	Dose % Rx
1		-0.43	3.50	0.46	1.73	57.6

Report created Apr/29/2019, 3:55 PM by HDRplus 3.0.5, Local Dongle Serial No.: 0123-6736-1078, Unique Id: FFD5 [Page 5 of 6]

APPENDIX G-2: DOSE CONTROL POINT REPORT OF THE TREATMENT PLAN FROM THE TPS SHOWING DOSE CALCULATION (CYLINDERS ONLY).

, Radiotherapy Centre, Korle- Bu Teaching Hospital, KB 369, Korle-Bu/ Accra, Ghana

Patient: research, phd Jan/3/1955 No.: 1234

Study last saved: Apr/29/2019, 3:23 PM Fraction 1 Study Type: Orthogonal

Dose Control Point Report

Rx = 2.80 Gy

Ctrl Point Group Name: Bladder

Min. Dose: 1.57 Gy; Average Dose: 1.57 Gy (56.01% Rx); Max. Dose: 1.57 Gy;

Idx	Name	X-Pos [cm]	Y-Pos [cm]	Z-Pos [cm]	Dose [Gy]	Dose % Rx
1		-0.57	-3.44	-1.17	1.57	56.0

Ctrl Point Group Name: RECTUM

Min. Dose: 1.61 Gy; Average Dose: 1.61 Gy (57.60% Rx); Max. Dose: 1.61 Gy;

Idx	Name	X-Pos [cm]	Y-Pos [cm]	Z-Pos [cm]	Dose [Gy]	Dose % Rx
1		-0.43	3.50	0.46	1.61	57.6

Report created Apr/29/2019, 3:23 PM by HDRplus 3.0.5, Local Dongle Serial No.: 0123-8738-1078, Unique Id: DF34 [Page 5 of 6]

APPENDIX G-3: DOSE CONTROL POINT REPORT OF THE TREATMENT PLAN FROM THE TPS SHOWING DOSE CALCULATION (FLETCHER SUITES OF APPLICATORS).

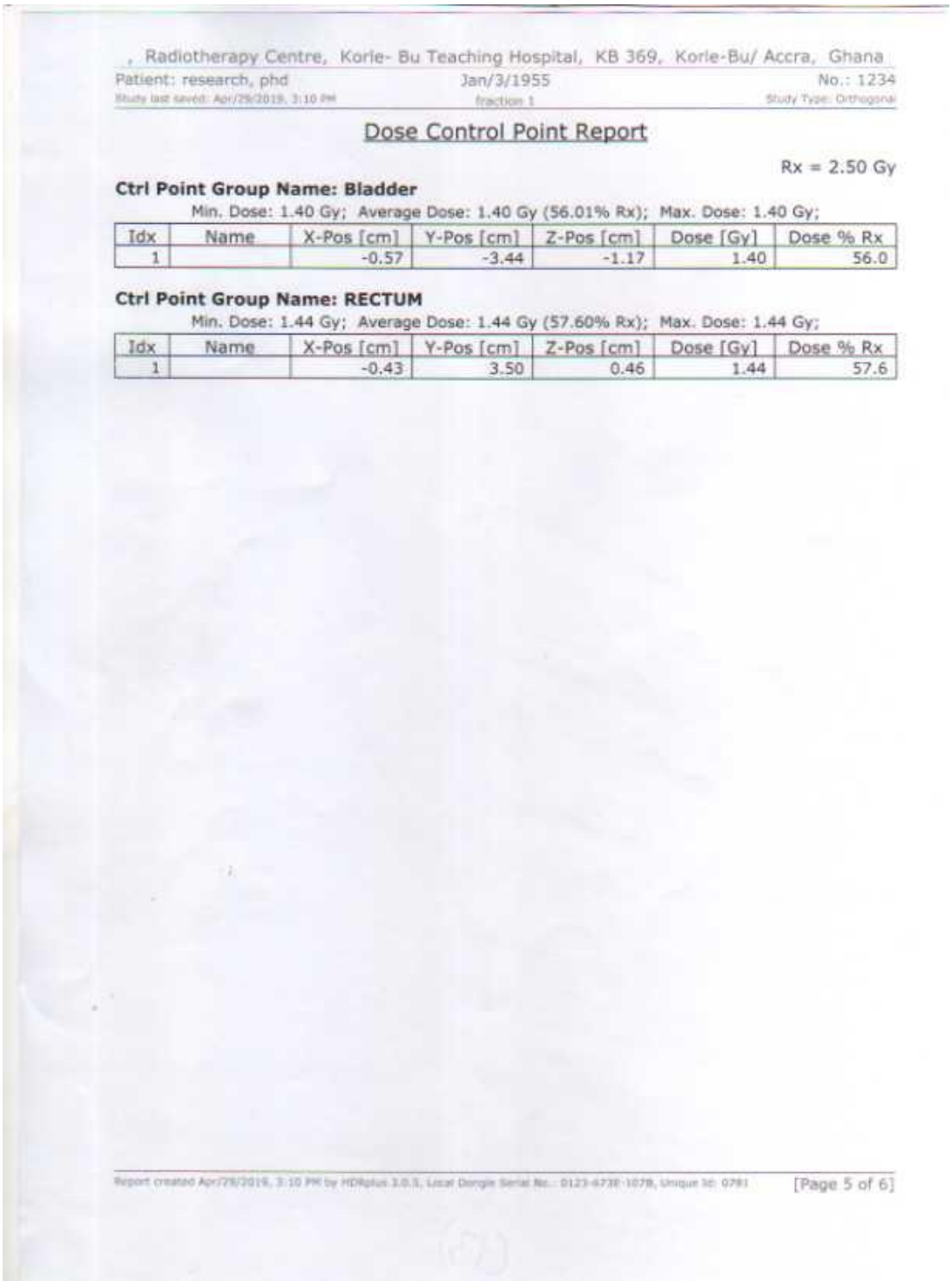

, Radiotherapy Centre, Korle- Bu Teaching Hospital, KB 369, Korle-Bu/ Accra, Ghana

Patient: research, phd | Jan/3/1955 | No.: 1234

Study last saved: Apr/29/2019, 3:10 PM | fraction 1 | Study Type: Orthogonal

Dose Control Point Report

Rx = 2.50 Gy

Ctrl Point Group Name: Bladder

Min. Dose: 1.40 Gy; Average Dose: 1.40 Gy (56.01% Rx); Max. Dose: 1.40 Gy;

Idx	Name	X-Pos [cm]	Y-Pos [cm]	Z-Pos [cm]	Dose [Gy]	Dose % Rx
1		-0.57	-3.44	-1.17	1.40	56.0

Ctrl Point Group Name: RECTUM

Min. Dose: 1.44 Gy; Average Dose: 1.44 Gy (57.60% Rx); Max. Dose: 1.44 Gy;

Idx	Name	X-Pos [cm]	Y-Pos [cm]	Z-Pos [cm]	Dose [Gy]	Dose % Rx
1		-0.43	3.50	0.46	1.44	57.6

Report created Apr/29/2019, 3:10 PM by HDRplus 3.0.5, Local Dongle Serial No.: 0123-6730-1078, Unique Id: 0781 [Page 5 of 6]

APPENDIX G-4: DOSE CONTROL POINT REPORT OF THE TREATMENT PLAN FROM THE TPS SHOWING DOSE CALCULATION (CYLINDERS ONLY).

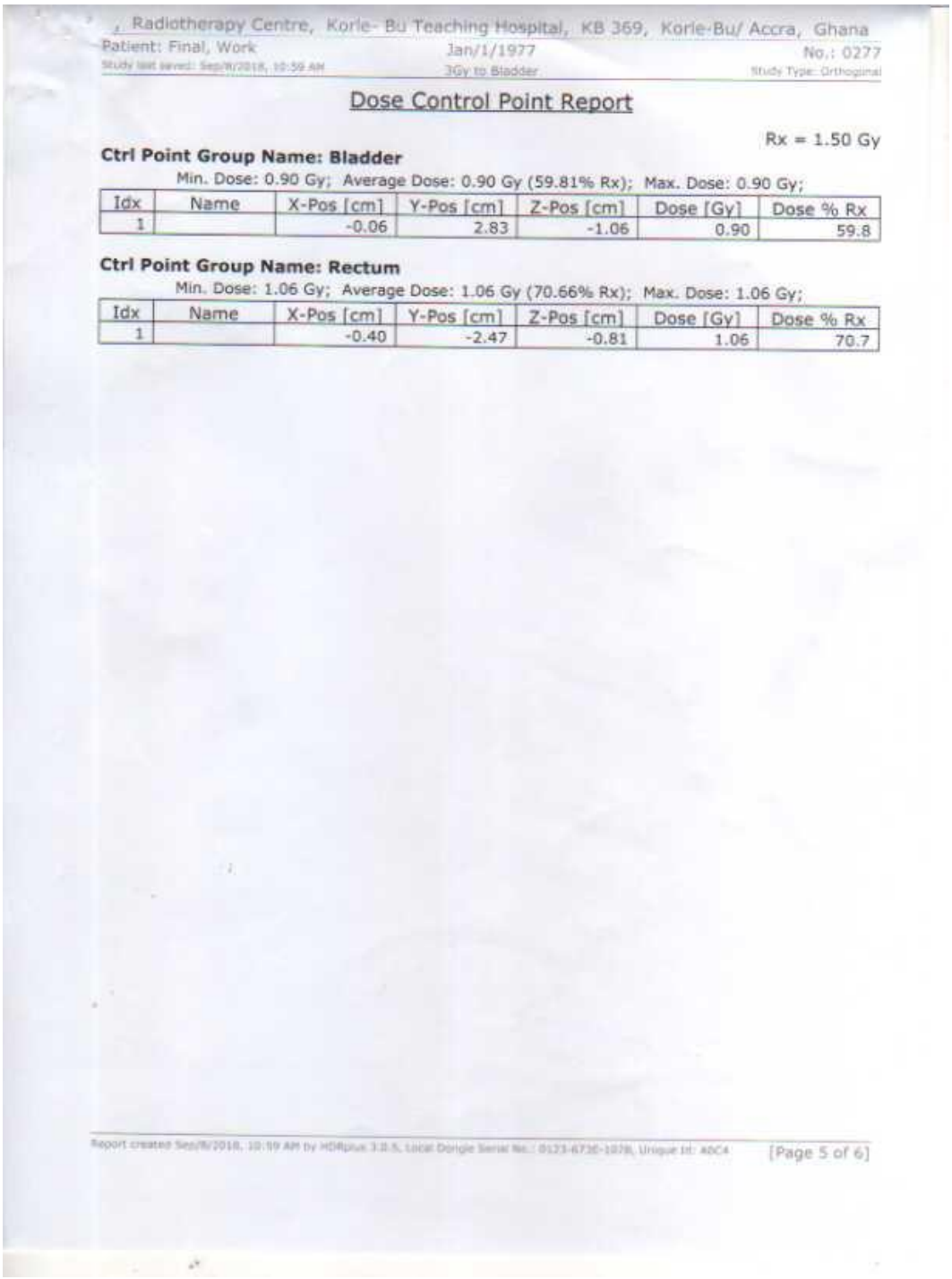

Radiotherapy Centre, Korle- Bu Teaching Hospital, KB 369, Korle-Bu/ Accra, Ghana

Patient: Final, Work — Jan/1/1977 — No.: 0277

Study last saved: Sep/8/2018, 10:59 AM — 3Gy to Bladder — Study Type: Orthogonal

Dose Control Point Report

Rx = 1.50 Gy

Ctrl Point Group Name: Bladder

Min. Dose: 0.90 Gy; Average Dose: 0.90 Gy (59.81% Rx); Max. Dose: 0.90 Gy;

Idx	Name	X-Pos [cm]	Y-Pos [cm]	Z-Pos [cm]	Dose [Gy]	Dose % Rx
1		-0.06	2.83	-1.06	0.90	59.8

Ctrl Point Group Name: Rectum

Min. Dose: 1.06 Gy; Average Dose: 1.06 Gy (70.66% Rx); Max. Dose: 1.06 Gy;

Idx	Name	X-Pos [cm]	Y-Pos [cm]	Z-Pos [cm]	Dose [Gy]	Dose % Rx
1		-0.40	-2.47	-0.81	1.06	70.7

Report created Sep/8/2018, 10:59 AM by HDRplus 3.0.5, Local Dongle Serial No.: 0123-6730-1078, Unique Id: A0C4 [Page 5 of 6]

APPENDIX G-5: DWELL POSITION REPORT OF THE TREATMENT PLAN SHOWING DWELL TIME FROM THE TPS (CYLINDERS ONLY).

, Radiotherapy Centre, Korle- Bu Teaching Hospital, KB 369, Korle-Bu/ Accra, Ghana

Patient: Final, Work Jan/1/1977 No.: 0277

Study last saved: Sep/8/2018, 10:59 AM 3Gy to Bladder Study Type: Orthogonal

Dwell Position Report

Applicator <1>: LCR01-01

Dwell-Index	from Tip [cm]	X-Pos [cm]	Y-Pos [cm]	Z-Pos [cm]	Dwell-Time [s]
1	0.64	0.01	0.02	-3.79	17.20
2	1.14	0.01	0.02	-3.29	17.20
3	1.64	0.01	0.02	-2.79	17.20
4	2.14	0.01	0.02	-2.29	17.20
5	2.64	0.01	0.02	-1.79	17.20
6	3.14	0.01	0.02	-1.29	17.20
7	3.64	0.00	0.03	-0.79	17.20
8	4.14	0.00	0.03	-0.29	17.20
9	4.64	0.00	0.03	0.21	17.20
10	5.14	0.00	0.03	0.71	17.20
11	5.64	0.00	0.03	1.21	17.20
12	6.14	0.00	0.03	1.71	17.20
13	6.64	-0.01	0.04	2.21	17.20
14	7.14	-0.01	0.04	2.71	17.20
15	7.64	-0.01	0.04	3.21	17.20
16	8.14	-0.01	0.04	3.71	17.20

Total Dwell Time for this Applicator : 275.18 s = 00:04:35

Total Dwell Time for this Study: 275.18 s = 00:04:35

Total Reference Air Kerma (TRAK) : 0.1029 cGy·m²

Report created Sep/8/2018, 10:59 AM by HDRplus 3.0.5, Local Dongle Serial No.: 0123-673F-107B, Unique Id: A0C4 [Page 4 of 6]

APPENDIX G-6: DOSE CONTROL POINT REPORT OF THE REATMENT FROM THE TPS SHOWING DOSE CALCULATION (CYLINDERS ONLY).

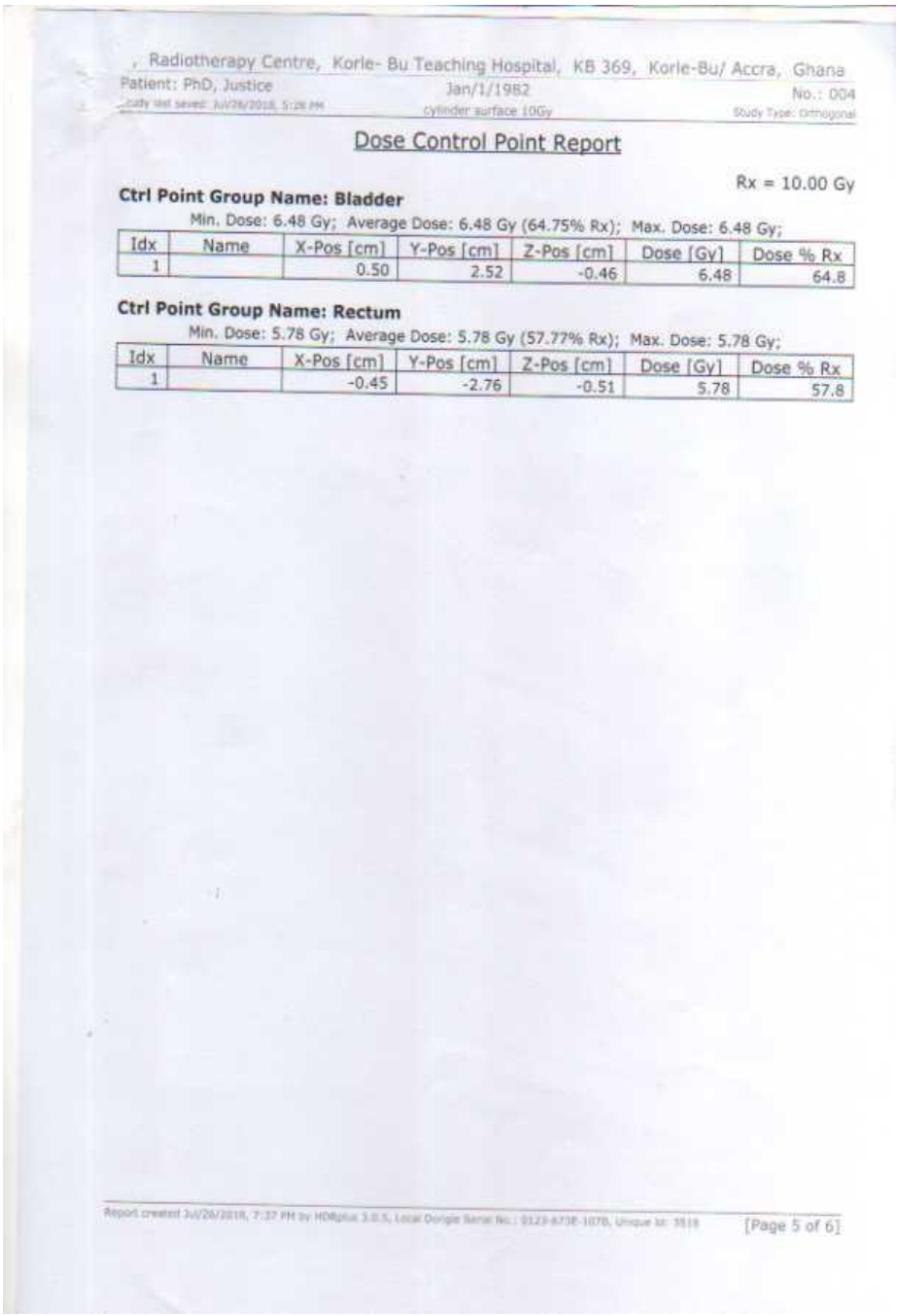

, Radiotherapy Centre, Korle- Bu Teaching Hospital, KB 369, Korle-Bu/ Accra, Ghana

Patient: PhD, Justice Jan/1/1982 No.: 004

Study last saved: Jul/26/2018, 5:26 PM Cylinder surface 10Gy Study Type: Orthogonal

Dose Control Point Report

Rx = 10.00 Gy

Ctrl Point Group Name: Bladder

Min. Dose: 6.48 Gy; Average Dose: 6.48 Gy (64.75% Rx); Max. Dose: 6.48 Gy;

Idx	Name	X-Pos [cm]	Y-Pos [cm]	Z-Pos [cm]	Dose [Gy]	Dose % Rx
1		0.50	2.52	-0.46	6.48	64.8

Ctrl Point Group Name: Rectum

Min. Dose: 5.78 Gy; Average Dose: 5.78 Gy (57.77% Rx); Max. Dose: 5.78 Gy;

Idx	Name	X-Pos [cm]	Y-Pos [cm]	Z-Pos [cm]	Dose [Gy]	Dose % Rx
1		-0.45	-2.76	-0.51	5.78	57.8

Report created Jul/26/2018, 7:37 PM by HDRplus 3.0.5, Local Dongle Serial No.: 0123-6738-1078, Unique Id: 3519 [Page 5 of 6]

APPENDIX G-7: DWELL POSITION REPORT OF THE TREATMENT PLAN SHOWING DWELL TIME FROM THE TPS (CYLINDERS ONLY).

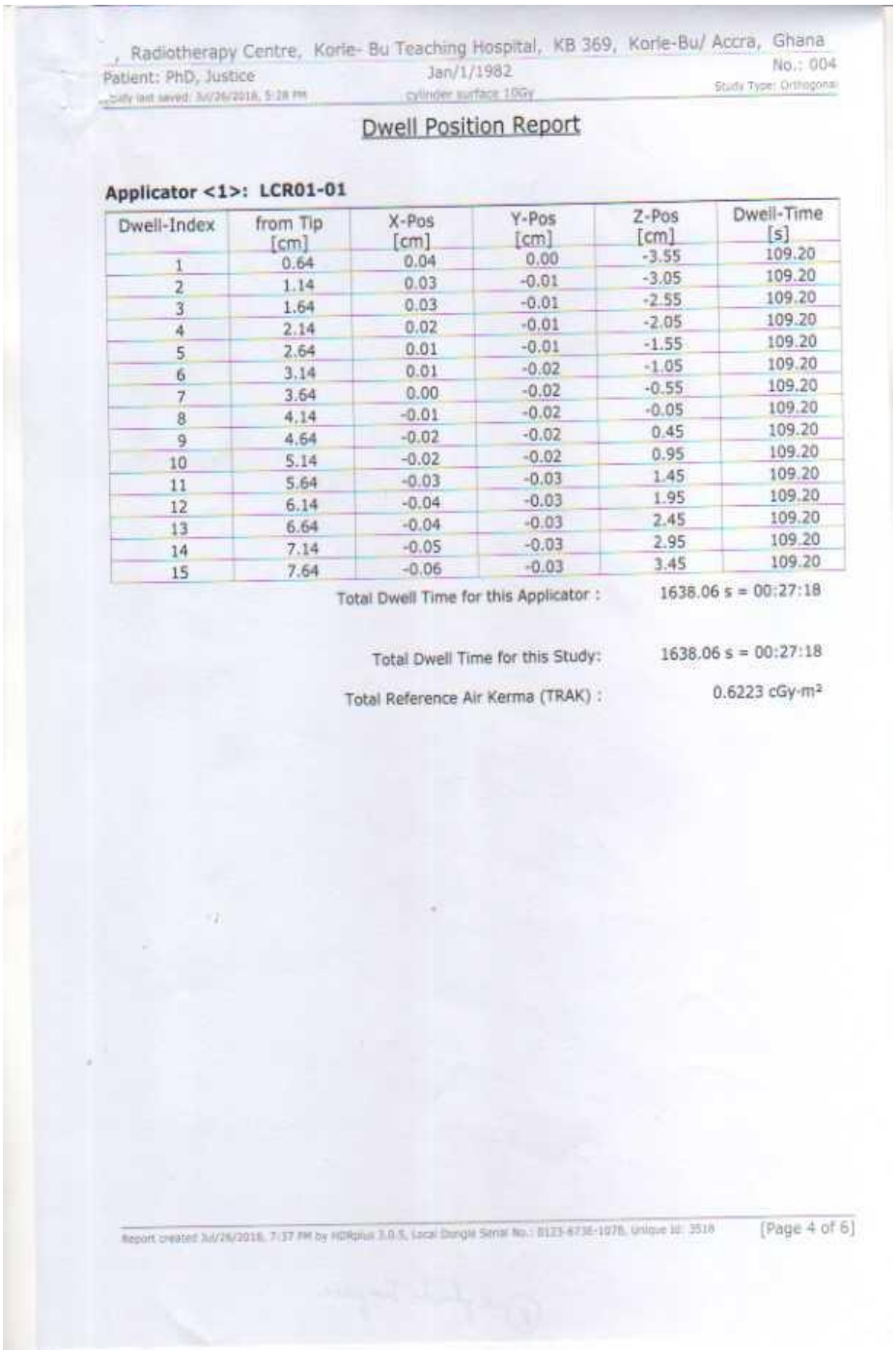

, Radiotherapy Centre, Korle- Bu Teaching Hospital, KB 369, Korle-Bu/ Accra, Ghana

Patient: PhD, Justice Jan/1/1982 No.: 004

Study last saved: Jul/26/2018, 5:28 PM cylinder surface 10Gy Study Type: Orthogonal

Dwell Position Report

Applicator <1>: LCR01-01

Dwell-Index	from Tip [cm]	X-Pos [cm]	Y-Pos [cm]	Z-Pos [cm]	Dwell-Time [s]
1	0.64	0.04	0.00	-3.55	109.20
2	1.14	0.03	-0.01	-3.05	109.20
3	1.64	0.03	-0.01	-2.55	109.20
4	2.14	0.02	-0.01	-2.05	109.20
5	2.64	0.01	-0.01	-1.55	109.20
6	3.14	0.01	-0.02	-1.05	109.20
7	3.64	0.00	-0.02	-0.55	109.20
8	4.14	-0.01	-0.02	-0.05	109.20
9	4.64	-0.02	-0.02	0.45	109.20
10	5.14	-0.02	-0.02	0.95	109.20
11	5.64	-0.03	-0.03	1.45	109.20
12	6.14	-0.04	-0.03	1.95	109.20
13	6.64	-0.04	-0.03	2.45	109.20
14	7.14	-0.05	-0.03	2.95	109.20
15	7.64	-0.06	-0.03	3.45	109.20

Total Dwell Time for this Applicator : 1638.06 s = 00:27:18

Total Dwell Time for this Study: 1638.06 s = 00:27:18

Total Reference Air Kerma (TRAK) : 0.6223 cGy·m²

Report created Jul/26/2018, 7:37 PM by HDRplus 3.0.5, Local Dongle Serial No.: 0123-673E-1078, Unique Id: 3518 [Page 4 of 6]

APPENDIX G-8: DOSE CONTROL POINT REPORTS OF THE TREATMENT PLAN FROM THE TPS SHOWING DOSE CALCULATION (FLETCHER SUITES OF APPLICATORS).

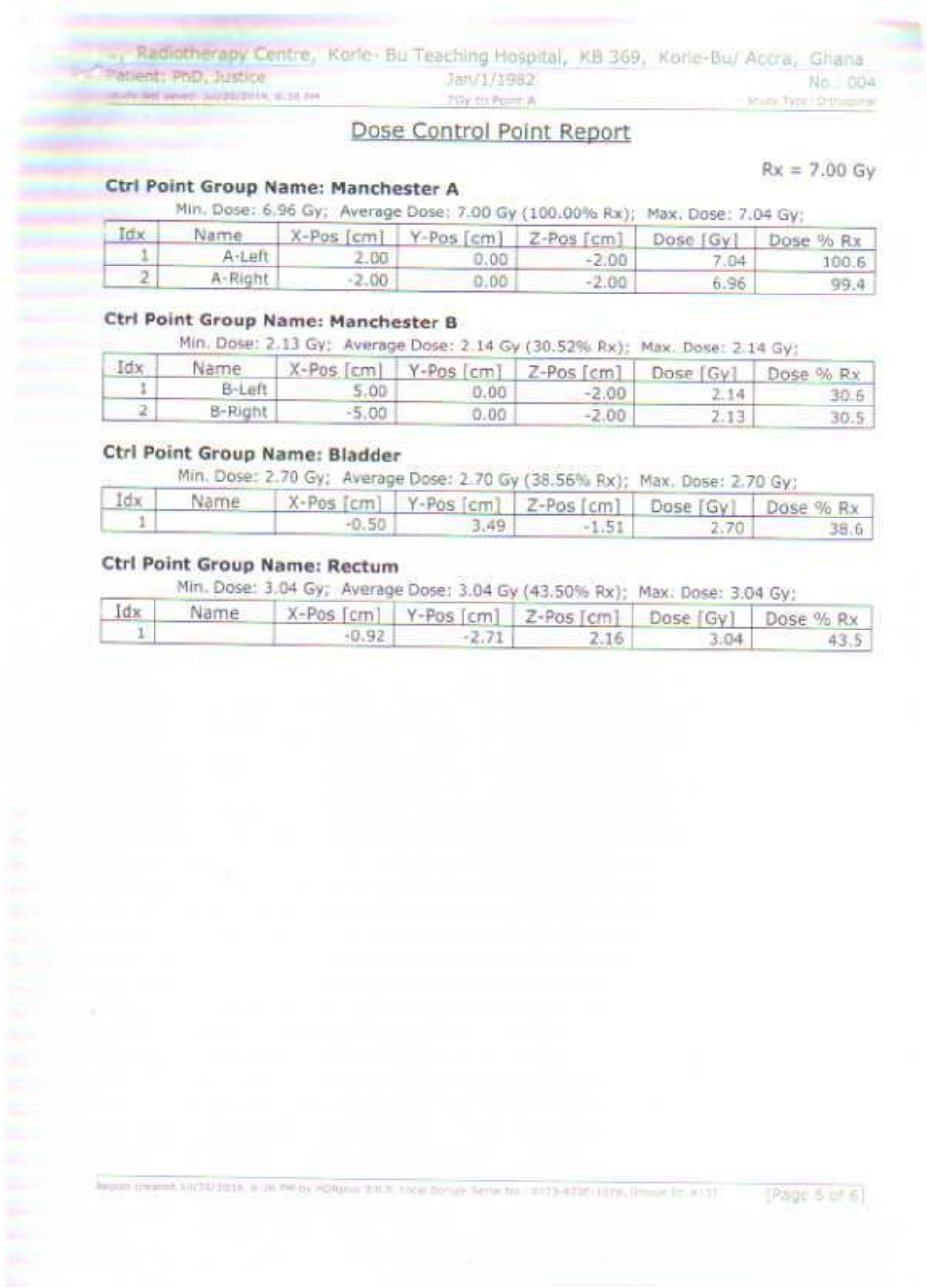

Radiotherapy Centre, Korle- Bu Teaching Hospital, KB 369, Korle-Bu/ Accra, Ghana

Patient: PhD, Justice Jan/1/1982 No.: 004

7Gy to Point A Study Type: Orthogonal

Dose Control Point Report

Rx = 7.00 Gy

Ctrl Point Group Name: Manchester A

Min. Dose: 6.96 Gy; Average Dose: 7.00 Gy (100.00% Rx); Max. Dose: 7.04 Gy;

Idx	Name	X-Pos [cm]	Y-Pos [cm]	Z-Pos [cm]	Dose [Gy]	Dose % Rx
1	A-Left	2.00	0.00	-2.00	7.04	100.6
2	A-Right	-2.00	0.00	-2.00	6.96	99.4

Ctrl Point Group Name: Manchester B

Min. Dose: 2.13 Gy; Average Dose: 2.14 Gy (30.52% Rx); Max. Dose: 2.14 Gy;

Idx	Name	X-Pos [cm]	Y-Pos [cm]	Z-Pos [cm]	Dose [Gy]	Dose % Rx
1	B-Left	5.00	0.00	-2.00	2.14	30.6
2	B-Right	-5.00	0.00	-2.00	2.13	30.5

Ctrl Point Group Name: Bladder

Min. Dose: 2.70 Gy; Average Dose: 2.70 Gy (38.56% Rx); Max. Dose: 2.70 Gy;

Idx	Name	X-Pos [cm]	Y-Pos [cm]	Z-Pos [cm]	Dose [Gy]	Dose % Rx
1		-0.50	3.49	-1.51	2.70	38.6

Ctrl Point Group Name: Rectum

Min. Dose: 3.04 Gy; Average Dose: 3.04 Gy (43.50% Rx); Max. Dose: 3.04 Gy;

Idx	Name	X-Pos [cm]	Y-Pos [cm]	Z-Pos [cm]	Dose [Gy]	Dose % Rx
1		-0.92	-2.71	2.16	3.04	43.5

Report created: 3/2/2019, 9:26 PM by HDRplus 3.0.5, Local Dongle Serial No.: 0173-4230-1019, Unique Id: 4137 [Page 5 of 6]

APPENDIX G-9: DOSE CONTROL POINT REPORTS OF THETREATMENT PLAN FROM THE TPS SHOWINGDOSE CALCULATION (FLETCHER SUITES OF APPLICATORS).

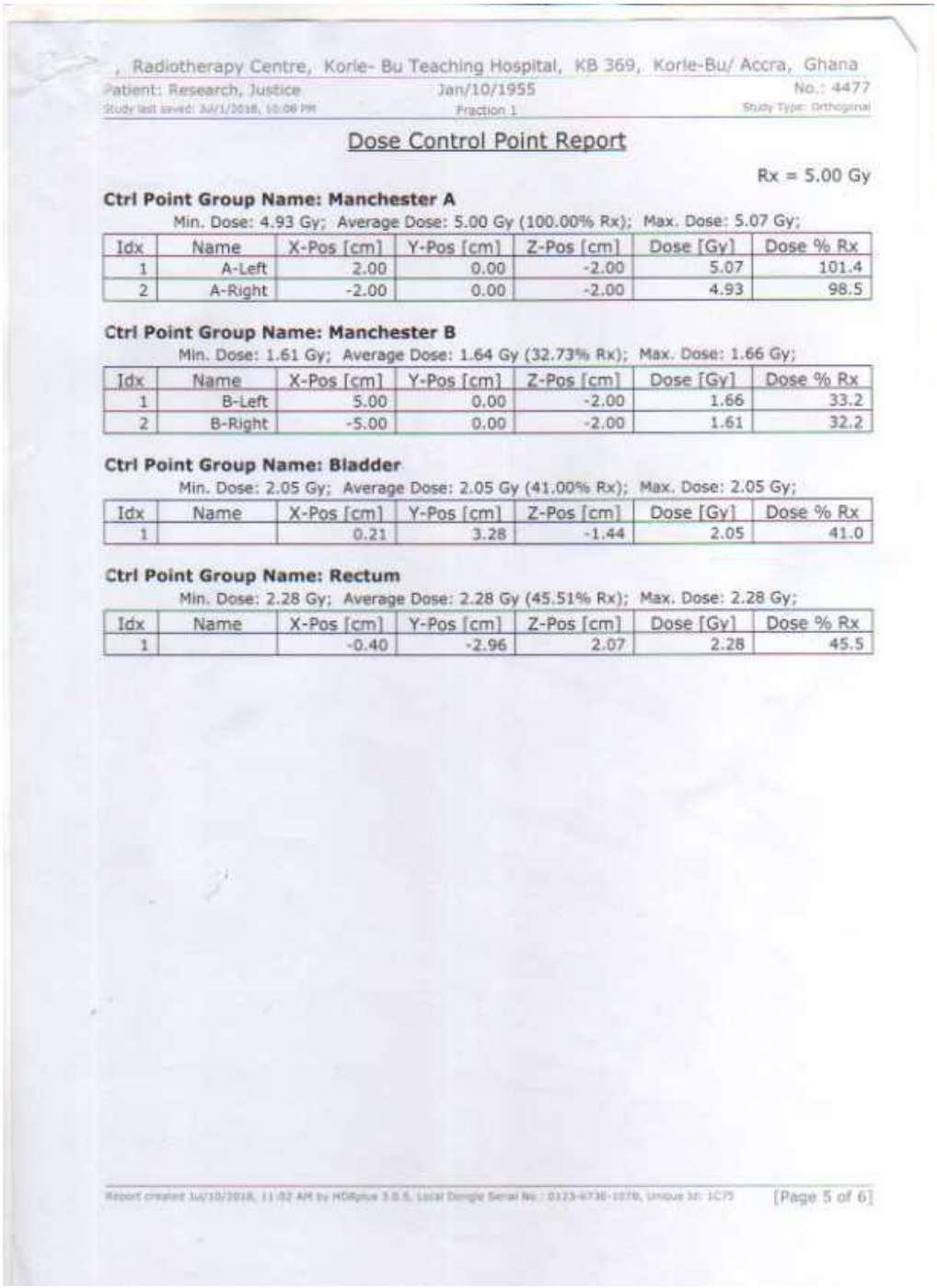

, Radiotherapy Centre, Korle- Bu Teaching Hospital, KB 369, Korle-Bu/ Accra, Ghana

Patient: Research, Justice — Jan/10/1955 — No.: 4477

Study last saved: Jul/1/2018, 10:08 PM — Fraction 1 — Study Type: Orthogonal

Dose Control Point Report

Rx = 5.00 Gy

Ctrl Point Group Name: Manchester A

Min. Dose: 4.93 Gy; Average Dose: 5.00 Gy (100.00% Rx); Max. Dose: 5.07 Gy;

Idx	Name	X-Pos [cm]	Y-Pos [cm]	Z-Pos [cm]	Dose [Gy]	Dose % Rx
1	A-Left	2.00	0.00	-2.00	5.07	101.4
2	A-Right	-2.00	0.00	-2.00	4.93	98.5

Ctrl Point Group Name: Manchester B

Min. Dose: 1.61 Gy; Average Dose: 1.64 Gy (32.73% Rx); Max. Dose: 1.66 Gy;

Idx	Name	X-Pos [cm]	Y-Pos [cm]	Z-Pos [cm]	Dose [Gy]	Dose % Rx
1	B-Left	5.00	0.00	-2.00	1.66	33.2
2	B-Right	-5.00	0.00	-2.00	1.61	32.2

Ctrl Point Group Name: Bladder

Min. Dose: 2.05 Gy; Average Dose: 2.05 Gy (41.00% Rx); Max. Dose: 2.05 Gy;

Idx	Name	X-Pos [cm]	Y-Pos [cm]	Z-Pos [cm]	Dose [Gy]	Dose % Rx
1		0.21	3.28	-1.44	2.05	41.0

Ctrl Point Group Name: Rectum

Min. Dose: 2.28 Gy; Average Dose: 2.28 Gy (45.51% Rx); Max. Dose: 2.28 Gy;

Idx	Name	X-Pos [cm]	Y-Pos [cm]	Z-Pos [cm]	Dose [Gy]	Dose % Rx
1		-0.40	-2.96	2.07	2.28	45.5

Report created Jul/10/2018, 11:02 AM by HDRplus 3.0.5, Local Dongle Serial No.: 0123-6730-1078, Unique Id: 1C75 [Page 5 of 6]

APPENDIX G-10: DOSE CONTROL POINT REPORTS OF THE TREATMENT PLAN FROM THE TPS SHOWING DOSE CALCULATION (FLETCHER SUITES OF APPLICATORS).

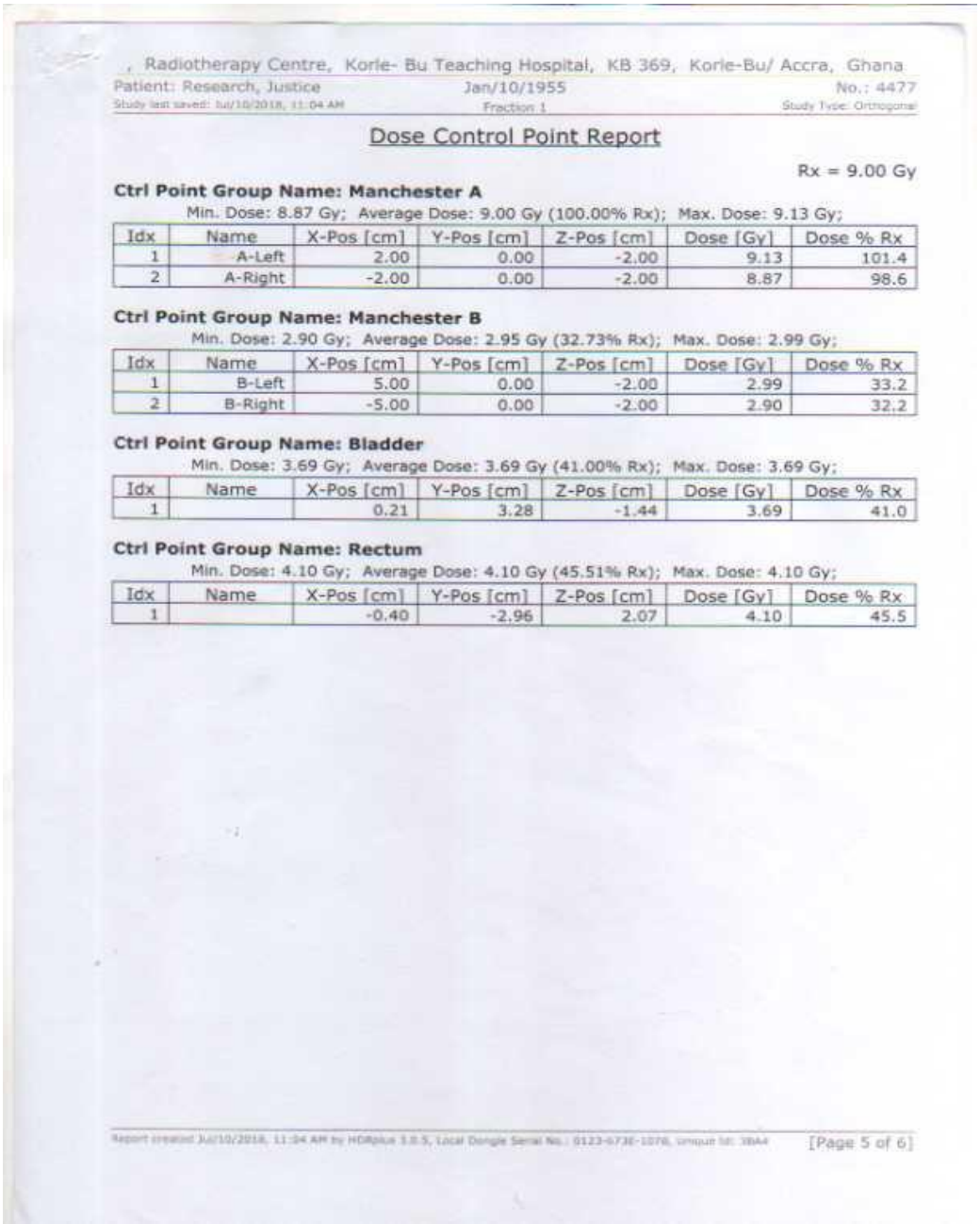

, Radiotherapy Centre, Korle- Bu Teaching Hospital, KB 369, Korle-Bu/ Accra, Ghana
Patient: Research, Justice Jan/10/1955 No.: 4477
Study last saved: Jul/10/2018, 11:04 AM Fraction 1 Study Type: Orthogonal

Dose Control Point Report

Rx = 9.00 Gy

Ctrl Point Group Name: Manchester A

Min. Dose: 8.87 Gy; Average Dose: 9.00 Gy (100.00% Rx); Max. Dose: 9.13 Gy;

Idx	Name	X-Pos [cm]	Y-Pos [cm]	Z-Pos [cm]	Dose [Gy]	Dose % Rx
1	A-Left	2.00	0.00	-2.00	9.13	101.4
2	A-Right	-2.00	0.00	-2.00	8.87	98.6

Ctrl Point Group Name: Manchester B

Min. Dose: 2.90 Gy; Average Dose: 2.95 Gy (32.73% Rx); Max. Dose: 2.99 Gy;

Idx	Name	X-Pos [cm]	Y-Pos [cm]	Z-Pos [cm]	Dose [Gy]	Dose % Rx
1	B-Left	5.00	0.00	-2.00	2.99	33.2
2	B-Right	-5.00	0.00	-2.00	2.90	32.2

Ctrl Point Group Name: Bladder

Min. Dose: 3.69 Gy; Average Dose: 3.69 Gy (41.00% Rx); Max. Dose: 3.69 Gy;

Idx	Name	X-Pos [cm]	Y-Pos [cm]	Z-Pos [cm]	Dose [Gy]	Dose % Rx
1		0.21	3.28	-1.44	3.69	41.0

Ctrl Point Group Name: Rectum

Min. Dose: 4.10 Gy; Average Dose: 4.10 Gy (45.51% Rx); Max. Dose: 4.10 Gy;

Idx	Name	X-Pos [cm]	Y-Pos [cm]	Z-Pos [cm]	Dose [Gy]	Dose % Rx
1		-0.40	-2.96	2.07	4.10	45.5

Report created Jul/10/2018, 11:04 AM by HDRplus 3.0.5, Local Dongle Serial No.: 0123-673E-1078, Unique Id: 3BA4 [Page 5 of 6]

APPENDIX G-11: DOSE CONTROL POINT REPORTS SHOWING DWELL POSITIONS FROM THE TPS (FLETCHER SUITES OF APPLICATORS).

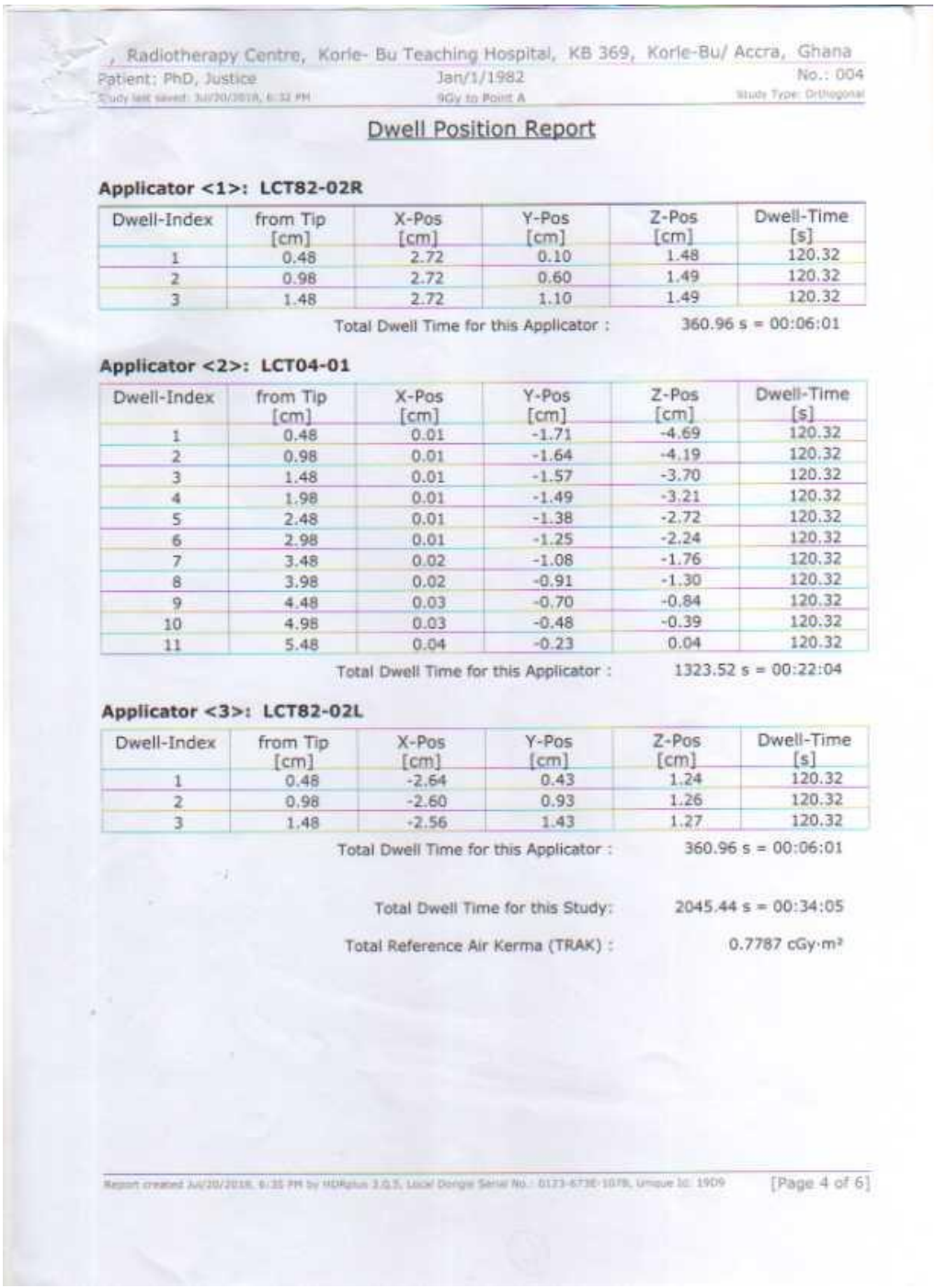

, Radiotherapy Centre, Korle- Bu Teaching Hospital, KB 369, Korle-Bu/ Accra, Ghana

Patient: PhD, Justice | Jan/1/1982 | No.: 004

Study last saved: Jul/20/2018, 6:32 PM | 8Gy to Point A | Study Type: Orthogonal

Dwell Position Report

Applicator <1>: LCT82-02R

Dwell-Index	from Tip [cm]	X-Pos [cm]	Y-Pos [cm]	Z-Pos [cm]	Dwell-Time [s]
1	0.48	2.72	0.10	1.48	120.32
2	0.98	2.72	0.60	1.49	120.32
3	1.48	2.72	1.10	1.49	120.32

Total Dwell Time for this Applicator : 360.96 s = 00:06:01

Applicator <2>: LCT04-01

Dwell-Index	from Tip [cm]	X-Pos [cm]	Y-Pos [cm]	Z-Pos [cm]	Dwell-Time [s]
1	0.48	0.01	-1.71	-4.69	120.32
2	0.98	0.01	-1.64	-4.19	120.32
3	1.48	0.01	-1.57	-3.70	120.32
4	1.98	0.01	-1.49	-3.21	120.32
5	2.48	0.01	-1.38	-2.72	120.32
6	2.98	0.01	-1.25	-2.24	120.32
7	3.48	0.02	-1.08	-1.76	120.32
8	3.98	0.02	-0.91	-1.30	120.32
9	4.48	0.03	-0.70	-0.84	120.32
10	4.98	0.03	-0.48	-0.39	120.32
11	5.48	0.04	-0.23	0.04	120.32

Total Dwell Time for this Applicator : 1323.52 s = 00:22:04

Applicator <3>: LCT82-02L

Dwell-Index	from Tip [cm]	X-Pos [cm]	Y-Pos [cm]	Z-Pos [cm]	Dwell-Time [s]
1	0.48	-2.64	0.43	1.24	120.32
2	0.98	-2.60	0.93	1.26	120.32
3	1.48	-2.56	1.43	1.27	120.32

Total Dwell Time for this Applicator : 360.96 s = 00:06:01

Total Dwell Time for this Study: 2045.44 s = 00:34:05

Total Reference Air Kerma (TRAK) : 0.7787 cGy·m²

Report created Jul/20/2018, 6:35 PM by HDRplus 3.0.5, Local Dongle Serial No.: 0123-673E-1078, Unique Id: 19D9 [Page 4 of 6]

APPENDIX H: CODE FOR DOSE CONVERSION MODEL

```
double Ir;  //Ir is the intensity of the irradiated film to the rectum
double Ib; // Ib is the intensity of the irradiated film to the bladder
double Db // VARIABLE TO STORE THE DOSE FOR THE BLADDER;
double Dr; // VARIABLE TO STORE THE DOSE FOR THE RECTUM;

#pragma endregion
        private: System::Void txtib_TextChanged(System::Object^  sender,
System::EventArgs^  e) {

                                    if (txtib->Text==""){
                                    lbldb->Text="";
                                    }
                                    else
                                    {
 Ib =Double::Parse(txtib->Text);
  // DOSE FOR THE BLADDER FORMULA
Db = 11.520 - 0.108 * Ib;
//---------------------------------------
lbldb->Text = System::Convert::ToString(Db);

                                    }


                                }


        private: System::Void txtir_TextChanged(System::Object^  sender,
System::EventArgs^  e) {
//          DOSE FOR THE RECTUM
                                    if (txtir->Text==""){
```

```
                                    lbldr->Text="";
                                    }
                                    else
                                    {
Ir =Double::Parse(txtir->Text);

// DOSE FOR THE RECTUM FORMULA
Dr = 11.611 - 0.110 * Ir;
//---------------------------
lbldr->Text = System::Convert::ToString(Dr);

                                    }

                    }

private: System::Void txtib_KeyPress(System::Object^  sender,
System::Windows::Forms::KeyPressEventArgs^  e) {

   if(e->KeyChar == '.'){
      if( this->txtib->Text->Contains(".") && !this->txtib->SelectedText-
>Contains(".") )
         e->Handled = true;
   }
   // Allow negative numbers
   else if(e->KeyChar == '-' && !(this->txtib->Text->Contains("-"))){
      e->Handled = true;
      txtib->Text = "-" + txtib->Text;
   }
   // Accept only digits ".", "-" and the Backspace character
   else if(!Char::IsDigit(e->KeyChar)&& e->KeyChar != 0x08){
      e->Handled = true;
   }
```

```
}

private: System::Void txtir_KeyPress(System::Object^  sender,
System::Windows::Forms::KeyPressEventArgs^  e) {

   if(e->KeyChar == '.'){
      if( this->txtir->Text->Contains(".") && !this->txtir->SelectedText-
>Contains(".") )
         e->Handled = true;
   }
   // Allow negative numbers
   else if(e->KeyChar == '-' && !(this->txtir->Text->Contains("-"))){
      e->Handled = true;
      txtir->Text = "-" + txtir->Text;
   }
   // Accept only digits ".", "-" and the Backspace character
   else if(!Char::IsDigit(e->KeyChar)&& e->KeyChar != 0x08){
      e->Handled = true;
   }
}

};
}
```

APPENDIX I: PUBLISHED ARTICLE FROM THESIS

1. Justice Avevor, Joseph Amoako, George Amoako, Samuel Nii Tagoe, "*Design and Fabrication of Water Phantom for Treatment Verification in High Dose Rate (HDR) Brachytherapy of the Cervix*", International Journal of Scientific Research in Science and Technology (IJSRST), Online ISSN: 2395-602X, Print ISSN: 2395-6011, Volume 6 Issue 5, pp. 211-214, September-October 2019. Available at doi: https://doi.org/10.32628/IJSRST196518

   Journal URL: http://ijsrst.com/IJSRST196518
2. Justice Avevor, Joseph Amoako, George Amoako. "*Empirical Validation of Absorbed Dose to the Rectum in the treatment of Cervical Cancer using High Dose Rate Brachytherapy".* International Journal of Scientific & Technology Research (IJSTR), Online ISSN: 2277-8616, Volume 8 Issue 11, pp 2687-2694, November 2019 Edition. Journal URL: http://ijstr.org/IJSTR-1119-25114